Precambrian Research xxx (xxxx) xxx

Contents lists available at ScienceDirect

Precambrian Research

journal homepage: www.elsevier.com/locate/precamres

A geochronological review of magmatism along the external margin of Columbia and in the Grenville-age orogens forming the core of Rodinia

Åke Johansson [a,*], Bernard Bingen [b], Hannu Huhma [c], Tod Waight [d], Rikke Vestergaard [d], Alvar Soesoo [e], Grazina Skridlaite [f], Ewa Krzeminska [g], Leonid Shumlyanskyy [h,s], Mark E. Holland [i], Christopher Holm-Denoma [j], Wilson Teixeira [k], Frederico M. Faleiros [k], Bruno V. Ribeiro [l], Joachim Jacobs [m], Chengcheng Wang [m], Robert J. Thomas [n], Paul H. Macey [n], Christopher L. Kirkland [o], Michael I.H. Hartnady [o], Bruce M. Eglington [p], Stephen J. Puetz [q], Kent C. Condie [r]

[a] Department of Geosciences, Swedish Museum of Natural History, Box 50 007, SE-104 05 Stockholm, Sweden
[b] Geological Survey of Norway, NO-7491 Trondheim, Norway
[c] Geological Survey of Finland, P.O. Box 96, FI-02151 Espoo, Finland
[d] Department of Geosciences and Natural Resource Management (Geology Section), University of Copenhagen, Øster Voldgade 10, 1350 Copenhagen K, Denmark
[e] Department of Geology, Tallinn University of Technology, Ehitajate tee 5, Tallinn, 19086, Estonia
[f] Institute of Geology and Geography, Nature Research Centre, Akademijos 2a, LT-8412 Vilnius, Lithuania
[g] Polish Geological Institute – National Research Institute, 4 Rakowiecka, 00975 Warszawa, Poland
[h] School of Earth and Planetary Sciences, Curtin University, Perth, Western Australia 6102, Australia
[i] Dept. of Life, Earth, and Environmental Sciences, West Texas A&M University, Canyon, TX 79016, USA
[j] Geology, Geophysics, and Geochemistry Science Center, U.S. Geological Survey, Denver, CO, USA
[k] Institute of Geosciences, University of São Paulo, Brazil
[l] School of Earth, Atmosphere & Environment, Monash University, Australia
[m] Department of Earth Science, University of Bergen, PB7803, NO-5020 Bergen, Norway
[n] Council for Geoscience, P.O. Box 572, Bellville 7535, South Africa
[o] Timescales of Mineral Systems Group, School of Earth and Planetary Sciences, Curtin University, Perth, Western Australia 6102, Australia
[p] University of Saskatchewan, Geological Sciences, 114 Science Place, Saskatoon, Saskatchewan S7N 5E2, Canada
[q] Progressive Science Institute, 475 Atkinson Drive # 704, Honolulu, HI 96814, USA
[r] Department of Earth and Environmental Science, New Mexico Institute of Mining and Technology, Socorro, NM 87801, USA
[s] M.P. Semenenko Institute of Geochemistry, Mineralogy and Ore Formation, Kyiv, Ukraine

ARTICLE INFO

Keywords:
U-Pb geochronology
Grenville
Geochronological database
Columbia
Rodinia
Supercontinents

ABSTRACT

A total of 4344 magmatic U-Pb ages in the range 2300 to 800 Ma have been compiled from the Great Proterozoic Accretionary Orogen along the margin of the Columbia / Nuna supercontinent and from the subsequent Grenvillian collisional orogens forming the core of Rodinia. The age data are derived from Laurentia (North America and Greenland, n = 1212), Baltica (NE Europe, n = 1922), Amazonia (central South America, n = 625), Kalahari (southern Africa and Dronning Maud Land in East Antarctica, n = 386), and western Australia (n = 199). Laurentia, Baltica, and Amazonia (and possibly other cratons) most likely formed a ca. 10 000-km-long external active continental margin of Columbia from its assembly at ca. 1800 Ma until its dispersal at ca. 1260 Ma, after which all cratons studied were involved in the Rodinia-forming Grenvillian orogeny. However, the magmatic record is not smooth and even but highly irregular, with marked peaks and troughs, both for individual cratons and the combined data set.

Magmatic peaks typically range in duration from a few tens of million years up to around hundred million years, with intervening troughs of comparable length. Some magmatic peaks are observed on multiple cratons, either by coincidence or because of paleogeographic proximity and common tectonic setting, while others are not. The best overall correlation, 0.617, is observed between Baltica and Amazonia, consistent with (but not definitive proof of) their being close neighbours in a SAMBA-like configuration at least in Columbia, and perhaps having shared the same peri-Columbian subduction system for a considerable time. Correlation factors between

* Corresponding author.
E-mail addresses: ake.johansson@nrm.se (Johansson), kcondie@nmt.edu (K.C. Condie).

https://doi.org/10.1016/j.precamres.2021.106463
Received 31 March 2021; Received in revised form 24 September 2021; Accepted 7 November 2021

Laurentia and Baltica, or Laurentia and Amazonia, are below 0.14. Comparison between the Grenville Province in northeastern Laurentia and the Sveconorwegian Province in southwestern Fennoscandia (Baltica) shows some striking similarities, especially in the Mesoproterozoic, but also exhibits differences in the timing of events, especially during the final Grenville-Sveconorwegian collision, when the Sveconorwegian evolution seems to lag behind by some tens of million years. Between the other cratons, the evolution before and during the final Grenvillian collision is also largely diachronous. After 900 Ma, magmatic activity had ceased in all areas investigated, attesting to the position of most of them within the stable interior of Rodinia.

1. Introduction

During the past decades, it has become increasingly clear that several earlier supercontinents existed prior to the Phanerozoic supercontinent Pangea, first proposed by Wegener (1912, 1915). Leaving aside the question of the existence of any late Archean supercontinent or supercraton (e.g. Bleeker, 2003; Liu et al., 2021), it is generally accepted that there was a late Paleoproterozoic to Mesoproterozoic supercontinent, Columbia (also known as Nuna), followed by a Neoproterozoic supercontinent, Rodinia (Evans, 2013; Mitchell et al., 2021). Parts of Rodinia then amalgamated into the megacontinent Gondwana (C. Wang et al., 2020), which later merged with the present-day northern continents to form the full supercontinent Pangea.

The external margins of supercontinents are characterized by prolonged subduction-related magmatism and accretionary orogenies that collectively may last for several hundred million years. The existence of these supercontinents may also have affected Earth's climate, mantle evolution, and crustal growth patterns (e.g. Pastor-Galán et al., 2019).

Much of Columbia apparently assembled through a global network of accretionary and collisional orogens at 1.9 to 1.8 Ga (e.g. Zhao et al., 2004, 2011; Wan et al., 2020), which collectively can be referred to as "proto-Columbian" orogens. However, parts of Columbia (eastern Amazonia, some African cratons, the Volgo-Uralian and Sarmatian parts of Baltica) were probably already assembled by 2.0 Ga. Final assembly of Columbia may not have taken place until 1.6 Ga, when Australia collided with western (in present-day coordinates) Laurentia (e.g. Furlanetto et al., 2013, 2016; Pourteau et al., 2018; Nordsvan et al., 2018; Kirscher et al. 2019; Gibson and Champion, 2019; Gibson et al., 2020) in a "proto-SWEAT" configuration. According to D'Agrella-Filho et al. (2016), final Columbia assembly may even have occurred as late as 1.4 Ga. The assembly of Columbia thus appears to have been similar to the assembly of Pangea, with a protracted period of collisions over several hundred million years, ending with final assembly through the collision of its two halves (cf. C. Wang et al., 2020).

The exact configuration of Columbia is still debated (cf. Rogers and Santosh, 2002; Zhao et al., 2004; Meert and Santosh, 2017; Zhang et al., 2012; Mertanen and Pesonen, 2012; Pisarevsky et al., 2014; Teixeira et al., 2007; Johansson, 2009; Grenholm, 2019; D'Agrella-Filho et al., 2016; Reis et al., 2013; Terentiev and Santosh, 2020; Mitchell et al., 2021), but it is usually agreed that a long-lived external active margin

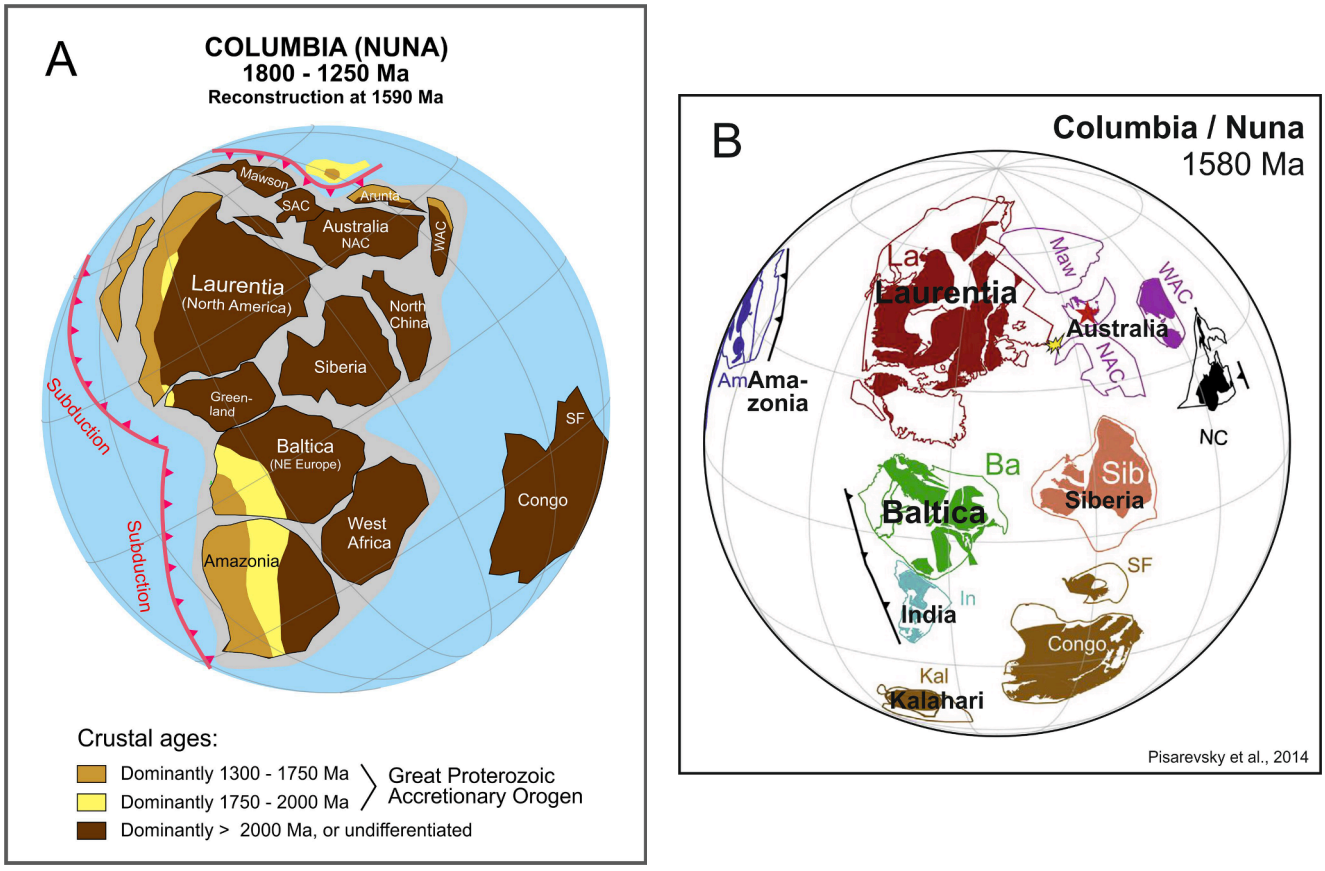

Fig. 1. a. The Great Proterozoic Accretionary Orogen (GPAO) in a Columbia (Nuna) configuration of Laurentia, Baltica and Amazonia that may have existed from around 1800 Ma to 1250 Ma, partly after Johansson (2009). The positions of the Congo-Sao Fransisco craton is highly uncertain. Kalahari is not visible in this view. **B.** Alternative reconstruction by Pisarevsky et al. (2014), with India instead of Amazonia attached to the Sarmatian part of Baltica, and Amazonia and West Africa (not seen in this view) forming a separate block that is not part of Columbia. Also Kalahari is separate from Columbia, at least at this stage.

extended from present-day southeastern Laurentia (North America) via the southern tip of Greenland to Baltica (northeast Europe), referred to as the NENA (Northern Europe – North America) connection by Gower et al. (1990). A further continuation of this active margin from Baltica to Amazonia – the SAMBA (South America – Baltica) connection – was proposed by Johansson (2009), and is outlined in Fig. 1A. However, an alternative configuration was proposed by Pisarevsky et al. (2014), in which India instead of Amazonia is attached to southwest Baltica, while Amazonia and West Africa form an independent block west of Baltica and Laurentia, not being part of the Columbian supercontinent (Fig. 1B).

Depending on where along the western Laurentian margin the different parts of Australia and Antarctica were attached, the Laurentian active margin may (or may not) have extended into southern Australia, as proposed by Karlstrom et al. (2001). This huge external accretionary belt was referred to as the Great Proterozoic Accretionary Orogen (GPAO) by Condie (2013), and would have been part of the subduction girdle encircling Columbia. Following the terminology proposed above, we could refer to these orogenies and orogens as "syn-Columbian" and "peri-Columbian", respectively, based on their position in time (simultaneous) and space (peripheral) relative to the Columbia supercontinent.

Break-up of Columbia is often assumed to have taken place around 1.25 Ga (e.g. Evans and Mitchell, 2011; Pesonen et al., 2012; Kirscher et al., 2021), but may also have been a protracted process. Through clockwise rotation of Baltica, Amazonia, and West Africa relative to Laurentia between 1.25 and 0.95 Ga, these cratons assembled in a new configuration that formed the core of Rodinia (e.g. Li et al., 2008; Johansson, 2009; Fig. 2). The details of this collision, such as which continent collided with which, are still controversial (cf. Karlstrom et al., 2001; Tohver et al., 2002, 2004; Li et al., 2008; Johansson, 2009; Cawood et al., 2010; Lorenz et al., 2012; Gee et al., 2015; Johansson, 2016; Cawood and Pisarevsky, 2017; Martin et al., 2020), and there are also non-collisional accretionary models both for the Sveconorwegian orogeny (Slagstad et al., 2013, 2017, 2018, 2020) and the Sunsás orogeny (Santos et al., 2008; Evans, 2009). However, in most reconstructions, Baltica and Amazonia form the conjugate margin of southeastern Laurentia. Further along the Laurentian margin, other parts of present-day South America, such as the Pampean block, would have accreted, in turn followed by the Kalahari craton (southern Africa) and East Antarctica (cf. Dalziel et al., 2000; Johansson, 2014). Because of the aforementioned rotation, the intervening ocean closed and the accretionary "syn- and peri-Columbian" GPAO became transformed into the collisional "proto-Rodinian" Grenville-Sveconorwegian-Sunsas orogenic belt and its further continuation into southern Africa and Antarctica.

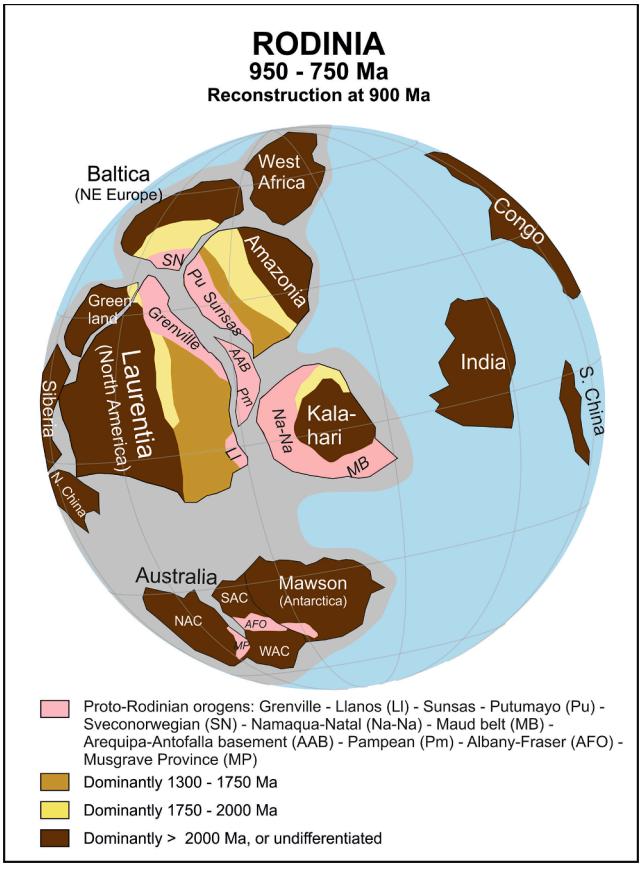

Fig. 2. Rodinia reconstruction at 900 Ma, with the Grenville-Sveconorwegian-Sunsas belts and related orogens at the heart of Rodinia, partly after Johansson (2009, 2014). The positions of India, S. China and Congo are highly uncertain in this reconstruction.

The purpose of this paper is to compare magmatic crystallization ages, and hence crust-forming or crust-recycling orogenic (and anorogenic or intraplate) events, during the timespan 2.3 to 0.8 Ga along the external "syn- and peri-Columbian" GPAO, including its "proto-Columbian" predecessors, and the subsequent collisional "proto-Rodinian" Grenville-Sveconorwegian-Sunsás orogen. Although accretionary, and subsequent collisional, orogenic activity was going on semi-continuously along this belt, over a distance of at least 10 000 km (Laurentia-Baltica-Amazonia part) for around 1 billion years (1900 to 900 Ma), this activity can be subdivided into different magmatic and orogenic events occurring at different times along different segments of this belt, separated by periods of relative quiescence. Our aim is to compare the ages of these events on the different continents and cratons involved (primarily Laurentia, Baltica, and Amazonia, but with extensions to southern Africa, Antarctica, and Australia), to determine whether these events occurred penecontemporaneously and can be correlated in more detail from continent to continent, or if subduction, arc-continent collisions, intra-plate magmatism, and final continent–continent collision occurred at different times along different segments of this orogen. The broad-scale and regional context of this compilation by necessity means that some local scale geological events will be obscured, particularly when identified on the basis of only limited outcrops and/or a restricted number of ages.

In addition to a better understanding of the Proterozoic geological and geotectonic evolution on each of the continents involved, and their inter-relationships, this study also aims to shed some light on the much-debated issue of whether global peaks in crustal formation ages (as seen from U-Pb zircon ages, Nd whole rock, or Hf in zircon model ages) are due to pulses of enhanced magmatic activity during periods of supercontinent formation, in turn reflecting changes in mantle geodynamics (Stein and Hofmann, 1994; Condie, 1998; Wang et al., 2009; Arndt and Davaille, 2013; Parman, 2015; Condie et al., 2015, 2017, 2018; Rollinson, 2017; Walzer and Hendel, 2017; Puetz and Condie, 2020), or if these peaks are due to better preservation of newly-formed crust during those periods, with actual crustal production being steady-state or slowly declining (Hawkesworth et al., 2009, 2010, 2019; Dhuime et al., 2011; Cawood et al., 2013).

2. Methods

U-Pb age determinations on Proterozoic magmatic rocks in the timespan 2.3 to 0.8 Ga from the above-mentioned continents have been compiled, building on pre-existing compilations and databases. The vast majority of ages in this compilation are from felsic to intermediate intrusive or extrusive rocks, or their metamorphic equivalents, with only a limited number of ages from mafic igneous rocks.

From Laurentia, relevant areas include the Makkovik, Penokean, Mojave, Yavapai, and Matatzal Provinces, the Granite-Rhyolite Province of the central US, the Grenville Province (including older rocks contained within it), and the Ketilidian Province and Gardar magmatic

rocks of southern Greenland.

For Baltica, the relevant areas include the Svecofennian (a.k.a. Svecokarelian) and Sveconorwegian Provinces and the Transscandinavian Igneous Belt of Fennoscandia, and corresponding units within the concealed basement of the Baltic countries and northeast Poland, sampled through drill holes. From the Sarmatian part of Baltica, rocks occurring along its western accretionary margin were included. Younger, intraplate (anorogenic) magmatic rocks occurring in these areas were also included, and grouped together with the orogenic province in which they occur.

From Amazonia, magmatic ages of rocks from the Central Amazonian, Maroni-Itacaiúnas, Ventuari-Tapajos, Rio Negro-Juruena, Rondonian-San Ignacio, and Sunsas Provinces, as well as the small Rio Apa Craton, were all included.

From southern Africa (Kalahari craton), rocks occurring within the Grenville-age Namaqua-Natal belt in Namibia and South Africa were included, and rocks of corresponding ages in northern Mozambique and Malawi, which represent the northwards continuation of the Maud belt of East Antarctica. From Antarctica, similar-aged rocks from the adjacent (in Proterozoic times) Maud belt in Dronning Maud Land were included. From western Australia, rocks from the Albany-Fraser Orogen, the Eucla Basement (Madura and Coompana Provinces) and Musgrave Province, which form a potential prolongation of the GPAO, were included. Since the positions of both Australia and Kalahari within Columbia is uncertain, our focus was restricted to the Grenville-age Rodinia-forming orogens from those cratons.

Rocks and ages representing internal collisional Proterozoic orogens within Columbia, such as the Trans-Hudson orogen of Laurentia or the Lapland-Kola belt of Baltica, were excluded, as this contribution is focused on activities along the external margin of Columbia. Dolerite dyke swarms were also excluded, since they do not represent any significant crustal growth but rather attempted or successful rifting. Furthermore, the dyke-based magmatic record has been the subject of a recent large international project involving age dating and "barcode matching" of continents (www.supercontinent.org; cf. Ernst et al., 2013; Srivastava et al., 2019). However, rocks forming part of the dominantly mafic early Paleoproterozoic Karelian magmatism in Baltica have been included, since this magmatism is more varied and also contains felsic components.

Terranes of uncertain, potentially exotic origin, were excluded. This includes Proterozoic rock units within younger mountain belts, such as the Andes, the Appalachians or the Scandinavian Caledonides, unless they represent (par)autochthonous basement.

Some effort has been made to separate magmatic events into subduction- or collision-related continental margin magmatism on the one hand, and intraplate magmatism such as siliceous large igneous provinces (SLIPs) and anorthosite-mangerite-charnockite-granite (AMCG) complexes on the other, at least for Baltica and Amazonia. Age data on intraplate magmatic rocks have been plotted within the province in which these rocks occur, even if they are not related to the orogenic development of that province. For example, the classical rapakivi granites of Finland and central Sweden have been plotted as part of the Svecofennian Province in which they occur, and the Mesoproterozoic A-type granites of southeast Sweden and the Danish island of Bornholm are included as part of the Transscandinavian Igneous Belt, despite having formed 200 to 300 million years later than the surrounding rock units.

From some of the countries (Canada, Sweden, Norway, Finland, Western Australia) geochronological databases had already been assembled by their respective geological surveys, which could be used after some filtering and editing. In other cases, the data were assembled from pre-existing partial compilations or captured directly from the published literature.

Filtering included removal of all ages except U-Pb ages (and a few Pb-Pb ages), mostly on zircon, but some baddeleyite, monazite or titanite ages were also included. Only ages interpreted as representing magmatic crystallization were kept, excluding all metamorphic, inherited, detrital, mixed or disturbed data. Furthermore, all ages with a reported uncertainty of more than ± 20 million years were excluded, to avoid imprecise data that may be erroneous. Nevertheless, there may be seemingly precise but still incorrect mixed or reset U-Pb ages, especially among older multigrain TIMS analyses, that will escape the filtering. Such data may result in some noise and scatter in the diagrams, but should not seriously disturb the age patterns presented. Although one could have considered using only modern, high-precision TIMS, SIMS or LA-ICP-MS data from the last twenty years, omitting all previously published age data might have lead to other problems and biases, for example by focusing the data on more restricted geographical areas or rock types studied in recent years, while excluding earlier more regional studies that will give more representative age patterns.

Consequently, we emphasize that our approach is at best semi-quantitative, and may not reflect the real volumes of crust formed at different time intervals, for a variety of reasons:

1. The data only show magmatic rocks (or metamorphosed equivalents), and not metasedimentary rocks (although in active continental margin environments, these can largely be assumed to fall within the same age intervals as the magmatic rocks, and ultimately all clastic sedimentary rocks must have a magmatic source);
2. The U-Pb ages do not reveal the age of mantle separation, which may have occurred several hundred million years earlier;
3. The U-Pb ages only show the age distribution at the present-day accessible land surface (or closely beneath the surface of the Precambrian basement in the case of drill core data), which may not necessarily be representative of the underlying volume of continental crust;
4. Well-exposed areas that are easily accessible and have a varied and complicated geology will have more data compared to concealed basement regions only known from drill cores, geographically remote areas, or areas with more homogeneous bedrock.
5. The number of U-Pb ages from one rock unit is not fully representative of the surface area (or volume) of that unit. Ore-bearing metavolcanic units may be over-represented, as well as pegmatites and other dyke rocks, while mafic rocks or homogeneous granitoids covering large tracts of land may be somewhat under-represented. A more sophisticated quantitative approach would be to compute the surface area of various local rock units or rock types (if not volume) and weight the age data accordingly, but this is beyond the scope of the present contribution.

Nevertheless, samples were weighted on a regional scale, proportional to the surface areas of the geological provinces and cratons, and this weighting was applied to the final relative probability curves, comparing the different cratons studied, since the sample density is much higher in well-exposed, accessible and well-studied regions, than in remote areas or areas where the Precambrian basement is covered, and only known through drill holes. Consequently, the surface areas of the different orogenic or geological provinces defined on each craton were estimated, including those areas overlain by younger sedimentary cover (e.g. East European Platform, Central United States, large parts of Amazonia), water (e.g. Baltic Sea), or ice (in Greenland and Antarctica). By relating the number of sample records from each province to its surface area, a weighing factor was computed and applied to the combined data.

The whole dataset, with a total of 4344 sample records, is available in the Appendix, which also includes area estimates and weighting factors for each craton as well as for the combined dataset. The data have been plotted on Google Earth maps of each craton investigated, with sample symbols colour-coded according to age. The time ranges for this subdivision (900–1260, 1260–1600, 1600–1820, 1820–2020, 2020–2300 Ma) were selected in order to subdivide as few magmatic peaks as possible in the cratons studied, placing the division lines where troughs in magmatic commonly activity occur.

In addition to presenting the data in map and diagram form in the figures of this paper, two animations are included as supplementary electronic material, one with the data points appearing at their respective age on a map of the present-day Earth, the other where they appear in a similar way on a set of plate tectonic reconstruction maps.

3. Laurentia data and results

3.1. Geological overview

Laurentia is the cratonic core of present-day North America, and taken here to include Greenland. Currently the largest craton on Earth, Laurentia is composed of an Archean core known as the Canadian Shield that was assembled from several distinct Archean cratons during the 1.83–1.80 Ga Trans-Hudson orogeny (Corrigan et al., 2005, 2009). The Canadian Shield is bound by numerous Proterozoic orogens, most notably a > 1000 km wide belt of dominantly accretionary orogens that record protracted crustal growth along the southeastern margin (present coordinates) of Laurentia from ca. 1.8 to 1.0 Ga (Condie, 1982; Karlstrom et al., 2001; Whitmeyer and Karlstrom, 2007). It is this long-lived orogenic collage that is the focus of this review.

A review of the Laurentian accretionary history provided by Whitmeyer and Karlstrom (2007) shows divisions of southern Laurentia into crustal provinces based on their age, isotopic character, and timing of orogenesis. Here, we summarize the major tectonic features of these crustal provinces with an emphasis on associated magmatism, starting with southern Greenland.

Relevant U-Pb ages from Laurentia for this study (1212 records) are plotted on a Google Earth map of Laurentia, together with a simplified outline of the geology, in Fig. 3. Relevant relative probability curves and corresponding cumulative age diagrams are shown in Fig. 4.

3.2. Ketilidian Province and Gardar Domain of southern Greenland

Proterozoic magmatic activity in South Greenland is dominated by the Palaeoproterozoic Ketilidian Orogen and the Mesoproterozoic Gardar alkaline igneous province (Steenfelt et al., 2016).

The Julianehåb Igneous Complex (formerly Julianehåb Batholith of Chadwick and Garde, 1996) of the Ketilidian Orogen is interpreted to result from northwards-dipping subduction under the Archean foreland, located to the present day north. It has a wedge-shaped outcrop area of ca. 30 000 km^2 and is composed of ca. 1.8 Ga calc-alkaline continental magmatic arc rocks (Garde et al., 2002) that constitute the Central Domain of the Ketilidian Orogen. Adjacent to the batholith to the south

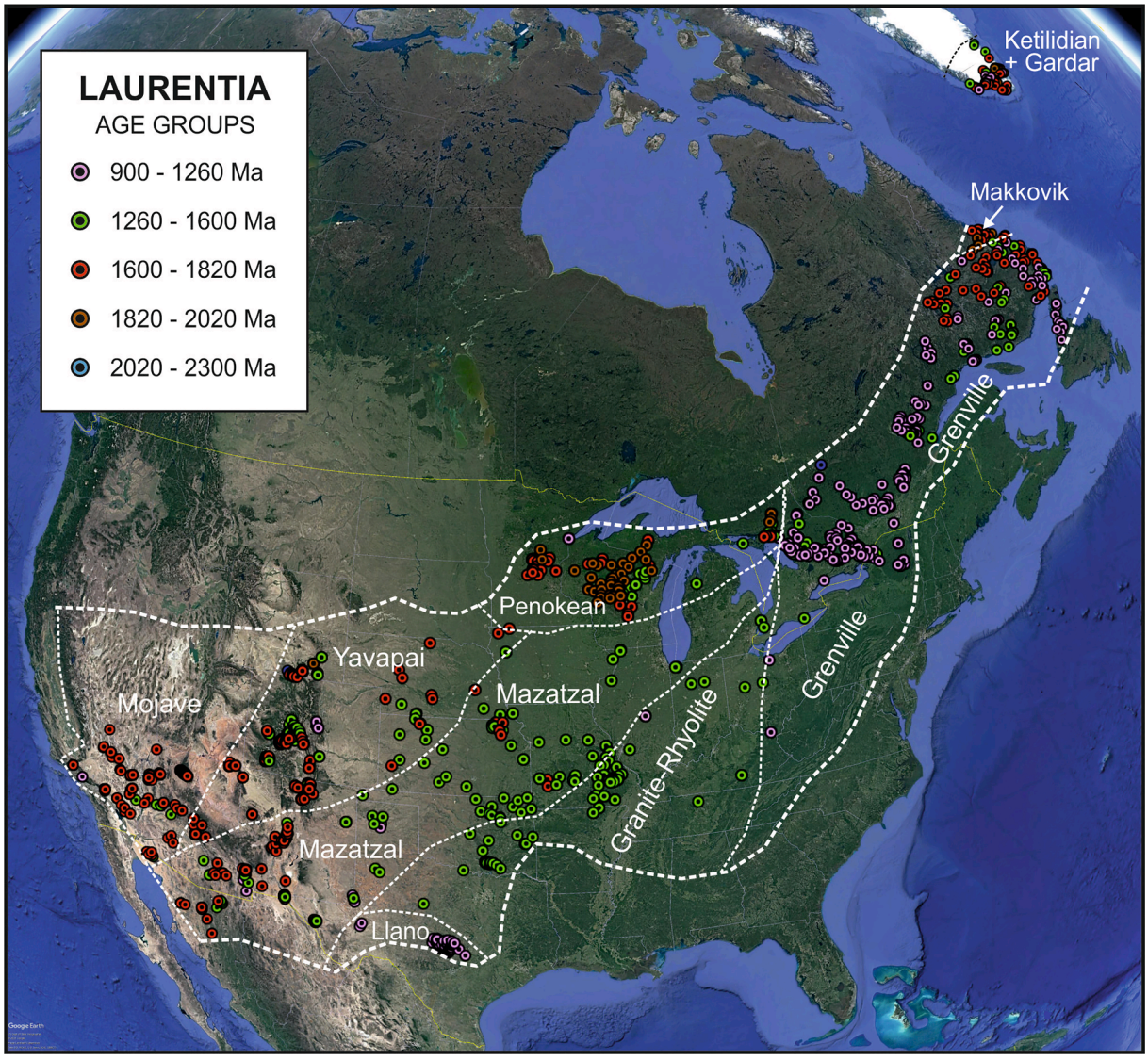

Fig. 3. Google Earth map of Laurentia with main geological provinces (white dashed lines) and magmatic U-Pb age data points indicated, colour-coded according to age.

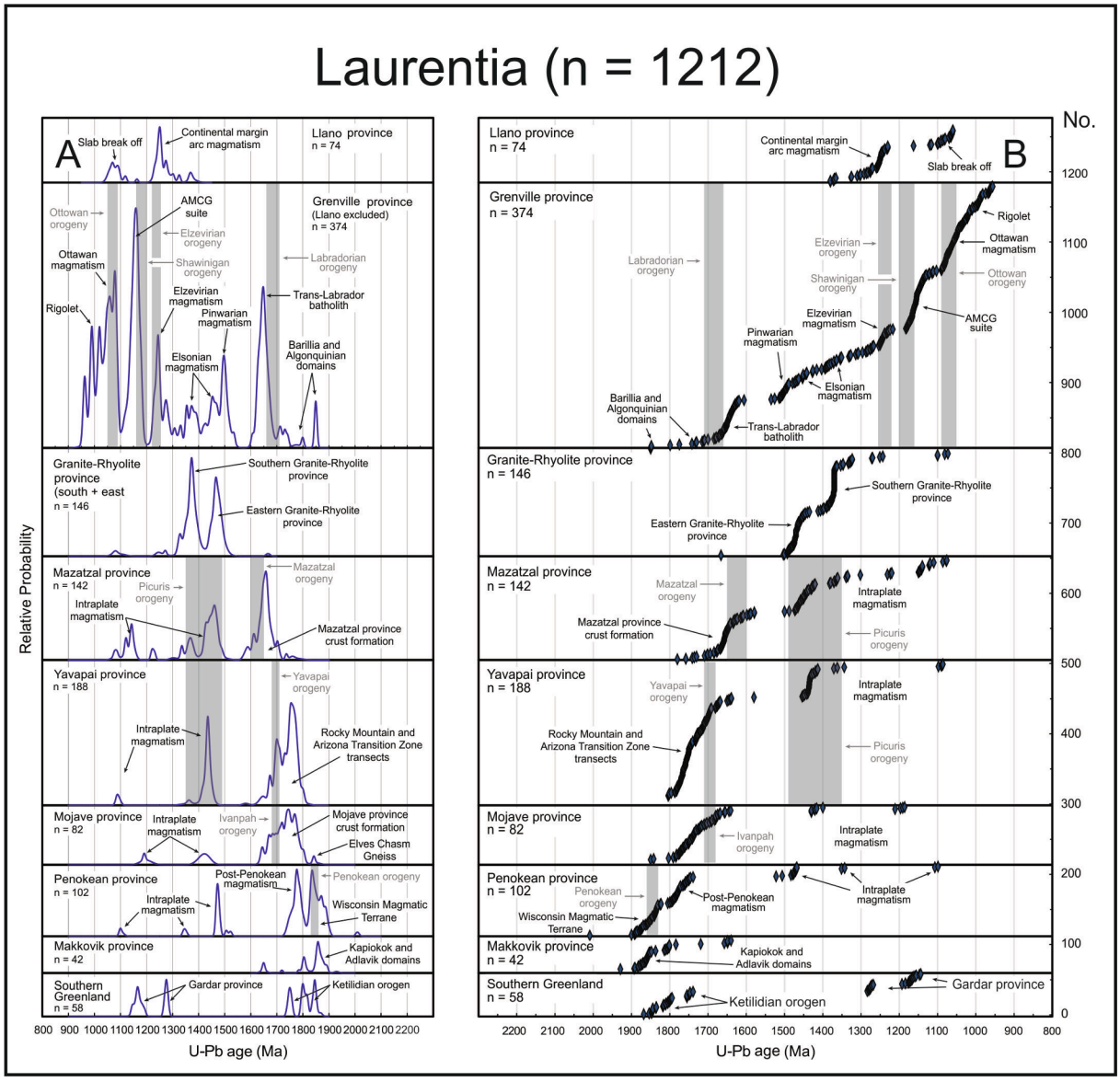

Fig. 4. A. Relative probability curves of magmatic U-Pb ages between 2300 and 800 Ma from various parts of the GPAO and Grenville Orogen in Laurentia. **B.** Cumulative age diagrams from the same units. Note that the age axis in panel B is reverse compared to in panel A.

is the Southern Domain (formerly the Psammite and Pelite Zone of Chadwick and Garde, 1996), which is a region dominated by deformed high-grade metamorphic rocks intruded by the Ilua Suite rapakivi granites which formed late in the Ketilidian orogeny at ca. 1.75 Ga (Garde et al., 2002; Steenfelt et al., 2016). The metamorphic rocks of the Southern Domain are interpreted as fore-arc rocks formed by material eroded off the uplifted and unroofed batholith (Garde et al., 2002), and were metamorphosed prior to the emplacement of the Ilua Suite. The Ketilidian Orogen has been correlated with similar aged events and crustal architectures in Canada (Makkovik Province; Ketchum et al., 2002) and Scandinavia (Transscandinavian Igneous Belt; Lahtinen et al., 2008).

In our data compilation, the Ketilidian Orogen is represented by 33 magmatic ages ranging from 1870 to 1740 Ma, subdivided into three sharp peaks at ca. 1850, 1800 and 1750 Ma (Fig. 4). These peaks correspond to two apparent groupings of ages in the Julianehåb Igneous complex at 1850–1830 and 1800–1780 Ma and the later post-tectonic Ilua Suite intrusives (Garde et al., 2002; Steenfelt et al., 2016).

The Gardar Domain (Gardar Province) encompasses igneous and supracrustal rocks emplaced during at least two events of continental rifting between 1.30 and 1.14 Ga and is exposed over most of South Greenland, either overlying or intruding the rocks of the other domains (Steenfelt et al., 2016). Magmatic products include several rift-related mafic dyke swarms (e.g. Bartels et al. 2015), ultramafic lamprophyres and carbonatites (e.g. Halama et al. 2005), and a suite of alkaline to agpaitic syenitic to nepheline syenitic intrusive complexes including the Ilímaussaq Complex (e.g. Sørensen, 2001; Upton, 2013).

The Gardar Domain is represented by 25 ages in our compilation, ranging from 1285 to 1140 Ma, with the two magmatic events mentioned above clearly visible as two peaks at ca. 1270 and 1160 Ma, separated by a gap in magmatic activity of 75 million years (Fig. 4).

3.3. *Makkovik Province*

The Makkovik Province in Labrador is generally considered to be the westerly equivalent of the Ketilidian Orogen in South Greenland (Fig. 3), although there are important differences (Ketchum et al. 2002). Historically, three main domains were identified, from northwest to southeast, the Kaipokok, Aillik and Cape Harrison domains (Kerr et al., 1996). Recent work suggests the previously defined Aillik and Cape

Harrison domains should be combined into the Adlavik Domain (Hinchey, 2021a). The northernmost Kaipokok Domain is part of the North Atlantic Craton and comprises reworked Archean gneisses, intruded by the calc-alkaline Island Harbour Bay Plutonic Suite (1895–1870 Ma), with isotopic signatures indicative of involvement of reworked older crust (Barr et al., 2001). The more southern Adlavik Domain consists of the Aillik Group, which is dominated by Paleoproterozoic metasediments and metavolcanics with ferroan (A-type) signatures as well as mafic rocks emplaced between 1.88 and 1.85 Ga and interpreted to represent a back-arc environment (Hinchey, 2021a). The composite arc itself is represented by various and abundant intrusive suites (ca. 1800, 1720, and 1650-1640 Ma) and orthogneiss of the Cape Harrison Metamorphic Suite (Hinchey, 2021b). Nd isotope data suggest reworking of Neoarchean to Paleoproterozoic crustal sources, or interactions between mantle melts and even older crustal components (Hinchey et al., 2020; Hinchey, 2021a, b, c, d; but see also Dickin, 2021). The Kaipokok Domain is considered equivalent to the Northern Domain of the Ketilidian Orogen, whereas the Adlivik Domain is equivalent to the Central Domain and Julianehåb Igneous Complex as defined by Steenfelt et al. (2016). However, the Adlivik Domain generally yields somewhat older ages and represents higher crustal levels, and the back-arc equivalents to the Aillik Group are not identified in Greenland. The metasediments of the Southern Domain of the Ketilidian Orogen are not recognized in the Makkovik Province, but a suite of post-orogenic undeformed A-type granites emplaced around 1720 Ma are considered equivalent to the Ilua Suite rapakivi granites (Ketchum et al, 2002).

In our compilation, the Makkovik Province is represented by 42 data points, ranging in age from 1930 to 1640 Ma, forming several peaks the largest of which is centered at 1800 Ma. The 1800 Ma peak, as well as a peak at 1650 Ma, is mainly due to the Trans-Labrador batholith (Kerr, 1989; Kerr et al., 1992). The ca. 1720 Ma A-type magmatism is only represented by one data record. The 1650 Ma peak is an age-equivalent of the Labradorian magmatism within the nearby Grenville Province (see below).

3.4. Penokean Province

The Penokean Province in the Great Lakes region (Fig. 3) is similar in age to the Makkovik Province, and together they form the oldest of several Paleoproterozoic orogenic terranes that accreted to the margin of the Archean Canadian Shield. The Penokean Province records the interaction between Paleoproterozoic arc successions and two Archean cratonic blocks, the Superior Craton and the Marshfield Terrane (Holm et al., 2020). South of the Superior Craton, the Wisconsin Magmatic Terrane includes an assemblage of ca. 1875–1835 Ma tholeiitic and calc-alkaline volcanic and plutonic rocks interpreted to have formed in an oceanic arc above a south-dipping subduction zone (Sims et al., 1989; Holm et al., 2020) (Fig. 3). Our database includes 46 ages from this magmatic suite. Cratonic passive margin rocks of the Superior Province are juxtaposed against the Wisconsin Magmatic Terrane along the Niagara Fault Zone, interpreted to record the suturing of the Paleoproterozoic Penokean Province rocks to the Archean Superior Craton at ca. 1860 Ma (Schulz and Cannon, 2007).

Following the accretion of the Wisconsin Magmatic Terrane to the Superior Province, north-dipping subduction occurred beneath this terrane until the accretion of the Archean Marshfield Terrane, juxtaposing the two provinces across the Eau Pleine shear zone at ca. 1840 Ma (Sims et al., 1989; Schulz and Cannon, 2007). A near-continuum of post-orogenic magmatism in the combined Penokean Province migrated from north to south from ca. 1800 to 1750, and is attributed to variations in plate convergence rates during continued north-dipping subduction (Holm et al., 2005) (Fig. 4). This magmatic episode is represented by 38 ages. South of the Marshfield Terrane, ca. 1700 Ma rocks broadly associated with the Yavapai crustal Province are present south of the Spirit Lake tectonic zone (NICE Working Group, 2007; Chichester et al., 2018). The Penokean Province experienced variable tectonic overprinting related to younger tectonism that is beyond the scope of this review.

3.5. Yavapai and Mojave provinces

The Yavapai crustal Province is exposed along two semi-continuous transects in the western United States; the north–south trending Rocky Mountains, and the northwest-southeast trending Arizona Transition Zone (Fig. 3). Paleoproterozoic (ca. 1.8–1.7 Ga; Fig. 4) rocks of both regions include a broadly similar assemblage of metasedimentary rocks, bimodal metavolcanic rocks, and granitoid intrusions generally interpreted to have formed in arc-related environments before their accretion to Laurentia in a series of orogenic episodes (Reed et al., 1987; Karlstrom and Bowring, 1988). The timing, regional extent, and tectonic setting of orogenesis throughout the western U.S. remains the subject of debate (Grambling, 1986; Shaw and Karlstrom, 1999; Selverstone et al., 2000; Daniel et al., 2013; Mako et al., 2015; Holland et al., 2020), but the magmatic framework of the Yavapai Province is very well established.

Similar to the Penokean Province, the Yavapai Province of Whitmeyer and Karlstrom (2007; which includes the Colorado Province of Reed et al., 1987) records the juxtaposition of Paleoproterozoic crust against Archean crust across the Cheyenne Belt of southern Wyoming. The Yavapai Province is locally divided into terranes or blocks (c.f. Whitmeyer and Karlstrom, 2007), though the tectonic significance of many proposed structural boundaries is uncertain (Karlstrom and Bowring, 1988; Tyson et al., 2002; Cavosie and Selverstone, 2003; Bickford and Hill, 2007; Holland et al., 2015). Immediately south of the Cheyenne Belt in the northern Rocky Mountains is the Green Mountain terrane, interpreted to be a juvenile 1.78–1.76 arc (Jones et al., 2010) accreted to the margin of the Wyoming Craton at ca. 1.75 Ga during the Medicine Bow orogeny (Chamberlain, 1998; Jones et al., 2010). Throughout the Rocky Mountain region of the Yavapai Province, several other magmatic suites have been proposed to represent juvenile arc successions that generally young southwards; these include the ca. 1.80–1.79 Irving Formation (Gonzales and Van Schmus, 2007), the ca. 1.77–1.60 Ga Dubois and ca. 1.74–1.72 Cochetopa successions (Bickford et al., 1989), and the 1.75–1.74 Ga Rawah Terrane (Premo and Van Schmus, 1989). We include 114 ages from this region (Fig. 4).

Paleoproterozoic rocks of the Arizona Transition Zone share numerous characteristics with those of the Rocky Mountain region. In central Arizona, the Yavapai Supergroup consists of interlayered metaturbidite and bimodal metavolcanic rocks inferred to have formed in a juvenile oceanic arc setting (Karlstrom and Bowring, 1988). The Yavapai Supergroup and related rocks are intruded by a suite of ca. 1.77–1.71 Ga arc-related granitoids (Karlstrom et al., 1987; Chamberlain and Bowring, 1990; Hawkins et al., 1996; Duebendorfer et al., 2001; $n = 21$). As in the Rocky Mountain region, the Yavapai Province of central Arizona is divided into multiple blocks bounded by shear zones that juxtapose rocks with varied metamorphic, deformational, and magmatic histories (Karlstrom and Bowring, 1988). Most blocks share a broadly similar tectonic history that probably represents the assembly of multiple arc terranes during the 1.71–1.68 Ga Yavapai orogeny (Karlstrom and Bowring, 1988; Ilg et al., 1996; Duebendorfer et al., 2001). Throughout the Yavapai Province, in both the Rocky Mountain region and central Arizona, the extent to which various magmatic suites and shear zone bounded blocks represent distinct arcs (e.g. Jessup et al., 2006) or dissected fragments of a longer-lived composite arc system (Jones et al., 2010) is poorly understood.

On the western edge of the Arizona Transition Zone and the Yavapai Province lies the Mojave Province, represented by 82 records in our compilation (Figs. 3 and 4). The Mojave Province is primarily distinguished from the Yavapai Province on the basis of isotopic composition, with igneous rocks of the Mojave Province showing evidence for the recycling of early Paleoproterozoic to Archean crust in every isotopic system yet applied to them (Bennett and DePaolo, 1987; Lee et al., 2001; Wooden et al., 1988; Wooden et al., 2012; Holland et al., 2015, 2018).

Direct evidence for the presence of older crust in the Mojave Province is found in the 1.84 Ga Elves Chasm Gneiss of the Grand Canyon (Hawkins et al., 1996), a remnant of the plutonic substrate upon which the Mojave Province was built (Holland et al., 2018). Otherwise, the main phase of magmatism in the Mojave Province began at ca. 1790 Ma and continued to ca. 1650 Ma (Barth et al., 2009; Wooden et al., 2012), with later pulses of magmatism at 1420 and 1190 Ma related to Granite-Rhyolite and Grenville Province magmatism (Fig. 4). Rocks of the Mojave Province also experienced a pulse of deformation and metamorphism at ca. 1.7 Ga, locally referred to as the Ivanpah orogeny that corresponds to the Yavapai orogeny in the Yavapai Province (Wooden and Miller, 1990; Duebendorfer et al., 2001; Strickland et al., 2013).

3.6. Mazatzal Province

The Mazatzal Province is exposed in the eastern Arizona Transition Zone and southern Rocky Mountains of New Mexico (Fig. 3). Throughout the Mazatzal Province, a suite of ca. 1.68–1.62 Ga granitoids (n = 61) intrudes metasedimentary and metavolcanic rocks of different character to those of the Yavapai Province (Karlstrom et al., 1987; Amato et al., 2008; Mako et al., 2015; Holland et al., 2020). Distinctive rhyolite-quartzite successions were deposited across the Mazatzal Province at ca. 1.70 and 1.65 Ga (Whitmeyer and Karlstrom, 2007), though felsic volcanism continued locally until at least 1.59 Ga (Holland et al., 2020). Rhyolite-quartzite successions and the granitoids which intrude them are interpreted to have formed in a continental arc developed above the previously assembled Yavapai Province (Condie, 1982; Bickford et al., 2019; Holland et al., 2020). Volcanism and sedimentation occurred during cyclic episodes of supra-subduction zone extension followed by basin inversion and regional deformation (Jones et al., 2010; Holland et al., 2020).

Tectonism contemporaneous with that in the Mazatzal Province is widely distributed across southern Laurentia (Duebendorfer et al., 2015; Papapavlou et al., 2017). Magmatism was also extensive throughout other provinces at this time, with numerous plutonic intrusions in the Yavapai and Mojave Provinces between ca. 1.70–1.62 Ga (Reed et al., 1987; Karlstrom et al., 1987; Jones et al., 2010; Wooden et al., 2012; Moscati et al., 2017; Holland et al., 2018). In addition, the Labradorian orogeny in northeastern Laurentia is contemporaneous with the Mazatzal orogeny (Papapavlou et al., 2017), and includes similarly-aged rock units located within the Grenville Province discussed below.

The relationship between crust-forming processes within the Mazatzal Province and tectonism within and surrounding it is poorly understood. Many of the structures previously attributed to deformation during the ca. 1.65–1.60 Ga Mazatzal orogeny are now believed to have formed during the Mesoproterozoic (ca. 1.49–1.35 Ga) Picuris orogeny (Doe et al., 2012; Daniel et al., 2013; Mako et al., 2015; Holland et al., 2020). Mesoproterozoic deformation and metamorphism is associated with ca. 1460–1370 Ma Granite-Rhyolite magmatism that extended into the Mazatzal Province (Fig. 3). Subsequent magmatism from ca. 1220 to 1080 Ma is primarily alkaline, and is attributed to extension prior to Grenville-aged tectonism on the southern margin of the province.

3.7. Granite-Rhyolite Province

The enigmatic Granite-Rhyolite Province comprises most of the known Proterozoic crust in the mid-continent region of southern Laurentia (Fig. 3). Due to thick Phanerozoic sedimentary cover, it is known primarily from drill cores and limited exposures (Sides et al., 1981; Barnes et al., 2002; Bickford et al., 2015). As its name suggests, the Granite-Rhyolite Province is composed of extensive ca. 1.5–1.3 Ga granitoids and felsic volcanic rocks of mainly ferroan composition (Sides et al., 1981; Bickford et al., 2015; du Bray et al., 2018). The province is broadly divided into two regions based largely on geochronological differences (Van Schmus et al., 1993). The eastern part is dominated by ca. 1.49–1.40 Ga magmatism, and is represented by 74 ages in our compilation. The southern part consists primarily of ca. 1.37–1.32 Ga rocks, and is represented by 72 ages in our compilation (Fig. 4). Rocks of both age groups are, however, locally present in both the eastern and southern parts (Bickford et al., 2015). Intrusive rocks of similar age and geochemical nature also occur in several of the other crustal provinces, from southwestern Laurentia through the midcontinent along a broadly northeasterly trend into northeasternmost Laurentia, where coeval intrusive rocks include anorthosite-mangerite-charnockite-granite complexes (Emslie et al., 1994), in some regions overprinted or reworked by Grenvillian orogenic deformation.

Magmatism associated with the Granite-Rhyolite Province is part of a regionally and globally significant event. Similar Mesoproterozoic magmatism extends into Antarctica and Baltica, and has been used to aid in Proterozoic supercontinent reconstructions (Anderson and Morrison, 2005; Goodge et al., 2008). Throughout the Yavapai, Mojave, and Mazatzal Provinces in southern Laurentia, ca. 1.48–1.38 Ga intrusions perforate older Paleoproterozoic rocks. Nd and Hf isotopic studies have shown that these coeval intracratonic magmas were derived in part from partial melting of older crust, with model ages roughly equal to the age of crust into which the plutons intrude (Bennett and DePaolo, 1987; Van Schmus et al., 1996; Goodge and Vervoort, 2006; Wooden et al., 2012).

The tectonic significance of Mesoproterozoic magmatism in Laurentia (and Baltica) has long been debated. The ferroan geochemistry of these magmas is generally considered to preclude a subduction-related origin, yet many workers invoke extensional processes in an overall convergent margin setting (Anderson and Morrison, 2005; Slagstad et al., 2009; Bickford et al., 2015; du Bray et al., 2018). In western Laurentia, Mesoproterozoic plutons are now known to be coeval with regionally extensive intracratonic deformation and metamorphism during the 1.49–1.35 Ga Picuris orogeny (Daniel et al., 2013; Mako et al., 2015; Aronoff et al., 2016; Holland et al., 2020).

3.8. Grenville Province

The Grenville Province extends along the entire southeastern margin of Laurentia, but is best exposed in its northeastern (Canadian) part, from where most of our geochronological data are derived (n = 350). It includes juvenile accretionary arc rocks as old as 1.85 Ga (Figs. 3 and 4) (e.g. Barillia and Algonquinian domains; Dickin, 2000; Gower et al., 2008). The US Grenville-aged rocks are mainly exposed in the Adirondack Mountains (n = 19) and the Llano uplift in Texas (n = 74; plotted separately in Fig. 4). Grenvillian inliers within the Appalachians have been excluded from the compilation, since they may be of exotic, non-Laurentian origin (Loewy et al., 2003; Fisher et al., 2010). In addition, there are plutonic intrusions, mostly with ages at, or slightly below, 1100 Ma, scattered in other geological provinces in the central and western USA far to the northwest of the Grenville Province, such as the ca 1090 Ma Pikes Peak batholith in the Yavapai Province in Colorado. These have been plotted together with other data from the province in which they intrude in Fig. 4.

Altogether, the Grenville Province represents a protracted accretionary history from 1800 to 1300 Ma along the margin of Columbia, followed by 350 million years of continued accretion and final collision, from 1300 to 950 Ma (Grenville orogeny *sensu strictu*), leading to the amalgamation of Rodinia.

The Labradorian orogeny ranged from ca. 1710 Ma to ca. 1600 Ma and included widespread juvenile, Andean-style felsic magmatism (Trans-Labrador batholith) around 1650 Ma (Gower et al., 1992, 2008: Gower and Krogh, 2002) which forms a prominent peak in Fig. 4. This orogeny likely represents an accretionary history that encompasses island arc formation and subsequent accretion (Gower et al., 2008). It is coeval with the Mazatzal orogeny in southwest Laurentia.

This is followed by another sharp peak at 1500 Ma, representing the Pinwarian orogeny, and a few more subdued peaks between 1460 and 1300 Ma, sometimes referred to as Elsonian (Gower and Krogh, 2002; Fig. 4). The Mesoproterozoic Pinwarian orogeny metamorphosed and

intruded Paleoproterozoic crust with voluminous plutons at ca. 1.50 Ga. Continuous magmatism from 1.50 to 1.30 Ga is suggested to be the result of a long-lived southeast-facing arc along the Laurentian margin (e.g. Rivers and Corrigan, 2000). This is supported by the juvenile nature of the magmatism (1.55 Ga Nd model ages; Dickin, 2000). It has been suggested that the Pinwarian-Elsonian belt is continuous with the Granite-Rhyolite Province (e.g. Rivers, 2008). The Elsonian phase of magmatism (ca. 1460–1300 Ma) coincides with early anorthosite-mangerite-charnockite-granite (AMCG) emplacement (Michikamau, Mistastin and Harp Lake complexes) and later magmatism including the Mealy dykes and other granitoids.

The Grenville orogeny proper can be considered to start at ca. 1300 Ma, and has been divided into four tectonic episodes - pre-collisional, Andean-style Elzevirian (ca. 1260–1220 Ma), arc accretion-collision Shawinigan (1200–1150 Ma), continent-collisional Ottawan (1090–1030 Ma), and post-orogenic Rigolet (1030–950 Ma), all visible as more or less separate peaks (in the case of the Rigolet phase a triple peak) in Fig. 4. Peak metamorphism occurred by ca. 1090 Ma (e.g. Rivers, 1997, Rivers et al., 2002; McLelland et al., 1996). Additionally, there is a recognized period of AMCG magmatism from ca. 1180 to 1130 Ma (McLelland et al., 1996) that forms part of the Shawinigan peak in the diagram.

In northeastern Laurentia, the Canadian Grenville Province proper and the Adirondack Mountains expose much of the infrastructure of the orogen. Grenville-aged intrusive rocks in inliers of the southern Appalachians (south of New York, USA) have unique isotope systematics compared to the Canadian Grenville Province, Adirondacks, northern Appalachian inliers, and Llano uplift. The Pb isotope signatures of these ca. 1.3–1.0 Ga rocks are more similar to Amazonian Grenville-aged rocks (Loewy et al., 2003; Fisher et al., 2010). Thus, it is likely that the Grenville basement in the southern Appalachian inliers is exotic to Laurentia and was accreted during the amalgamation of Rodinia (Tohver et al., 2004a), and it has thus been excluded from this compilation.

Further southwest, the Llano uplift in Texas and basement uplifts to the west and south into Mexico (Mosher, 1998; Bickford et al., 2000) are the southernmost known components of the Grenville in Laurentia. In the Llano uplift proper, both pre-to-early Grenville rocks and Grenville-age rocks proper are preserved (Fig. 4). The eastern portion contains a likely exotic ca. 1300–1200 Ma continental margin arc assemblage and adjacent ophiolite assemblage accreted during Grenville orogenesis (Mosher et al., 2008 and references therein). Accretion was followed by

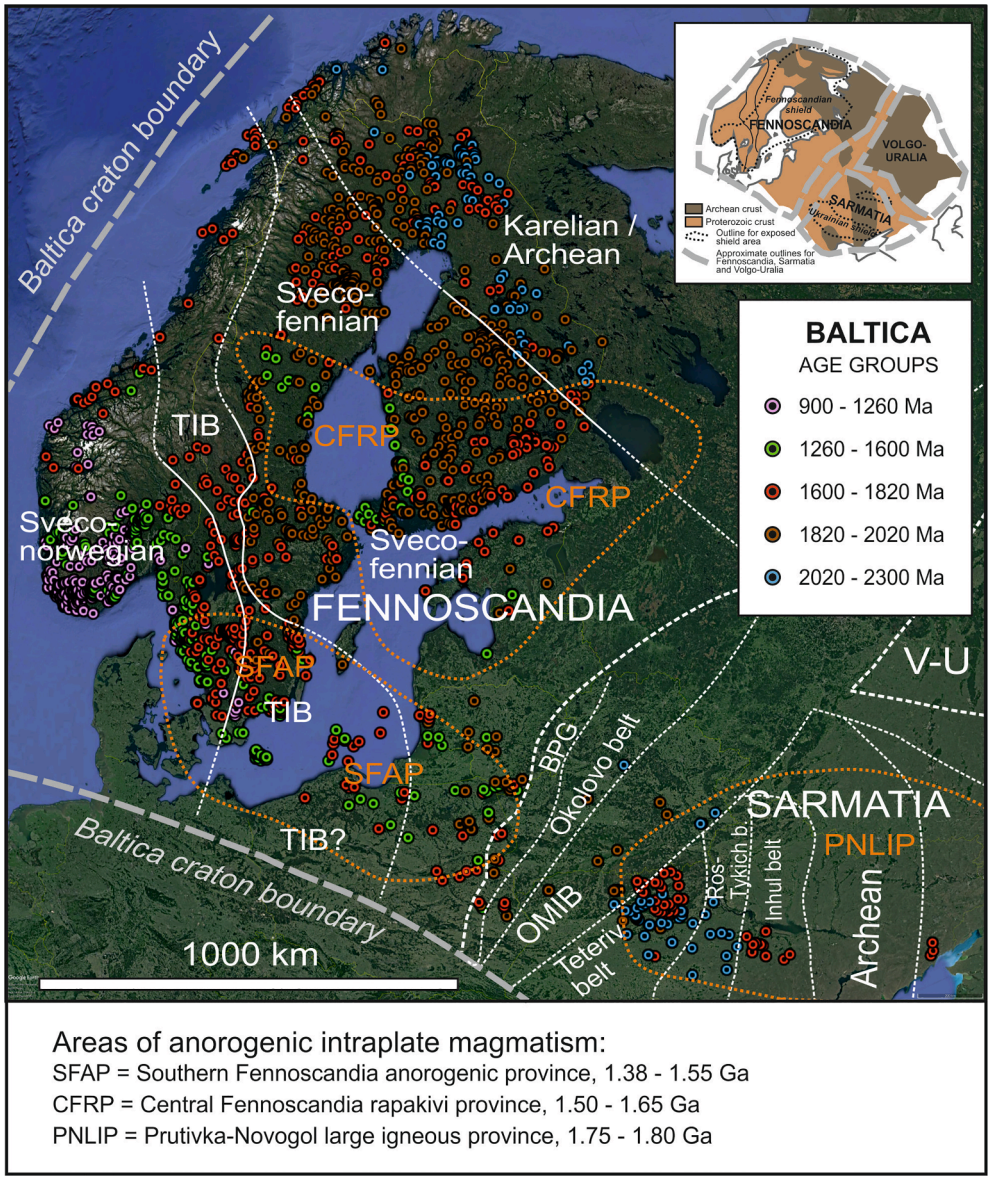

Fig. 5. Google Earth map of Baltica with main Proterozoic geological provinces and magmatic U-Pb age data points indicated. Dashed white lines are concealed or otherwise uncertain boundaries. Thick dashed grey line marks the approximate cratonic boundary of Baltica. V-U = Volgo-Uralia; OMIB = Osnitsk-Mikashevychi Igneous Belt; BPG = Belarus-Podlasie Granulite Belt; TIB = Transscandinavian Igneous Belt. Dotted orange lines show approximate outlines of anorogenic intraplate magmatic provinces: PNLIP = Prutivka-Novogol large igneous province (1.80–1.75 Ga); CFRP = Central Fennoscandia rapakivi province (1.65–1.50 Ga); SFAP = Southern Fennoscandia anorogenic province (1.55–1.38 Ga). The latter also includes area of penecontemporaneous Hallandian magmatism within the Eastern Segment of the Sveconorwegian Orogen. Inset map shows Fennoscandia, Sarmatia and Volgo-Uralia as parts of Baltica, and their exposed parts (Fennoscandian and Ukrainian Shields, including Voronezh massif).

attempted subduction of the Laurentian margin and slab break-off. Subsequent upwelling of the asthenosphere led to intrusion of juvenile granitoids at ca. 1120–1070 Ma, and terminal collision with associated high-pressure metamorphism (Mosher et al., 2008).

Models of Grenville orogenesis envisage it to be a large, hot orogen (e.g. Rivers, 2008), long in duration and leading to massive crustal shortening, especially in the northern, Canadian sector, where rocks spanning some 900 million years (ca. 1800–900 Ma) have been juxtaposed. Large volumes of melt were generated during crustal thickening and anatexis, and resulted in voluminous additions of crustal material.

4. Baltica data and results

4.1. Geological overview

Baltica, also known as the East European Craton (EEC), consists of the northeastern half of present-day Europe to the NE of the Trans-European Suture Zone. It comprises three proto-cratons: Fennoscandia in the west, Sarmatia in the southeast, and Volgo-Uralia in the northeast (Gorbatschev and Bogdanova, 1993; inset in Fig. 5). Sarmatia and Volgo-Uralia collided at around 2.1 Ga along the Volga-Don orogen (e.g. Shchipansky et al., 2007; Bibikova et al., 2009; Terentiev and Santosh, 2020; Terentiev and Santosh, 2020, and references therein), and the combined Volgo-Sarmatia craton collided with Fennoscandia along the Central Russian orogen and its southerly continuation, the Osnitsk-Mikashevychi Igneous Belt (OMIB) at around 1.8 Ga (Gorbatschev and Bogdanova, 1993; Shumlyanskyy, 2014; Bogdanova et al., 2015), forming the combined Baltica paleocontinent.Fig. 6a.

The Fennoscandian (Baltic) Shield is exposed in Sweden, Norway, Finland, and adjacent parts of Russia (Kola peninsula and Karelia), whereas unexposed parts of Fennoscandia covered by younger rocks occur beneath Denmark, northernmost Germany, northeastern Poland

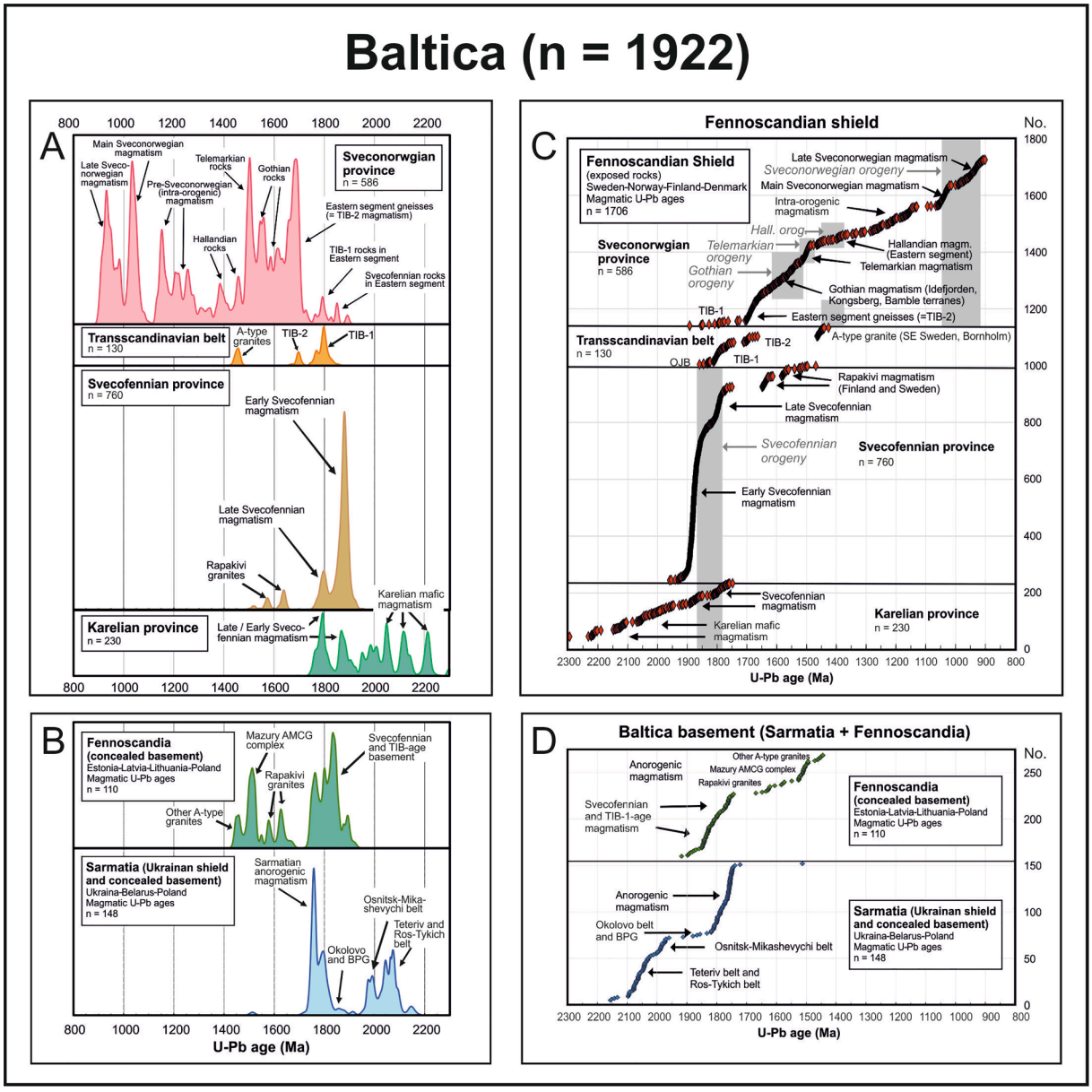

Fig. 6. A. Relative probability curves of magmatic U-Pb ages between 2300 and 800 Ma from the exposed Fennoscandian shield. **B.** Relative probability curves of magmatic U-Pb ages between 2300 and 800 Ma from the concealed parts of Fennoscandia and from Sarmatia. **C.** Cumulative age diagrams for the different parts of the exposed Fennoscandian shield. **D.** Cumulative age diagrams for the concealed parts of Fennoscandia and for Sarmatia. Note that the age axes in panels C and D are reverse compared to in panel A and B.

and the Baltic countries, as well as beneath the Scandinavian Caledonides in Sweden and Norway. The shield consists of an Archean core in the northeast (Kola and Karelia protocratons), with Proterozoic orogenic belts in its central and southwestern parts, younging towards the southwest (e.g Gorbatschev and Bogdanova, 1993). Shorter overview articles of Fennoscandia have been written by Nironen (1997), Korja et al. (2006), and Lahtinen et al. (2005, 2008), while the geology of Sweden has been compiled by Stephens and Bergman Weihed (2020), that of Finland by Lehtinen et al. (2005), and that of Norway by Ramberg et al. (2008).

Sarmatia is exposed in the smaller Ukrainian Shield and Voronezh Crystalline Massif, but otherwise only known through drill cores and geophysics. It is dominated by Archean and early Paleoproterozoic rocks, rimmed by slightly younger Paleoproterozoic orogens in the northeast (Volga-Don Orogen, 2.2 – 2.05 Ga; Terentiev et al., 2016) and the northwest (Teteriv Orogenic Belt, Osnitsk-Mikashevychi Igneous Belt, Okolovo Belt and Belarus-Podlasie Belt, 2.1 – 1.8 Ga; Bogdanova et al., 2015, 2016; Shumlyanskyy et al., 2018, 2021). The Okolovo and Belarus-Podlasie belts form part of the collision zone between Sarmatia and Fennoscandia, and may alternatively be included in Fennoscandia (as in the Polish basement map by Krzeminska et al., 2017), but for practical reasons data points from these belts have been included here with the Sarmatia data. Volgo-Uralia is entirely covered by younger sedimentary rocks, but from studies of drill core material, it appears to be totally dominated by Archean rocks (Bogdanova et al., 2010, 2016).

In the present context, we are only concerned with the dominantly accretionary Proterozoic orogens in southwestern Baltica, and younger anorogenic or intraplate rocks within those orogens. This includes the Svecofennian (a.k.a. Svecokarelian) Orogen in central Fennoscandia, the Transscandinavian Igneous Belt (TIB), and the Sveconorwegian Orogen in southwest Fennoscandia, and their southwards continuations in the concealed basement beneath the southern Baltic Sea, Estonia, Latvia, Lithuania, northeast Poland and Denmark (Fig. 5). Karelian (early Paleoproterozoic) and Svecofennian intrusive rocks within the Archean Karelian Province in northeast Finland have also been included, but not the internal collisional 1.9 Ga Lapland-Kola belt between the Archean Kola and Karelia protocratons. Younger anorogenic intrusions within each province, such as rapakivi massifs within the Svecofennian Province of central Fennoscandia, have been included and plotted within the province in which they occur. From Sarmatia, the Paleoproterozoic belts along its western margin in Ukraine, Belarus and Poland, and younger anorogenic granite intrusions within that area, are included, but not Paleoproterozoic rocks further east (Fig. 5). Volgo-Uralia is not included in our study.

Relevant U-Pb ages from Baltica on a simplified geological map are plotted in Fig. 5, with relative probability curves and corresponding cumulative age diagrams shown in Fig. 6.

4.2. Sarmatia

The oldest Baltica ages in our compilation (disregarding the dominantly mafic Karelian magmatism in northeast Fennoscandia) are from the western margin of Sarmatia, consisting of a peak representing the Teteriv and Ros-Tykich Belts between 2.16 and 2.02 Ga (n = 43), and a second peak at 2.04 to 1.95 Ga representing the Osnitsk-Mikashevychi Belt (n = 23; Figs. 4 and 5). A few ages from the Okolovo Belt and Belarus-Podlasie Granulite Belt (BPG) in eastern Poland (n = 17) scatter between 1.98 and 1.78 Ga, with one older and one younger outlier. At this time, Sarmatia (and Volgo-Uralia) had not yet joined Fennoscandia to form a coherent Baltica.

Another major peak from Sarmatia at 1.82 to 1.75 Ga (n = 65) represents intraplate anorogenic magmatism, such as the Korosten and Korsun-Novomyrhorod plutons and related mafic dykes, which were emplaced at the approximate time of Sarmatia – Fennoscandia collision (Bogdanova et al., 2013; Shumlyanskyy et al., 2013, 2016a, 2016b, 2017, 2021). This magmatism was referred to as the Prutivka-Novogol large igneous province by Shumlyanskyy et al. (2021; Fig. 5). It overlaps in time with the TIB-1 magmatic phase of the Transscandinavian Igneous Belt in Fennoscandia (see below). There is no subsequent magmatic activity within the Sarmatian part of Baltica during our time of interest.

4.3. Svecofennian Orogen

The geology and evolution of the Swedish part of the Svecofennian (in their terminology the Svecokarelian) Orogen have been described in several chapters in Stephens and Bergman Weihed (2020), with overviews presented by Stephens and Bergman (2020) and Stephens (2020). Examples of relatively recent papers with discussions of Finnish geology and geochronology are Huhma et al. (2011) and Lahtinen et al. (2015a, 2015b, 2016). Geotectonic models for the Svecofennian orogeny range from purely accretionary (Hermansson et al., 2008; Stephens, 2020) to collisional (Lahtinen et al., 2005; Korja et al. 2006) or combinations of accretion and oblique collision with Sarmatia (Bogdanova et al., 2015).

In the exposed part of Fennoscandia, Karelian magmatism within the Archean Karelian protocraton in northeast Finland occurred in several pulses between 2.5 and 2.0 Ga. It is strongly dominated by mafic rocks (layered intrusions, gabbros, dolerite dyke swarms and mafic volcanics; Figs. 4 and 5). Early Svecofennian magmatism began at ca. 1.95 Ga and shows a major peak between 1.90 and 1.85 Ga (n = 541; Fig. 6). This peak represents felsic to intermediate volcanic and intrusive activity in a large area of subduction-related crustal growth in central Fennoscandia, encompassing southwestern Finland, northern and central Sweden, but also Svecofennian intrusions within the Archean craton in northeast Finland and northernmost Norway. Its height reflects both the size of this area (approximately 940 000 km^2, including intervening sea areas and concealed basement areas) and the large number of U-Pb age determinations carried out in these parts of Sweden and Finland, not the least because of its importance as host for major iron and sulfide ore deposits (Bergslagen, Skellefte and Norrbotten districts in Sweden, and the Savo, Outokumpu and Orijärvi districts in Finland; Hanski, 2015).

Following a clear minimum, representing a quieter 'intra-orogenic' phase, a second peak of late-orogenic Svecofennian magmatism is seen in Fig. 6 at around 1.8 Ga (n = 218). This magmatism includes both anatectic pure granites (the Granite-Pegmatite suite of Stephens et al. (2009) and Stephens and Bergman Weihed (2020)) that could be related to crustal thickening during the collision between Fennoscandia and Sarmatia, and more varied and alkali-rich intrusions referred to as the Granitoid-Syenitoid-Dioritoid-Gabbroid suite by the same authors. Such intrusions do not only occur within the Svecofennian Province *sensu stricto*, but also within the Archean Karelian Province in northeast Finland (Fig. 5).

4.4. Transscandinavian Igneous Belt

Magmatism within the Transscandinavian Igneous Belt (TIB), which stretches some 1400 km along the western margin of the Svecofennian Province from southeastern Sweden across central Sweden and then beneath the Caledonian nappes to the Lofoten archipelago in northern Norway (Högdahl et al., 2004), was divided into a 1.81 – 1.76 Ga TIB-1 phase, a 1.71 – 1.69 Ga TIB-2 phase, and a 1.67 – 1.65 TIB-3 phase by Larson and Berglund (1992), based on early U-Pb dating. The TIB-2 and TIB-3 phases have subsequently been merged into a continuous 1.71 – 1.66 Ga TIB-2/3 phase, whereas an earlier, minor TIB-0 phase at around 1.85 Ga, consisting of granitoids along the southwestern Svecofennian boundary to the TIB in south-central Sweden, has been recognized (cf. Högdahl et al., 2004). The TIB dominantly consists of largely undeformed granitoids and volcanic rocks (porphyries) having I- to A-type

alkali-calcic geochemistry (Granitoid-Syenitoid-Dioritoid-Gabbroid type in the classification of Stephens et al. (2009) and Stephens and Bergman Weihed (2020)), interpreted to be related to renewed subduction beneath the Andean-type continental margin in the present-day west.

In the more recent subdivisions of the Swedish bedrock by the Geological Survey of Sweden (SGU), shown on the 1:1 million geological map of Sweden by Bergman et al (2012), and also in Stephens and Bergman Weihed (2020), the Transscandinavian Igneous Belt is not distinguished as a separate unit, since it is not an orogenic province. Instead, the TIB-0 and TIB-1 rocks are included within the Svecofennian (in their terminology Svecokarelian) Province (Wahlgren and Stephens, 2020a), whereas the TIB-2 rocks are grouped with other younger units as "post-Svecokarelian rocks" (Ripa and Stephens, 2020a). As can be seen in Fig. 6, the 1.81–1.76 Ga TIB-1 magmatism (n = 84) clearly overlaps in time with the late Svecofennian magmatism, forming a joint peak in combined diagrams, perhaps reflecting the complex geotectonic situation during this period with penecontemporaneous collision with Sarmatia from the southeast, and renewed subduction from the west.

Following the TIB-1 magmatism, including here also the 1.77 – 1.75 Ga magmatism in Blekinge in southeasternmost Sweden (n = 16; Johansson et al., 2006; Johansson, 2016; Wahlgren and Stephens, 2020b), there was a magmatic gap with very limited activity until the TIB-2 (or TIB-2/3) magmatism starting at 1.71 Ga (n = 21). Within the Transscandinavian Belt *sensu stricto*, this is mainly confined to the 1.71 – 1.68 Ga Dala-Rätan region in west-central Sweden (Lundqvist and Persson, 1999; Högdahl et al., 2004; Ripa and Stephens, 2020a), whose well-preserved granites and porphyries have an intraplate, anorogenic character and may be regarded as precursors to the classical rapakivi magmatism further east. However, U-Pb dating in recent decades has shown that the bulk of granitoid gneisses within the Eastern Segment of the Sveconorwegian Orogen further southwest also have ages between 1.71 and 1.65 Ga and could be regarded as strongly deformed TIB-2 granitoids (cf. Stephens and Wahlgren, 2020a, and references therein). In Figs. 4 and 5, the latter rocks are, however, included within the Sveconorwegian Orogen, and not within the Transscandinavian Belt.

4.5. The basement beneath Estonia, Latvia, Lithuania, and Poland

In the concealed basement beneath Estonia, Latvia, Lithuania, and northeast Poland, it is difficult to make a clear distinction between rocks belonging to the Svecofennian Orogen and those of the Transscandinavian Igneous Belt, since the ages overlap, the rocks may occur intermixed in some places, all rocks have undergone regional deformation and metamorphism as deduced from drill core observations, and boundaries between geological units can not be mapped out. However, there is a marked tendency for older (Svecofennian) rocks to occur in the north and east, within the basement of Estonia, Latvia, central and eastern Lithuania and eastern Poland (along the boundary to Sarmatia), while younger rocks that may tentatively be assigned to the TIB predominate in southwestern Lithuania and northwest Poland (Fig. 5).

The main early Svecofennian peak at 1.90 to 1.86 Ga is only represented by nine data points in this region, largely because of lack of age-data from these rock units, especially in Estonia and Latvia. Hence, the curve seen for the Fennoscandian basement in Fig. 6 may not be very representative. The magmatic peak around 1.85 to 1.82 Ga (n = 25; Fig. 6) is dominated by age data from Lithuania (cf. Skridlaite et al., 2021) and northeast Poland where such rocks are abundant. Possibly, this reflects a southwards migration of subduction-related magmatism and crustal formation from central to southern Fennoscandia. In Poland, there is a continuum of ages down to 1.75 Ga (n = 33), mostly coming from rocks which could be considered to belong to a southwards continuation of the TIB (Fig. 4 and 5). Most of the youngest ages are found in Pomerania in northwest Poland, a region that may be correlated with the Blekinge region in southeast Sweden (Krzeminska et al., 2021).

4.6. Anorogenic intraplate magmatism

Within the Svecofennian Province and the Transscandinavian Belt, there are much younger (1.65–1.44 Ga) intraplate intrusions that could be considered anorogenic, since they have a typical A-type geochemistry and are 200 to 300 million years younger than their surrounding rock units and any associated orogenic deformation (cf. Andersson et al., 2002; Ripa and Stephens, 2020b; Wahlgren and Stephens, 2020b). Nevertheless, like in Laurentia (cf. Bickford et al., 2015, and references therein), they may have a distant relationship to orogenic activity along the continental margin in the west or southwest. For the rapakivi granites within the Svecofennian Province in central Fennoscandia, such a distant relationship with the Gothian activity in southwest Fennoscandia was suggested by Åhäll et al. (2000), and for the Danopolonian magmatism in southern Fennoscandia (Bogdanova, 2001) a similar link with the Hallandian event in southwest Sweden may be envisaged.

The classical rapakivi magmatism came in two distinct pulses, visible both in the exposed parts of Fennoscandia (intrusions in southern Finland and adjacent parts of Russia (Rämö and Haapala, 2005), in central Sweden (Persson, 1999; Andersson et al., 2002; Ripa and Stephens, 2020b)) and in the concealed basement of Estonia and Latvia (Rämo et al., 1996; Soesoo et al, 2004; Soesoo and Hade, 2012) (Fig. 4 and 5). The first pulse at 1.65 to 1.60 Ga (n = 43) includes the large Viborg intrusion across the Finnish-Russian border, as well as several smaller rapakivi-type granite intrusions in the basement of Estonia (Soesoo et al, 2004, Soesoo et al., 2020). The second pulse at 1.60 to 1.55 Ga (n = 38, including a tail down to 1.50 Ga) includes the Salmi intrusion in Russian Karelia (not included here), the Laitila and Åland intrusions in southwest Finland (Suominen, 1991), and the large Riga intrusion in the basement of Latvia and Estonia (Rämo et al., 1996). The rapakivi-type intrusions in central Sweden, such as Ragunda (Persson, 1999) and Nordingrå, also belong to this age group, but trend down to even younger ages around 1.50 Ga.

The younger group overlaps in age with the large, E-W-elongated Mazury AMCG-complex in the basement of northeast Poland, southern Lithuania, the Kaliningrad area, and western Belarus, which has U-Pb ages between 1.50 and 1.55 Ga (n = 13; Figs. 4 and 5; Dörr et al., 2002; Morgan et al., 2000; Skridlaite et al., 2003, 2008; Wiszniewska and Krzeminska, 2021). This magmatism is, however, not traditionally included within the rapakivi suite, but rather the Mesoproterozoic Danopolonian magmatism of southern Fennoscandia (Bogdanova, 2001). Most remaining granitic intrusions within the latter group, in southeast Sweden, the Danish island of Bornholm, and in the basement of Lithuania, northern Poland and the southern Baltic Sea, fall in a relatively narrow age range of 1.44 to 1.46 Ga (n = 43; Figs. 4 and 5). Whereas the rapakivi granites of central Fennoscandia have been plotted together with the Svecofennian Province in Fig. 6, since they are hosted by rocks of this province, the Danopolonian intrusions are dominantly hosted by rocks belonging to the Transscandinavian Igneous Belt or its southerly prolongation, and have been plotted together with the TIB.

4.7. Sveconorwegian Orogen

The Sveconorwegian Orogen encompasses southwest Sweden and southern Norway, and presumably also constitutes the concealed basement of Denmark (cf. Olivarius et al., 2015). Related rocks are found in the Western Gneiss Region of western Norway, west of the Caledonian nappes (Fig. 5). It is composed of five N-S-trending lithotectonic units, separated by crustal-scale shear zones and affected by the late Mesoproterozoic to early Neoproterozoic (1.15 – 0.9 Ga) Sveconorwegian orogeny. Most of the rocks in the orogen are substantially older than the Sveconorwegian orogeny and have been affected by earlier Mesoproterozoic orogenic events. In this regard, the Sveconorwegian Orogen is different in character from the mostly juvenile Svecofennian orogenic province. The oldest rocks within each lithotectonic unit show a younging tendency towards the west. Reviews of the geology and

evolution of the Sveconorwegian Orogen are found in Bingen et al. (2008b, 2021), Roberts and Slagstad (2015), Stephens et al. (2020) and Stephens and Wahlgren (2020b).

The bedrock in the easternmost of these units, referred to as the Eastern Segment, contains some reworked Svecofennian and TIB-1 rocks (n = 17), but is dominated by granitoid gneisses with ages between 1.73 and 1.66 Ga (n = 82), which have in recent years been correlated with the TIB-2 phase within the neighboring Transscandinavian Igneous Belt (cf. Appelquist et al., 2011; Stephens et al., 2020), with which it forms overlapping age peaks (Fig. 6). This magmatism has been interpreted to mark renewed subduction along the western continental margin of Fennoscandia after a period of quiescence (Stephens and Wahlgren, 2020a).

The Eastern Segment is juxtaposed in the west against the Idefjorden lithotectonic unit (formerly known as the Western segment), followed west of the Permian Oslo rift by the smaller Kongsberg and Bamble lithotectonic units. Subduction-related magmatism in these units started at 1.66 Ga, and continued until ca. 1.50 Ga (n = 121), accompanied by deformation (Bingen and Viola, 2018; Bergström et al. 2020; Bingen et al., 2021). This orogenic event is known as the Gothian orogeny. As mentioned above, it overlaps in time with the rapakivi magmatism in central Fennoscandia.

Gothian magmatism lasted for about 150 million years, with two or three different sub-peaks visible in the age data. It was as long-lived as the Svecofennian magmatism but encompassed a much smaller geographic area. Gothian magmatism, metamorphism and deformation are restricted to the Idefjorden, Kongsberg and Bamble lithotectonic units, and not seen in the Eastern Segment, suggesting some degree of separation between these crustal units in the Mesoproterozoic. The southern part of the Eastern Segment in southern Sweden instead was affected by Hallandian magmatism, metamorphism and deformation at 1.46 to 1.37 Ga (Stephens and Wahlgren, 2020a), an event that, on the other hand, is not seen in the more westerly terranes. Hallandian magmatism in the Eastern Segment appears to come in two pulses, at around 1.45 Ga (overlapping with the intraplate Danopolonian magmatism further east in Fig. 6), and around 1.38 Ga. However, this pattern could be an artefact of relatively few age data (n = 31) from a limited area.

The tectonic setting of the Hallandian and Danopolonian events and the relationship between them has been a controversial issue in Fennoscandian geology (cf. Bogdanova et al., 2008; Ulmius et al., 2015). On the one hand, the Danopolonian granites in the east are mostly undeformed and have an intraplate setting and A-type geochemistry (e.g. Johansson et al., 2016). On the other hand, some (but not all) of the Danopolonian Bornholm granites were pervasively deformed into gneisses penecontemporaneously with their formation around 1.45 Ga (Johansson et al., 2016), and they are closely related in time and space to the Hallandian metamorphism and deformation further west. It may be that the strong deformation at Bornholm occurred along an intraplate shear zone that is only seen on this island. It may also be that the Danopolonian A-type granites east of the Sveconorwegian Front / Protogine Zone (the eastern boundary of the Eastern Segment and the Sveconorwegian Orogen in southern Sweden) are upper crustal manifestations of the Hallandian melting and metamorphism seen west of this zone in the Eastern Segment, which represents a deeper crustal section.

West of Kongsberg and Bamble, the Telemarkia lithotectonic unit encompasses most of southern Norway. Crustal formation in Telemarkia appears to start with a short but intense pulse of magmatism at 1.52 – 1.48 Ga, seen as a relatively sharp peak in Fig. 6 (n = 39). This magmatism is spatially zoned with a volcanic arc signature westwards (Suldal arc) and a back-arc rift signature eastwards (Rjukan rift) (Bingen et al., 2005; Roberts et al., 2013). In Fig. 6, the Telemarkian event fills the gap between the Gothian and Hallandian events further east.

After these events, the future Sveconorwegian Orogen underwent several periods of intraplate magmatism. In the Idefjorden lithotectonic unit, the N-S-trending Kungsbacka bimodal suite intruded between 1.36 and 1.30 Ga (n = 8; Bergström et al., 2020). In the Eastern Segment, bimodal magmatism was mainly confined to an extensional event along the future Sveconorwegian Front / Protogine Zone (also N-S-trending) at 1.22 to 1.20 Ga (n = 9; cf. Stephens and Wahlgren, 2020a). In southern Norway (Telemarkia, Kongsberg and Bamble), several pulses of Pre-Sveconorwegian magmatism took place between 1.28 and 1.13 Ga (n = 72; Fig. 6) (Andersen et al., 2007; Bingen et al., 2003; Bingen and Viola, 2018; Brewer et al., 2004; Bingen et al., 2021). The last pulse between 1170 and 1130 Ma overlaps with the first phase of Sveconorwegian high-grade metamorphism restricted to the Bamble and Kongsberg lithotectonic units, which culminated in granulite-facies conditions between 1150 and 1120 Ma (Bingen and Viola, 2018; Bingen et al., 2021). A magmatic hiatus is observed over the entire orogen between 1130 and 1065 Ma.

The main Sveconorwegian orogeny took place between ca. 1065 and 910 Ma and it is characterized by convergent tectonics and high-grade metamorphism between ca. 1050 and 930 Ma. Several peaks of regional metamorphism are recorded, with an increasingly high-pressure signature eastwards in the orogen (Bingen et al., 2008a; Laurent et al., 2018; Möller et al., 2015, Möller and Andersson, 2018; Söderlund et al., 2008). These are high-pressure granulite-facies in the Idefjorden lithotectonic unit at ca. 1050 Ma, ultra-high-temperature granulite-facies in the Telemarkia lithotectonic unit (Rogaland) between 1030 and 1000 Ma, granulite- and locally eclogite-facies metamorphism in the Eastern Segment at ca. 990 Ma, and renewed ultra-high temperature - low pressure granulite-facies metamorphism in Telemarkia at ca. 930 Ma (cf. Bingen et al., 2021).

Sveconorwegian syn-orogenic magmatism increases dramatically in volume westwards in the orogen (Coint et al., 2015; Granseth et al., 2020; Vander Auwera et al., 2011). It is divided into three main magmatic suites: the (high-K) calc-alkaline Sirdal Magmatic Belt between 1065 and 1020 Ma (n = 64), the ferroan hornblende-biotite granite suite between 985 and 920 Ma and the AMCG-type Rogaland anorthosite complex between 935 and 915 Ma (n = 66 for the two latter combined). In the Eastern Segment, Sveconorwegian magmatism is restricted to some granitic and pegmatitic dykes with ages around 950 Ma (n = 6). In the other units, unfoliated pegmatite fields close the orogeny between 915 and 900 Ma. In Fig. 6, the Sveconorwegian magmatism forms a double peak with a trough at around 1000 Ma, where the first peak (Main Sveconorwegian magmatism) represents the Sirdal Belt, and the second peak (Late Sveconorwegian magmatism) constitutes the two later suites combined.

Three main geodynamic models have been proposed for the Sveconorwegian orogeny: (1) collision between Baltica and another major continent with all lithotectonic units endemic to Baltica (Li et al., 2008; Bingen et al., 2008b, 2021; Cawood and Pisarevsky, 2017), (2) collision between Baltica and a landmass consisting of the four western lithotectonic units of the orogen (Sveconorwegia) (Petersson et al., 2015; Möller and Andersson, 2018), and (3) a non-collisional (Andean) orogeny (Slagstad et al., 2013, 2017, 2018, 2020). In the first model, one or several oceanic basins closed to the west of the exposed orogen, followed by collision between Baltica and another major plate at ca. 1065 Ma (which corresponds to the start of the main syn-orogenic magmatism and metamorphism). In the second model westwards subduction of an oceanic plate below the four western lithotectonic units is followed by closure of ocean basins between them (the Eastern Segment and the Idefjorden unit, and/or the Idefjorden and Telemarkia units) and underthrusting of the Eastern Segment to granulite- and eclogite-facies conditions at ca. 990 Ma. In the third model, orogeny is controlled by long-lived east-dipping subduction of an oceanic plate below Baltica from at least 1150 to after 900 Ma.

After 900 Ma, magmatic activity ceased within Fennoscandia and Baltica, and did not resume until 620 Ma with mafic dykes heralding opening of the Iapetus Ocean. This 300 million year magmatic lull is best explained by the southwestern Fennoscandian margin of Baltica being trapped in an inboard continental position within Rodinia after continent–continent collision along the Grenville-Sveconorwegian-Sunsas belt.

4.8. Comparison between orogenic and intraplate magmatism in Baltica

Fig. 7 provides a comparison between (mainly) orogenic magmatism along the continental margin of Fennoscandia/Baltica from 2000 to 900 Ma, and anorogenic intraplate magmatism during the same period. The latter includes the 1.80–1.75 Ga Sarmatian anorogenic magmatism (Prutivka-Novogol SLIP), the 1.65–1.50 Ga Central Fennoscandia rapakivi province, and the Danopolonian 1.55–1.44 Ga Southern Fennoscandia anorogenic province (Mazury AMCG complex and younger A-type granites). Also the ca. 1.7 Ga TIB-2 magmatism of the Dala-Rätan complex in central Sweden, with its intraplate character, has been assigned to the anorogenic intraplate group, in contrast to the penecontemporaneous TIB-2 magmatism further west, in what is now the Eastern Segment of the Sveconorwegian Orogen. All magmatism within the Sveconorwegian Orogen was assigned to the orogenic group, for the sake of simplicity and because of its overall vicinity to the continental margin, although the inta-orogenic (pre-Sveconorwegian) magmatism during the 1300 to 1100 Ma time period, and the late Sveconorwegian Rogaland AMCG complex could perhaps equally well be assigned to the intraplate group.

As can be seen in Fig. 7, the early phase of Sarmatian anorogenic magmatism is penecontemporaneous with the main phase of TIB-1 magmatism along the Fennoscandian margin around 1.8 Ga, while the main Sarmatian phase coincides with the waning stages of TIB-1 magmatism at ca 1.75 Ga. The intraplate TIB-2 magmatism within the Dala-Rätan complex at 1.7 Ga naturally coincides with the TIB-2 magmatism within the Eastern Segment. The different pulses of rapakivi magmatism in central Fennoscandia (centered at 1.63, 1.57 and 1.50 Ga) may coincide with different pulses of Gothian magmatism along the continental margin, as proposed by Åhäll et al. (2000), although it is not that obvious from the present figure, where Gothian magmatism appears to be more continuous. Magmatism within the Mazury AMCG complex in NE Poland coincides in time with Telemarkian magmatism in southern Norway around 1.5 Ga, and the 1.45 Ga A-type Danopolonian granites in southern Fennoscandia with the early phase of Hallandian magmatism within the adjacent future-to-be Eastern Segment of the Sveconorwegian Orogen.

5. Amazonia data and results

5.1. Geological overview

Amazonia is a large crustal segment forming the core of South America. The exposed parts constitute the Guiana Shield and Central Brazil Shield, whose southwesterly extension is locally known as the Bolivian Shield. The central part of the craton is largely overlain by the Phanerozoic Amazonas sedimentary basin while the western and northern margins are overlain by Andean foreland basins. In the context

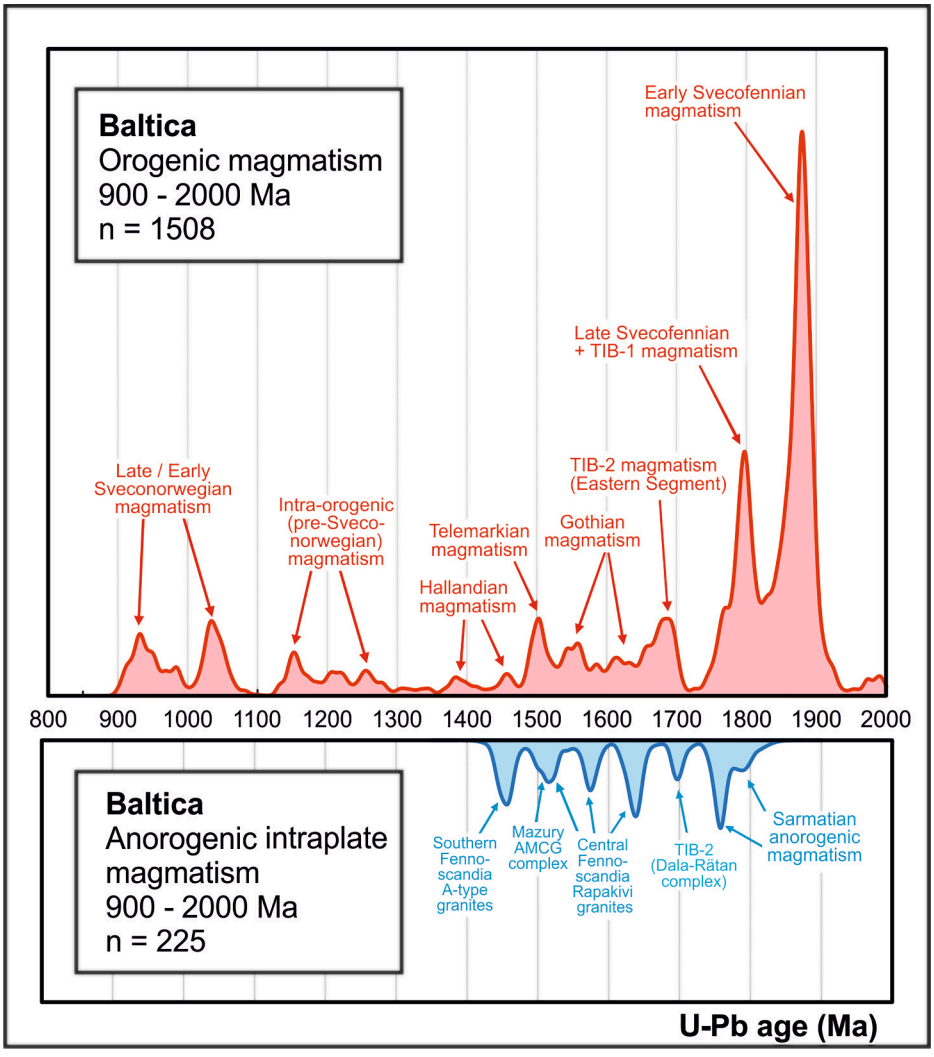

Fig. 7. Comparison of (mainly) orogenic magmatism along the active continental margin of Fennoscandia/ Baltica, and anorogenic intraplate magmatism in Baltica, during the 2000 to 900 Ma period.

of the Columbia and Rodinia supercontinents, Proterozoic Amazonia (i.e. the proto-Amazonian Craton) correlates well with the orogenic framework in West Africa, Laurentia, and Baltica, exemplified by accretionary-collisional belts, silicic large igneous provinces (SLIPs) and intraplate AMCG magmatism (Sadowski and Bettencourt, 1996; Cordani et al., 2009; Teixeira et al., 2019). This is also at least in part supported by the paleomagnetic evidence (e.g. D'Agrella Filho et al., 2016, 2020). However, the position of Amazonia in these supercontinents is still debatable, essentially due to the insufficient number of robust paleomagnetic poles on key units, but also to lack of geological and geochronological data from more remote and inaccessible areas.

Amazonia is composed of an Archean core in the east and several orogenic belts that are products of a long-lived accretionary-collisional regime in Proterozoic times (Cordani and Teixeira, 2007). Archean crust, partly reworked in Paleoproterozoic times, is apparent in the Guiana Shield, exemplified by the Imataca block and Amapá domain (Tassinari and Macambira, 1999; Borghetti et al., 2018; Milhomem Neto and Lafon, 2019). In the Central Brazil Shield the ancient core comprises the Carajás granite-greenstone domain, the Rio Maria granitoid domain and the adjoining Xingu-Iriri domain that together constitute the Central Amazonian Province (Tassinari and Macambira, 1999; Cordani and Teixeira, 2007; Oliveira et al., 2011; Almeida et al., 2017). These Archean domains are surrounded by the early Paleoproterozoic crust of the Maroni-Itacaiunas Province, largely formed during the 2.26 – 1.95 Ga Transamazonian orogeny, but also encompassing younger igneous rocks.

About half of the continental crust of the Amazonian Craton constitutes the Proterozoic Ventuari-Tapajós (2.01 – 1.80 Ga), Rio Negro-Juruena (1.82 – 1.60 Ga), Rondonian-San Ignacio (1.59 – 1.30 Ga), and Sunsas-Aguapeí (1.20 – 0.95 Ga) Provinces, located towards the southwest, as well as the peripheral Rio Apa Terrane (e.g. Cordani and Teixeira, 2007; Bettencourt et al., 2010; Teixeira et al., 2010, 2020; Scandolara et al., 2017). The tentative boundaries between these provinces, including the Archean core, are largely based on geological inferences, geochronological data, and Nd isotopic constraints. In addition, areas of three SLIPs (Orocaima, Uatumã, and Alta Floresta) have been marked separately on the map (Fig. 8), and their records have been plotted in a separate relative probability diagram in Fig. 9, together with other A-type and AMCG magmatism. The outlines of the SLIPs are drawn from the geologic evidence rather than from the low number of ages in key areas (Fig. 8), except for the Uatumã SLIP which is represented by many data points in the Central Brazil shield.

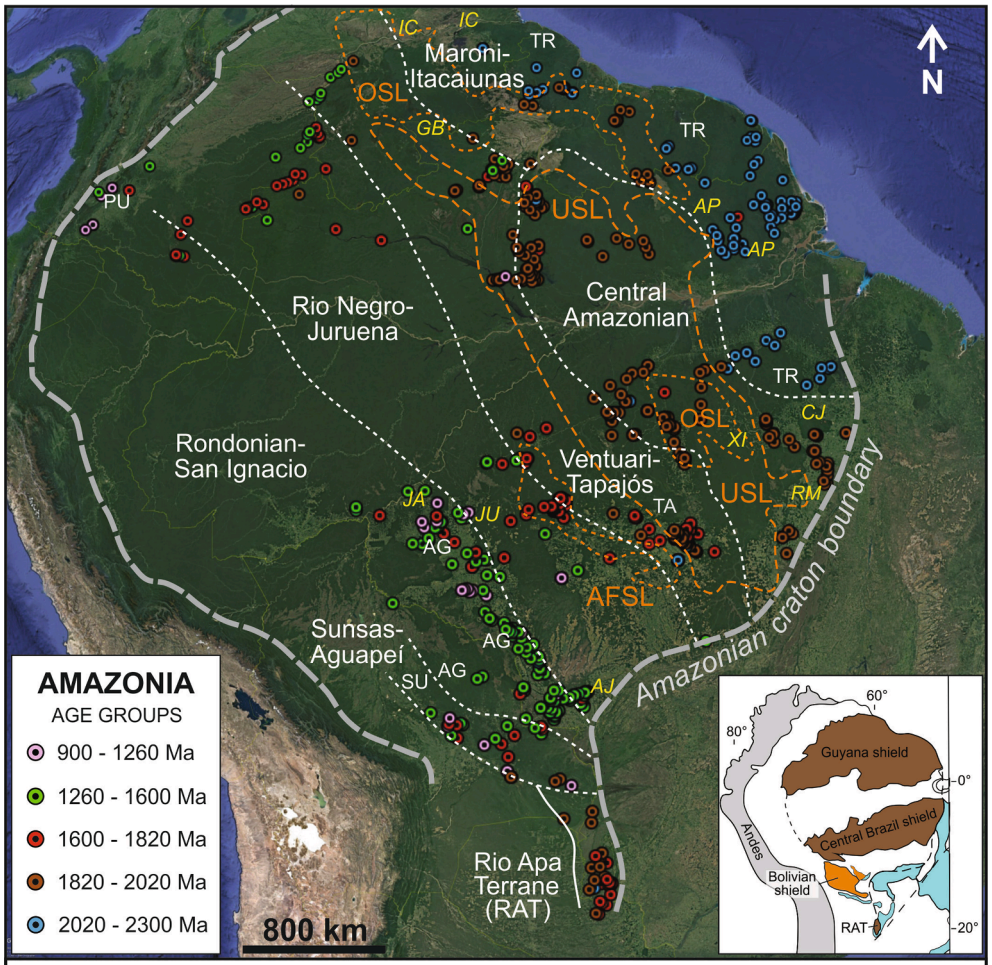

Orogenies:
TR = Transamazonian (2.26–1.95 Ga)
TA = Tapajós (2.10–1.90 Ga)
AJ = Alto Jauru (1.79–1.39 Ga)
AG = Alto Guaporé (1.45–1.33 Ga)
PU = Putumayo (1.45–0.90 Ga)
SU = Sunsas (1.11–1.00 Ga)

Tectonic domains:
RM = Rio Maria (3.05–2.87 Ga)
CJ = Carajás (2.98–2.73 Ga)
IC = Imataca (> 2.6 Ga)
AP = Amapá (> 2.6 Ga)
XI = Xingu-Iriri (1.99–1.86 Ga)

GB = Granulite belts (2.07–2.01 Ga)
JU = Juruena (1.82–1.78 Ga)
PA = Paraguá (1.82–1.34 Ga)
JA = Jamari (1.79–1.74 Ga)
AJ = Alto Jauru (1.79–1.42 Ga)

Anorogenic intraplate magmatism (SLIPs):
OSL = Orocaima (1.98–1.96 Ga) USL = Uatumã (1.88–1.87 Ga) AFSL = Alta Floresta (1.80–1.79 Ga)

Fig. 8. Google Earth map of Amazonia, with main geological provinces (white dashed lines), outlines of siliceous large igneous provinces (SLIPs; orange dashed lines), and magmatic U-Pb age data points indicated. Thick dashed grey line marks the approximate cratonic boundary of Amazonia. Inset map shows the exposed parts of Amazonia, the Guyana, Central Brazil and Bolivia Shields and the Rio Apa Terrane (RAT). Blue areas are Neoproterozoic orogenic belts partly surrounding the Amazonian Craton.

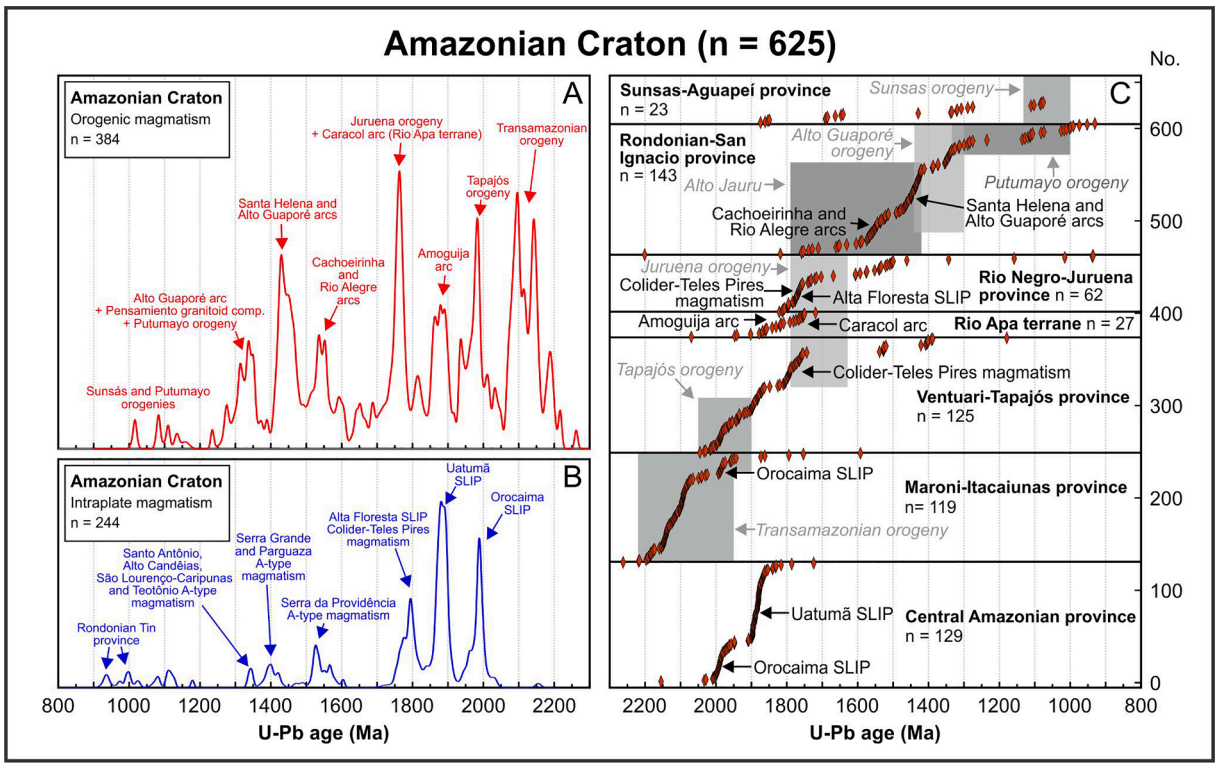

Fig. 9. A. Relative probability curves of magmatic U-Pb ages between 2300 and 800 Ma from orogenic rocks in the Amazonian Craton (including the adjacent Rio Apa Terrane). **B.** Relative probability curves of magmatic U-Pb ages between 2300 and 800 Ma from intraplate rocks (SLIPs and AMCG complexes) in the Amazonian Craton. **C.** Cumulative age diagrams for Amazonia, subdivided into the different orogenic provinces shown in Fig. 8. Note that the age axis in C is reverse compared to in panel A and B.

The geochronological data (625 U–Pb zircon ages) are grouped into five age intervals, 2.30 – 2.02, 2.02 – 1.82, 1.82 – 1.60, 1.60 – 1.26 and 1.26 – 0.90 Ga, which largely coincide with the age ranges for the Proterozoic provinces Maroni-Itacaiunas, Ventuari-Tapajós, Rio Negro-Juruena, Rondonian-San Ignacio, and Sunsas-Aguapeí, respectively (Fig. 8). These intervals illustrate the accretionary growth of Proterozoic Amazonia marked by a general southwestward decrease in age. The Central Brazil-Bolivia Shield including the Rio Apa Terrane is represented by a large number of data records (n = 392), especially in its southwestern part, compared to the Guiana Shield (n = 236). However, there is a remarkable coherence also in areas with less numerous data between age distribution patterns and tectonic framework.

5.2. *Paleoproterozoic orogenies*

Crust formation in Amazonia resumed during the early Paleoproterozoic due to the development of accretional-collisional arcs, as documented in the northern and eastern parts of the Amazonian Craton. The crustal growth continued towards the present-day southwest until 1.1 – 1.0 Ga, leading to the final consolidation of the Amazonian Craton (Cordani and Teixeira, 2007; Vasquez et al., 2008; Bettencourt et al., 2010; Teixeira et al., 2010; Fernandes et al., 2011; Scandolara et al., 2017).

The Maroni-Itacaiunas Province is a product of early Paleoproterozoic magmatic arcs which amalgamated during the Transamazonian orogeny (2.23 – 1.95 Ga). The geology is complex with the most prominent magmatic components forming three age peaks at 2.22 – 2.17 Ga (n = 14), 2.16 – 2.13 Ga (n = 28), and 2.12 – 2.06 Ga (n = 48) (Fig. 9), including granite-greenstone assemblages associated with TTG gneisses and gneissic-granitoid rocks. These magmatic events were succeeded by the formation of two adjoining granulite belts: the Bakhuis complex with igneous protoliths at ca. 2.07–2.06 Ga and the Cauarane-Coereni-Kanuku supracrustal association at ca. 2.04–2.01 Ga. Another belt composed of 1.99–1.94 Ga A-type granitoids (n = 8), gneisses, charnockites and migmatites occurs to the south (e.g. Vanderhaege et al., 1998; Tassinari and Macambira, 1999; Cordani and Teixeira 2007; Borghetti et al., 2018; Fraga and Cordani, 2019). Earlier Paleoproterozoic gneisses (2.5 – 2.4 Ga) and metavolcanic-sedimentary associations (2.4 – 2.3 Ga) occur, but in subordinate amounts, in the Bacajás domain that bounds the Carajás domain to the north (Vasquez et al., 2005, 2008; Macambira et al., 2009).

All these rocks have classically been referred to the Paleoproterozoic Transamazonian orogeny, and mainly show variable assimilation of pre-existing crustal material, as suggested by the available Hf–Nd isotopic signatures and model ages (Cordani and Teixeira, 2007; Kroonenberg et al., 2016; Milhomem Neto and Lafon, 2020). Two plutonic-volcanic belts (SLIPs), post-collisional to the Transamazonian orogeny, are widespread over the Maroni-Itacaiunas Province (section 5.4).

The Transamazonian orogeny is coeval with the Eburnean orogeny in the West African counterpart of Amazonia, during which the convergence and eventual collision between Amazonia and West Africa occurred (Delor et al., 2003; Cordani and Teixeira, 2007; Kroonenberg et al., 2016; Grenholm et al., 2019). From a paleomagnetic perspective, the amalgamation of Amazonia and West Africa is consistent with their 2.00–1.98 Ga Apparent Polar Wandering Paths (Nomade et al., 2003; Cordani et al., 2009; Bispo-Santos et al., 2014).

Two alternative geodynamic scenarios have been postulated for the evolution of the Maroni-Itacaiunas Province. The first envisages that all the Paleoproterozoic units originated from successive oceanic arcs with a final collision between the Amazonia and West Africa blocks, where the high-grade belts resulted from mantle upwelling in a zone of crustal stretching during plate convergence. This final process renewed the metamorphism in the high-grade belts along an anticlockwise cooling path, accompanied by anatexis and subsequent emplacement of plutonic rocks (e.g. Delor et al., 2003; Kroonenberg et al., 2016). The second scenario (e.g. Fraga et al., 2009b; Fraga and Cordani, 2019) postulates

the formation of a magmatic arc and associated back arc basin along an active continental margin, marked by the Cauarane-Coereni-Kanuku supracrustal association, and its eventual collision with the newly formed continental crust around ca. 2.02 – 2.01 Ga (Fraga et al., 2020), enclosing the older granite-greenstone areas formed during the preceding Transamazonian orogenic stages. The collisional process led to strong reworking of the pre-existing crust, including renewed metamorphism of the granulite belts. The ensuing A-type magmatism is considered to be related to a transpressional, post-collisional setting.

Large portions of the continental crust in the Central Brazil Shield became consolidated in the Paleoproterozoic, such as the Xingu-Iriri (weastern part of the Central Amazonian Province) and Tapajós Domains (2.05 – 1.80 Ga; Santos et al., 2001; Fernandes et al., 2011), and the Juruena and Jamari Terranes (1.82 – 1.60 Ga; Scandolara et al., 2017) (Figs. 8, 9C). From a geodynamic perspective, the continued accretionary-collisional processes also involved the Precambrian crust of Bolivia (e.g. Paraguá Terrane) as well as the peripheral Rio Apa Terrane.

The Xingu-Iriri and Tapajós Domains were formed from distinct accretionary-collisional arcs (Lamarão, 2005; Semblano et al., 2016a, b; Vasquez et al., 2019) collectively assigned here to the Tapajós orogeny that presents an age peak of 2.05 – 1.92 Ga (n = 56; Figs. 9A, C) along with a 1.98 – 1.96 Ga intraplate magmatic event (Orocaima SLIP, n = 29, section 5.4). The orogenic setting is complex, with rocks consisting of polyphase calc-alkaline and sub-alkaline tonalitic, monzogranitic and monzonitic gneisses, amphibolites and associated metavolcanic-sedimentary sequences that are extensively overlain or intruded by the volcanic-plutonic rocks of the 1.88 – 1.87 Ga Uatumã SLIP (n = 74; Klein et al., 2012). Thus, there is an ongoing debate about the number of magmatic arcs that formed the Xingu-Iriri and Tapajós Domains (Santos et al., 2001, 2004; Cordani and Teixeira, 2007; Fernandes et al., 2011).

The Xingu-Iriri Domain, bounded to the east by the Archean Carajás and Rio Maria Domains, hosts successive 1.99–1.84 Ga continental arcs, extensively overlain and intruded by volcanic and plutonic rocks of the Uatumã SLIP. These arc rocks are derived predominantly from Archean protoliths according to the available Nd isotopic evidence. Consequently, this domain has been tentatively included within the Archean Central Amazonian Province (Sato and Tassinari, 1997; Tassinari and Macambira, 1999; Cordani and Teixeira, 2007). Conversely, the adjoining Tapajos Domain essentially contains roots of juvenile magmatic arcs active between 2.01 and 1.90 Ga, as well as metavolcanic-sedimentary relicts (ca. 2.1 Ga), and volcano-plutonic rocks of the Uatumã SLIP (e.g. Tassinari and Macambira, 1999; Santos et al., 2000, 2001, 2004; Lamarão, 2005; Fernandes et al., 2011; Klein et al., 2012; Vasquez et al., 2019). A roughly similar geologic setting is seen immediately to the north in the Guiana Shield where 2.05–1.95 Ga K-rich calc-alkaline and shoshonitic rocks (n = 15) related to melting of juvenile mantle-derived magmas are again extensively overlain or intruded by the Uatumã volcano-plutonic association (e.g. Leal et al., 2018; Teixeira et al., 2019; Macambira et al., 2020). The Uatumã SLIP has Nd-isotopic signatures suggestive of large-scale fusion of young accreted oceanic lithosphere, rather than derivation from Archean crust (e.g. Klein et al., 2012). Therefore, a tectonic affinity with the Tapajós Domain to the south is apparent.

The southwestern limit of the Tapajós Domain with the younger Rio Negro-Juruena Province is tentatively placed along a set of NW-SE trending tectonic zones (Cordani and Teixeira, 2007). This region is composed of calc-alkaline gneisses (2.05–2.03 Ga), intruded by granitoid suites aged 1.99 – 1.93 and 1.89 – 1.87 Ga, the youngest of which has an intraplate setting (Scandolara et al., 2013; Rizzotto et al., 2019). These basement rocks are intruded or overlain by plutonic and volcanic rocks of the 1.79 – 1.75 Ga Teles Pires Suite and the 1.83 – 1.79 Ga Colíder Group (e.g. Neder et al., 2002; Santos et al., 2004; Cordani and Teixeira, 2007; Scandolara et al., 2017; Rizzotto et al., 2019; Trevisan et al., 2021; Saar de Almeida et al., 2021). From a geochemical point of view the Teles Pires Suite displays mainly alkaline A-type geochemical characteristics in contrast with the sub-alkaline to calc-alkaline trend of the Colider Group volcanics (e.g. Rizzotto et al., 2014, Rizzotto et al., 2019). These plutonic-volcanic rocks roughly bound a rift-type basin composed of a lower unit with 1.77–1.75 Ga volcanics and an associated sedimentary succession as young as 1.74 Ga (detrital zircon age), intruded by 1.57 Ga gabbro sills. The volcanic-sedimentary succession is overlain by much younger sedimentary packages representing a post-rift phase (Reis et al., 2021, and references therein).

The Rio Negro-Juruena Province formed from successive magmatic arcs continually succeeding the Ventuari-Tapajós Province arc-systems, as described by Cordani et al. (2016) for the Colombian basement in the westernmost part of the Guiana Shield. This portion comprises magmatic rocks aged 1.82 – 1.75 Ga (n = 26) and 1.74 – 1.70 Ga (n = 7), and two sets (1.60 – 1.50 Ga, n = 12; 1.48 – 1.33 Ga, n = 2) of crustal-derived granites (e.g. Tassinari et al., 1996; Santos et al., 2000; Ibañez-Mejia and Cordani, 2020). Of note, the basement rocks show Hf–O and Nd isotope characteristics indicating that reworking of older crust might have played an important role in the geological and geochemical evolution (Ibañez-Mejia and Cordani, 2020). This finding contrasts with granitoid rocks of similar ages exposed in the Central Brazil Shield, where positive to slightly negative Nd isotopic signatures are apparent (e.g. Tassinari et al., 1996; Tassinari and Macambira, 1999; Cordani and Teixeira, 2007), indicating a more juvenile origin.

The evolution of the southwestern part of the Rio Negro-Juruena Province is debated, including issues such as the tectonic interaction between the Juruena accretionary-collisional orogeny (1.82 – 1.63 Ga) and the older Tapajós arc system (e.g. Cordani and Teixeira, 2007; Scandolara et al., 2017; Rizzotto et al., 2019). This portion is divided into the 1.82 – 1.78 Ga Juruena and 1.79 – 1.74 Ga Jamari arc terranes according to geochronological and structural evidence (Scandolara et al., 2017). The available Nd isotopic evidence indicates that the crustal generation processes involved juvenile mantle sources and variable proportions of older recycled crust. According to these authors, the collision of these arcs against the pre-existing continental margin (i.e. consolidated Tapajós Orogen rocks) resulted in a complex tectono-structural framework under granulite facies metamorphism dated at 1.69 – 1.63 Ga. Subsequent 1.50 – 1.30 Ga crustal reworking is recorded in the Jamari Terrane (Tassinari et al., 1996; Santos et al., 2008; Scandolara et al., 2013, 2017). As such, this particular terrane is considered as an orogenic component of the adjoining Rondonian-San Ignacio Province rather than of the Rio Negro-Juruena Province (Bettencourt et al., 2010), as followed hereafter.

Roughly coeval tectono-magmatic events are documented in the Alto Jauru Terrane in the southeastern portion of the Rio Negro-Juruena Province. This portion is composed of 1.76 – 1.71 Ga (n = 6) granite-greenstone associations and juvenile granite-gneissic rocks that display Sm–Nd T_{DM} ages between 2.0 and 1.8 Ga and positive to slightly negative $\varepsilon_{Nd(t)}$ signatures (Geraldes et al., 2001, 2004, and references therein). Noteworthy the Alto Jauru Terrane like the Jamari Terrane displays Mesoproterozoic crustal reworking and A-type and intraplate magmatic activity representing peaks at 1.60–1.49 Ga (n = 21) and 1.47–1.39 Ga (n = 11), indicating its affinity with the adjoining Rondonian-San Ignacio Province (Bettencourt et al., 2010).

Rio Apa Terrane: The Rio Apa Terrane constitutes a Paleo- to Mesoproterozoic allochthonous fragment exposed in a basement window surrounded by Phanerozoic sediments, south of the Amazonian craton proper. It has been extensively studied in recent years, and is represented by 42 data points in our compilation (Fig. 9A), in spite of its relatively small size. Its affinity with Proterozoic Amazonia has been inferred by robust geochronological and Nd and zircon Hf isotopic constraints (Faleiros et al., 2016; Teixeira et al., 2020; Ribeiro et al., 2020). The Rio Apa Terrane is a product of three tectonic-magmatic events: 2.10 –1.94 Ga, 1.90 – 1.82 Ga (Amoguija arc), and 1.80 – 1.72 Ga (Caracol arc) (Fig. 9C). The two older events represent continental arcs with protoliths as old as 2.7 Ga indicated by the isotopic constraints. The younger arc likely evolved in an oceanic setting with

significant juvenile input according to Nd and zircon Hf isotopic evidence (Teixeira et al., 2020; Ribeiro et al., 2020).

The crustal evolution of the Rio Apa Terrane is penecontemporaneous with orogenic episodes recognized in the southeastern portions of the Ventuari-Tapajós and Rio Negro-Juruena Provinces, as also reinforced by the roughly similar initial $\varepsilon_{Hf(t)}$ signatures (Faleiros et al., 2016; Teixeira et al., 2020; Ribeiro et al., 2020). Hence, the Rio Apa Terrane was probably located along the southeastern extension of the boundary between the Ventuari-Tapajos and Rio Negro-Juruena Provinces during Paleoproterozoic times (e.g. Faleiros et al., 2016; Teixeira et al., 2020).

5.3. Mesoproterozoic orogens

The Rondonian-San Ignacio Province (1.59 – 1.30 Ga) is a product of a Mesoproterozoic orogeny that lasted ca. 260 Myr (Fig. 9C), involving successive stacking of accretionary-collisional magmatic arcs within the Jauru and Paraguá Terranes located to the west in the Bolivian Precambrian Shield (e.g. Boger et al., 2005; Bettencourt et al., 2010; Rizzotto et al., 2014; Teixeira et al., 2020). Age peaks at 1.59–1.48 Ga (n = 28), 1.47–1.39 Ga (n = 44), and 1.37–1.28 Ga (n = 22) (Fig. 9A) are primarily related to four orogenic pulses of continental or oceanic settings: Cachoeirinha (1.59 – 1.52 Ga), Rio Alegre (1.51 – 1.48 Ga), Santa Helena (1.44 – 1.42 Ga), and Alto Guaporé (1.44 – 1.33 Ga) (Bettencourt et al., 2010). The latter pulse generated the Alto Guaporé belt (e.g. Rizzotto et al., 2013; Teixeira et al., 2020), and represents the most prominent tectonic-magmatic event of Mesoproterozoic Amazonia, before the 1.1 – 1.0 Ga Sunsás orogeny that marks the final consolidation of the Amazonian Craton.

The history of the Alto Guaporé belt involved an early accretionary phase (1.44 – 1.43 Ga) marked by ophiolitic remnants and associated chemical ocean sediments (e.g. Bettencourt et al., 2010; Rizzotto and Hartmann, 2012; Rizzotto et al., 2013, 2014). The tectonic setting is similar during the 1.51–1.48 Ga orogenic pulse, indicating that an oceanic environment existed between the Alto Jauru and the Paraguá Terrane for at least 90 million years. The collisional stage (1.35 – 1.33 Ga) marks the suturing of the Paraguá Terrane onto the Rio Negro-Juruena Province and eventual consolidation of the Rondonian-San Ignacio Province (e.g. Boger et al., 2005; Cordani and Teixeira, 2007; Rizzotto et al., 2013, 2014). The Paraguá Terrane in the Bolivian Shield hosts crustal-derived granitoid rocks (1.37 – 1.34 Ga) collectively known as the Pensamiento Granitoid Complex (Litherland et al., 1986). These rocks have traditionally been assigned to the San Ignacio orogeny (Litherland et al., 1986; Boger et al., 2005; Matos et al., 2009), which was renamed the Alto Guaporé orogeny by Rizzotto et al. (2014).

The collisional phase was accompanied by inboard syn- to late tectonic plutonism in the Jamari Terrane, exemplified by the 1.36–1.34 Ga Alto Candeias suite, coeval with the Pensamiento suite in the Paraguá Terrane, and the slightly younger (1.31 – 1.28 Ga) São Lourenço-Caripunas suite. The Paraguá, Jamari and Alto Jauru Terranes experienced penecontemporaneous regional metamorphism and deformation and partial melting of pre-existing material at 1.35 – 1.30 Ga related to the Alto Guaporé orogeny (Rizzotto et al., 2013; Nedel et al., 2017; Teixeira et al., 2020).

The Alto Guaporé orogeny correlates well with the early phases of the Putumayo orogeny (Fig. 9A, C). The latter is recorded in basement inliers of the northern Andes in Colombia and in the westernmost portion of the Guiana Shield (Ibañez-Mejia, 2020 and references therein). The Putumayo convergence and arc–related magmatism and sedimentation mark a protracted orogenic history, lasting ca. 400 Myr (Fig. 9C), being penecontemporaneous with both the Alto Guaporé and Sunsás orogenies further south. The igneous protoliths associated with the early accretionary arcs yielded ca. 1.46 – 1.31 Ga ages (n = 3), and involved both the generation of juvenile crust and reworking of older crustal material.

The main arc development included subduction-driven magmatism and deformation, arc-terrane accretion (1.10 – 1.02 Ga, n = 3), and eventual AMCG magmatism (ca. 1.0 Ga, n = 1). According to Ibañez-Mejia (2020), the AMCG magmatism in the Putumayo Orogen postdates arc accretion but pre–dates the main collisional event, and most likely took place in a convergent tectonic environment. The final collisional stage and crustal exhumation of the Putumayo orogen is represented by ages at 1.05 –1.00 Ga (n = 2) and ~ 0.95 Ga (n = 1) (Fig. 9A–C). This stage is somewhat younger than the 1.11 – 1.00 Ga collisional stage in the Sunsás belt at the SW edge of the Amazonian Craton, in the Bolivian Shield (Litherland et al., 1989; Boger et al., 2005; Teixeira et al., 2010).

The Sunsás belt (1.20 – 1.00 Ga) southwest of the Paraguá Terrane is essentially composed of metasedimentary sequences and syn-, late and post-collisional granitic intrusive suites with variable I-, S- and hybrid A-type characteristics represented by a small peak at 1.15 – 1.05 Ga (n = 4) in Fig. 9A. This peak coincides with the mafic 1.11 Ga Rincón del Tigre-Huanchaca LIP recognized at the SW edge of the Amazonian Craton (Teixeira et al., 2010, 2015, 2020; Nedel et al., 2020) but not included in our compilation. The Sunsás belt is roughly contemporaneous with two intraplate supracrustal belts: the Nova Brasilândia Belt in the Jamari Terrane and the Aguapeí Belt along the eastern side of the Paraguá Terrane. In particular, the Nova Brasilândia Belt (Tohver et al., 2004a, 2004b, 2006), also termed Nova Brasilândia Terrane (e.g. Bettencourt et al., 2010; Teixeira et al., 2010), hosts 1.11 Ga bimodal magmatism, the Rio Branco suite, whose age matches the Rincón del Tigre-Huanchaca LIP (Teixeira et al., 2015, 2019).

The syn- to late-orogenic granites (1.1 – 1.0 Ga) have tectonic relations with several shear zones along the southern edge of the Paraguá Terrane, indicating the general transport of the Sunsás belt from southwest to northeast (Litherland et al., 1989; Teixeira et al., 2010, 2020). The emplacement of post-collisional to anorogenic granites accompanied the orogenic collapse and crustal exhumation (Litherland et al., 1986; Teixeira et al., 2010), like in the Putumayo orogen. These granites transect the Paraguá basement as well as the Jamari Terrane to the north, exemplified by the youngest granite generation of the Rondonian Tin Province with ages of 0.99 – 0.97 Ga (n = 4), and continue to 0.93 Ga (e.g. Payolla et al., 2002; Teixeira et al., 2010; Bettencourt et al., 2016).

5.4. Paleoproterozoic silicic large igneous provinces

Three SLIP events (Fig. 9B), namely the 1.98 – 1.96 Ga Orocaima (n = 29), 1.88 – 1.87 Ga Uatumã (n = 74), and 1.80 – 1.79 Ga Alta Floresta (n = 24), are signs of significant plutonic and volcanic activity throughout the late Paleoproterozoic within the older northeastern parts of Amazonia, accompanying the stepwise southwestward growth (Klein et al., 2012; Teixeira et al., 2019; Fraga et al., 2020; Reis et al., 2021). In addition, the Amazonian Craton hosts the 1.79 Ga Avanavero LIP composed of voluminous mafic sills and dykes, and the 1.11 Ga mafic Rincón del Tigre-Huanchaca LIP (Reis et al., 2013, 2021; Teixeira et al., 2019, 2020). However, these two mafic LIPs are beyond the scope of this paper.

The Orocaima SLIP roughly bounds the Cauarane-Coerene-Kanuku high-grade supracrustal belt in the central portion of the Maroni-Itacaiunas Province to the north, in the eastern part of the Guiana Shield. It extends to the south in the Central Brazil Shield, althought extensively overlain by Uatumã SLIP rocks. The Orocaima SLIP is composed of rocks with high-K calc-alkaline, A-type and shoshonitic chemistry, signatures of a post-collisional setting in relation to the Transamazonian orogeny (Reis et al., 2003, 2021).

The Uatumã SLIP crops out in a large oval area in the eastern parts of the Guiana and Central Brazil shields and forms a high-K calc-alkaline and A-type volcanic and plutonic association. This magmatism is a post-collisional to intraplate counterpart to the youngest continental arc that formed the Xingu-Iriri and Tapajós Domains (Fernandes et al., 2011; Klein et al., 2012; Teixeira et al., 2019; Reis et al., 2021). The Uatumã SLIP also includes the 1.88 Ga alkaline to sub-alkaline A-type granites

and mafic dykes that transect the Archean Carajás and Rio Maria domains (Antonio et al., 2017, 2021; Fernandes et al., 2011; Giovanardi et al., 2019; Teixeira et al., 2019). This SLIP forms a prominent age peak (Fig. 9B)

The 1.80 – 1.79 Ga Alta Floresta SLIP (Reis et al., 2021), which occurs in the Central Brazil Shield to the south of the Uatumã SLIP, matches the age of the Avanavero LIP in the Guiana Shield (Reis et al., 2013). This SLIP consists of spatially associated volcanic, subvolcanic and plutonic rocks of medium to high-K calc-alkaline to alkaline affinity along the southernmost fringe of the Tapajós Domain. These particular geochemical rock types were distinguished from the Colider volcanics and the Teles Pires Suite, collectively grouped into a 1.82 – 1.76 Ga magmatic belt in the same area (Rizzotto et al., 2019). We note that the Alta Floresta magmatism has a much shorter age range (10 myr) than the Colider-Teles Pires magmatism, but it could perhaps be considered the peak event of the whole Colider-Teles Pires magmatic episode.

5.5. Mesoproterozoic intraplate magmatism

The Amazonian Craton hosts scattered 1.61–1.34 Ga (n = 38) intraplate intrusions (Fig. 9B), exemplified by rapakivi plutons with A-type geochemistry and much younger ages than the surrounding crystalline basement. These magmatic episodes can be considered as discrete extension episodes within the already stable parts of the continental crust, contemporaneous with the crustal growth of southwestern Amazonia in the Mesoproterozoic. Their quite large distribution across the Guiana and Central Brazil-Bolivia shields is consistent with other LIP scale events (Teixeira et al., 2019). At a broader scale, the intermittent intraplate activity manifested by pulses of rapakivi granite and co-magmatic charnockite, anorthosite and mangerite have age matches with roughly correlative events composed of similar rocks formed in similar geologic environments in eastern Laurentia and Baltica (e.g. Sadowski and Bettencourt, 1996; Bettencourt et al., 1999; McLelland, 1989; Söderlund et al., 2002; Gower and Krogh, 2002; Payolla et al., 2002; Cordani and Teixeira, 2007).

In the Guiana Shield these intraplate intrusions include the Surucucus Suite (1.55 Ga), the Mucajaí AMG complex (1.53 – 1.51 Ga), the Repartimento Anorthosite (1.52 Ga), and the Serra Grande MCG complex (1.43 – 1.42 Ga) in Brazil, the Parguaza Suite (1.40 – 1.39 Ga) in Venezuela, and coeval rapakivi rocks in eastern Colombia (Santos et al., 2011; Fraga et al., 2009a, 2009b; Heinonen et al., 2012; Bonilla et al., 2016; Teixeira et al., 2019; Ibañez-Mejia and Cordani, 2020). Mesoproterozoic intraplate activity is also present in the Central Brazil Shield, such as the 1.61 – 1.51 Ga Serra da Providência, the 1.40 – 1.36 Ga Santo Antônio, and the 1.39 Ga Teotônio Suites (Payolla et al., 2002; Bettencourt et al., 2010; Scandolara et al., 2013, 2017) (Fig. 9B). The Serra da Providência Suite is post-collisional to the granulite metamorphism of the Juruena orogeny (e.g. Scandolara et al., 2013). These younger igneous pulses may be considered inboard magmatic counterparts to the distinct orogenic events that constructed the Rondonian–San Ignacio Province. Many of these granites show juvenile Nd isotopic signatures, indicating a high proportion of mantle-derived material in their magmas (Bettencourt et al., 1999).

6. Kalahari Craton data and results

6.1. Geological overview

Kalahari consists of the old pre-Neoproterozoic core of southern Africa and a small part of East Antarctica (Fig. 10). Its position within Columbia remains highly uncertain, and here we are mainly concerned with its relationship to the other continents within Rodinia. In Rodinia,

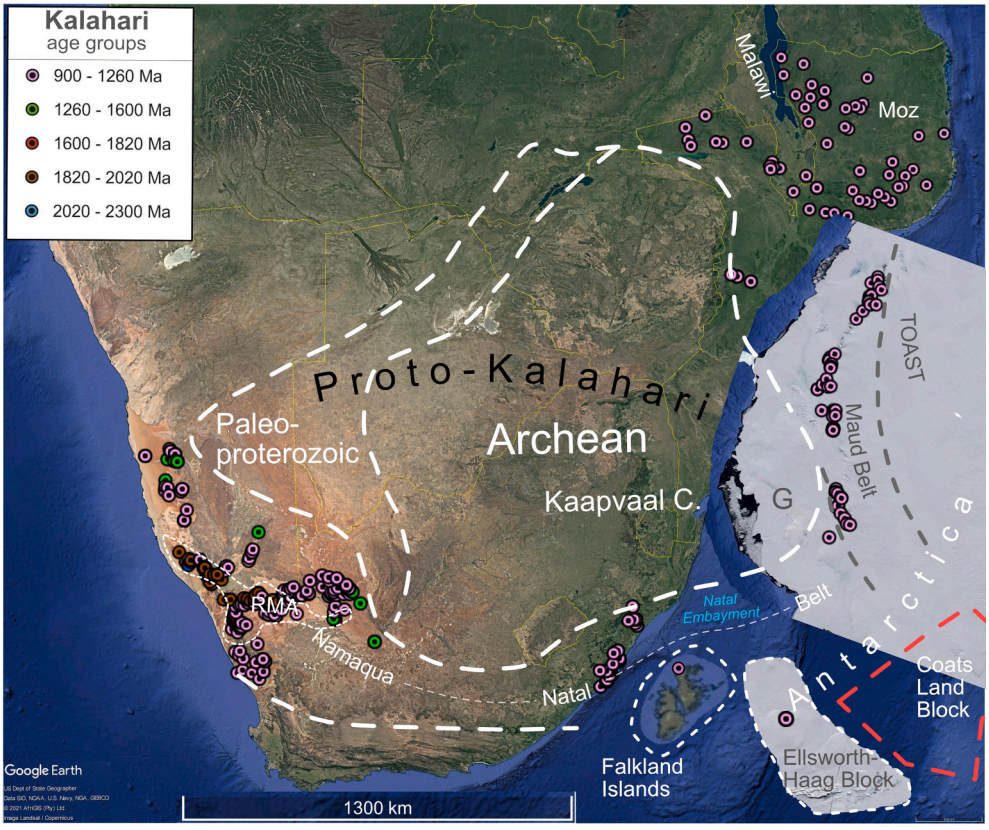

Fig. 10. Google Earth map of the Kalahari Craton (southern Africa and adjacent parts of East Antarctica) with main geological provinces (white dashed lines) and magmatic U-Pb age data points indicated. G = Grunehogna craton; Moz. = Mozambique; RMA = Richtersveld Magmatic Arc; TOAST = Tonian Oceanic Arc Superterrane.

Proto-Kalahari (pre-Mesoproterozoic Kalahari) is surrounded by Grenville-age rocks on all sides. These are related to different tectonic processes operative along three major sections of Proto-Kalahari. Whilst the Namaqua-Natal Belt represents continental collision with Laurentia, the Maud Belt in East Antarctica and its continuation into northern Mozambique is interpreted as a major continental arc. The present-day western and northern sides of the Proto-Kalahari Craton in northern Namibia-Botswana largely formed an extensional margin in late Grenville-age times (ca. 1200–1000 Ma; e.g. Singletary et al., 2003; Jacobs et al., 2008), and is not the focus of the current study.

Although only partly exposed, the Namaqua-Natal Belt can be traced by geophysical means underneath thick younger cover rocks in central South Africa and projects eastward into formerly adjacent parts of East Antarctica. Mesoproterozoic rocks of the Falkland Islands and the Haag block in Antarctica are part of this mobile belt and are restored within the Natal Embayment. Whilst the Namaqua sector is characterised by significant reworking of older crust, the Natal side is dominated by juvenile additions prior to continental collision. Proto-Kalahari formed an indenter during the final stage of continental collision, resulting in dextral shear geometries in the Namaqua and sinistral shear geometries in the Natal sectors, respectively (Jacobs et al., 1993).

In contrast, the Maud Belt, exposed in East Antarctica, represents a major long-lived continental arc that formed perpendicular to, and slightly after, the Namaqua-Natal Belt. The Maud Belt extends into northern Mozambique, and possibly correlates with the Southern Irumide Belt in Malawi and Tanzania (e.g. Bingen et al., 2009; Macey et al., 2010; Wang et al., 2020a). The entire Maud Belt underwent medium- to high-grade Pan-African reworking during the assembly of Gondwana (Jacobs et al., 1998; Wang et al., 2020b).

The protracted orogenic magmatism in the Namaqua-Natal and Maud belts shows a marked peak at ca. 1100 Ma, which coincides with widespread within-plate magmatism at 1112–1106 Ma inside the Proto-Kalahari Craton (Umkondo LIP) (e.g. Hanson et al., 1998). This event was synchronous with the within-plate magmatism of the Mid-Continental Rift System of Laurentia and in the Coats Land block of East Antarctica. The latter is interpreted as a fragment of Laurentia that remained attached to Kalahari, when Kalahari was rifted from Laurentia in the Neoproterozoic (e.g. Loewy et al., 2011).

A total of 386 U-Pb zircon ages from Kalahari between 2000 and 950 Ma in age, but mostly below 1400 Ma, have been compiled and their locations are plotted in Fig. 10. Relevant relative probability curves for the different segments of the Namaqua-Natal-Maud-Mozambique belt are shown in Fig. 11A, and corresponding cumulative age diagrams in Fig. 11B. Since only age data from the Grenville-age Namaqua-Natal and Maud Belts have been compiled, but not data from older Proterozoic provinces surrounding the Archaean nucleii, these diagrams do not give the full picture of the evolution of the entire Kalahari craton during the Proterozoic.

6.2. *Namaqua Sector*

The Namaqua Sector of the Namaqua-Natal Belt is composed of a number of Paleoproterozoic (~2.05–1.81 Ga) and Mesoproterozoic (~1.3–1.0 Ga) tectonostratigraphic 'subprovinces', 'terranes' or 'domains' (e.g. Cornell et al., 2006; Miller, 2008 and references therein; Macey et al., 2017). Broadly speaking, the domains occur as a stack of SW-vergent thrust sheets that were juxtaposed and reworked during the polyphase, high temperature, moderate/low pressure Namaqua orogeny between ~ 1220 and 960 Ma (e.g. Clifford et al., 2004; Hartnady et al., 1985; Eglington, 2006; Bial et al., 2015; Bailie et al., 2017; Macey et al., 2018b). The Paleoproterozoic domains occur in the western part of the Namaqua Sector and consist predominantly of igneous rocks formed during at least three distinct pulses. The oldest pulse, the ca. 2020 Ma calc-alkaline granodioritic orthogneisses in the Sperrgebiet Domain of southern Namibia (n = 5) are interpreted to have formed in an island-arc setting (Thomas et al., 2016). The second and most extensive phase of Paleoproterozoic magmatism developed in the Richtersveld Subprovince (Richtersveld Magmatic Arc) and intruded and enveloped the

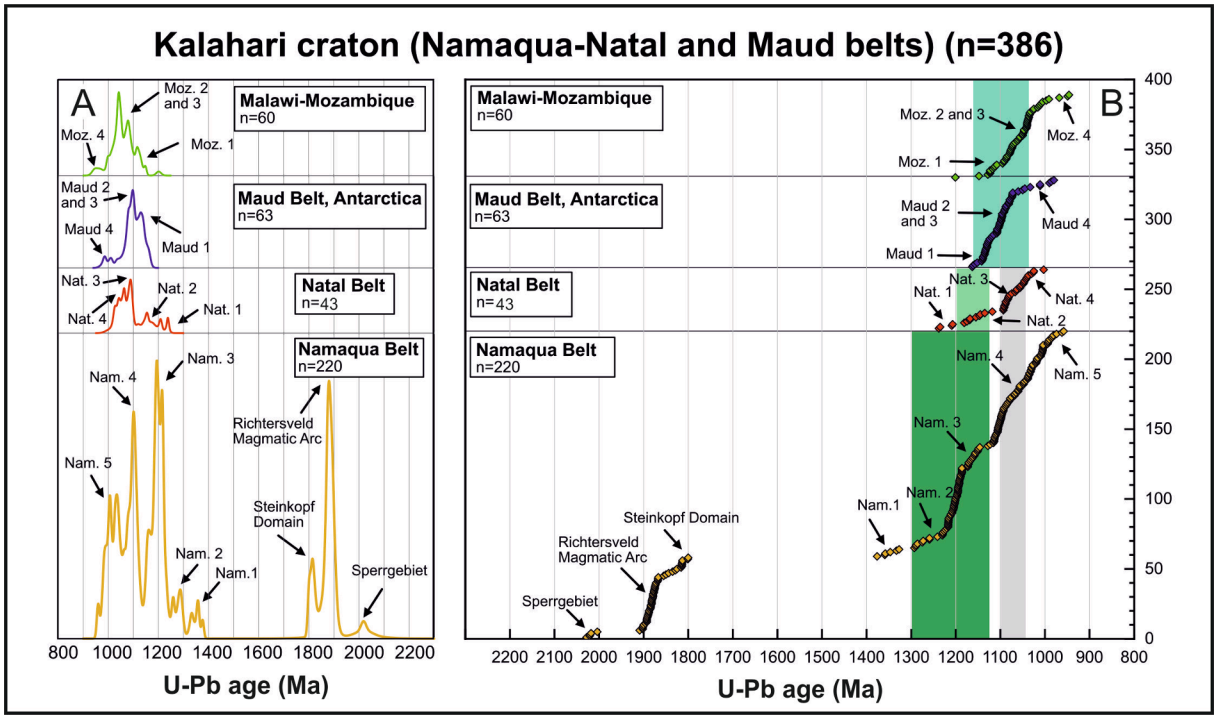

Fig. 11. A. Relative probability curves of magmatic U-Pb ages from the Namaqua-Natal Belt in southern Africa, the Maud Belt in Antarctica, and its continuation into northern Mozambique and Malawi. **B.** Cumulative age diagrams from the same rock units. Age ranges of accretionary orogenies in greenish hues, of collisional orogeny in grey. Note that the age axis in B is reverse compared to in panel A. For Kalahari, only age data from the Grenville-age Namaqua-Natal and Maud Belts were compiled, but not data from older Proterozoic provinces that would have yielded much more Paleoproterozoic age peaks.

Sperrgebiet Domain, including its scattered Neoarchean-early Paleoproterozoic crustal remnants (Bankwasser Migmatite, Macey et al., 2017). It is composed of 1910–1875 Ma calc-alkaline volcanic rocks and minor quartzite (Orange River Group; n = 8; Fig. 11), intruded by vast amounts of coeval granodiorite and granite of similar age (Vioolsdrif Suite; n = 36), associated with the low-grade Orange River orogeny (Reid, 1979; Blignault et al., 1983; Macey et al., 2017). The third pulse of Paleoproterozoic granitic magmatism at 1825–1800 Ma (Gladkop Suite; n = 9) was recognized just south of the Richtersveld Magmatic Arc and forms the Steinkopf Domain (Fig. 11) in the northern Bushmanland Subprovince (Robb et al., 1998; Nke et al., 2020).

The Paleoproterozoic block in the western Namaqua Sector is surrounded to the northeast, east and south by tectonic domains dominated by Mesoproterozoic plutonic rocks. However, isotopic studies indicate most of these were derived from the melting of a significant amount of Palaeoproterozoic crust. Mesoproterozoic igneous activity was also poly-episodic, with five pulses at 1360–1330 Ma, 1300–1240 Ma, 1230–1150 Ma, 1125–1030, and 1010–960 Ma during multiple cycles of collisional juxtaposition and extension of the tectonic domains around the Proto-Kalahari Craton (Fig. 11). The earliest magmatic phase at ca. 1350 Ma (n = 6) produced gabbro – granite hybrid rocks in the northeast Namaqua Sector (Konkiep Domain), possibly in a rift setting, which resulted in development of an ocean basin to the west (Cornell et al., 2015). The subsequent 1300–1240 Ma magmatism (n = 9), mainly recorded by mafic to intermediate metavolcanics and their redeposited equivalents rocks in the east of the Namaqua Sector (Areachap Domain), was interpreted as juvenile arc magmatism associated with inboard (eastward) subduction of the oceanic crust (Pettersson et al., 2007). In the Kakamas Domain (located between the Richtersveld Magmatic Arc and Konkiep-Areachap domains) and the Bushmanland Subprovince (located to the south of the Richtersveld Magmatic Arc), the earliest period of intrusion at ca. 1230–1150 Ma (n = 64) was characterised by minor early mafic magmatism followed by voluminous granites and youngest leucogranite (e.g. Clifford et al., 2004; Eglington, 2006; Pettersson, 2008; Groenewald and Macey, 2020). The ~ 1200 Ma granite magmas intruded supracrustal successions which had been deposited just before (e.g. McClung, 2006; Cornell and Pettersson, 2007) and was accompanied by high grade metamorphism (e.g. Clifford et al., 2004; Bial et al., 2015). A second Mesoproterozoic depositional event at ~ 1150 Ma (Raith et al., 2003; Cornell et al, 2009) was accompanied by minor mafic magmatism (Robb et al., 1998).

The fourth magmatic pulse between 1125 and 1030 Ma (n = 64 ; Fig. 11) produced the voluminous late- to post-tectonic granite and charnockite of the Keimoes and Komsberg Suites in the Kakamas and Areachap Domains (Bailie et al., 2017; Macey et al., 2018a) and the 1100–1040 Ma Spektakel Suite in the Bushmanland Subprovince (Macey et al., 2018b), which marked the end of the main phase of the Namaqua orogeny, the final juxtaposition of the various Namaqua domains, and final collision with Laurentia. The magmatism has been variably attributed to slab break-off and mantle upwelling (e.g. Waters, 1986; Bailie et al., 2017; Macey et al., 2018b) or to the influence of the Umkondo plume (Cornell et al., 2012). In the Bushmanland Subprovince the prolonged period of granitic and mafic (Koperberg Suite) magmatism is spatially and temporally related to low-P, high-T thermal metamorphism (1050–1020 Ma; e.g. Robb et al., 1998) of the western and southern Namaqua sector, suggesting that the ascending melts were responsible for the transfer of the heat into the surrounding crust. The fifth and final phase of magmatism in the Namaqua Sector is characterized by swarms of pegmatite sheets and associated leucogranites (e.g. Melcher et al., 2017; Doggart, 2019) that intruded between 1010 and 960 Ma (n = 19; Fig. 11). They are related to coeval large-scale, NW-trending, sub-vertical transcurrent dextral shear zones (e.g. Pofadder shear) which also reactivated the older major tectonic domain boundaries (e.g. Thomas et al., 1994; Lambert, 2013).

6.3. Natal Sector

The Natal Sector of the Namaqua-Natal Belt (Fig. 10) was divided into three Mesoproterozoic crustal blocks termed, from south to north, the Margate, Mzumbe, and Tugela Terranes (Thomas, 1989). Unlike the complexities and controversies attached to the Namaqua Sector, the Natal terranes have been interpreted as remnants of discrete juvenile island arcs that were accreted onto the margin of the Proto-Kalahari Craton during Rodinia assembly. The Tugela Terrane, adjacent to the Archean Kaapvaal Craton, also contains remnants of ophiolitic rocks (Matthews, 1972). Compiled geochronology data show that the igneous activities in the Natal Sector mainly occurred during four periods at 1250–1200 Ma, 1180–1130 Ma, 1090–1070 Ma, and 1060–1020 Ma (Fig. 11).

The first period (n = 4), interpreted as the early-stage island arc magmatism, is recorded by the Quha Gneiss in the Mzumbe and Margate Terranes, dated at 1235 ± 9 Ma (Thomas et al., 1999), which was intruded by the Mzumbe Granitoid Suite at ca. 1207 and 1175 Ma, respectively (Thomas and Eglington, 1990; Spencer et al., 2015). This magmatic phase has also been recognized in the Tugela Terrane, where the Kotongweni tonalite gneiss was dated at 1209 ± 5 Ma (Johnston et al., 2001). The second stage of magmatism (n = 8) took place in all the three terranes including, for example, the Sikombe and Margate granites in the Margate Terrane and the Mzimlilo granite of the Mzumbe Terrane. This period of magmatism is interpreted to possibly represent a phase of extensional activity during the latest stages of arc magmatism lasting to ca. 1130 Ma, when the Tugela and Mzumbe Terranes were accreted to the Proto-Kalahari Craton (Mendonidis et al., 2015). The ca. 1090–1070 Ma stage (n = 13) is characterized by synchronous intrusion of granites and mafic/ultramafic and alkaline intermediate magmatic suites, interpreted as syn- to post-tectonic magmatism related to the accretion of the Margate Terrane (Mendonidis and Armstrong, 2009). After this, late-stage post-accretional magmatism occurred at ca. 1060–1020 Ma (n = 13), exemplified by the emplacement of the voluminous A-type rapakivi-type granites and charnockites of the Oribi Gorge Granite Suite in the Margate and Mzumbe terranes (Eglington et al., 2003), which probably coincides with the final juxtaposition of Kalahari and Laurentia.

Paleogeographic reconstructions place the Falkland Islands (n = 3) and Haag Nunataks (n = 3) on the southern margin of the Proto-Kalahari Craton, and Grenville-age magmatism in these areas can be correlated with the adjacent Natal Sector (e.g. Jacobs et al., 1999; Riley et al., 2020). Furthermore, the Margate Terrane of the Natal Belt probably extends into the Vardeklettane Terrane in the south-westernmost part of the Maud Belt (Bauer et al., 2009; Mendonidis et al., 2015).

6.4. Maud Belt (Antarctica) and its continuation into northern Mozambique and Malawi

The Maud Belt in East Antarctica represents a Grenville-age continental arc that is complex due to both late Mesoproterozoic as well as intense late Neoproterozoic/early Paleozoic tectono-thermal reworking (e.g. Jacobs and Thomas, 2004). The Maud Belt fringes the Grunehogna Craton (Archean fragment of Proto-Kalahari Craton), as well as the extension of the Natal Belt into East Antarctica, to the east (coordinates as seen in Fig. 10; e.g. Groenewald et al., 1995). The contact with the Natal Belt coincides with the late Neoproterozoic/early Paleozoic Heimefront Shear Zone (e.g. Jacobs et al., 2003b; Wang et al., 2020a). On its eastern side, the Maud Belt is limited by the Tonian Oceanic Arc Super Terrane (TOAST), a remnant of the Neoproterozoic Mozambique Ocean (Jacobs et al., 2015).

The oldest rocks recognized in the Maud Belt are related to a metavolcano-sedimentary sequence that was deposited between ca. 1200 and 1100 Ma (Jacobs et al., 1998; Bauer et al., 2003; Ksienzyk and Jacobs, 2015). Major periods of magmatic activity are recorded at ca. 1140–1120 Ma, 1110–1100 Ma and 1090–1070 Ma, which form

overlapping peaks in Fig. 11 (n = 54). Whilst the first major magmatic event mostly represents volcanic arc activity, the second period is synchronous with a magmatic event that affected the entire Kalahari Craton (Hanson et al., 1998). The last period is associated with major plutonic intrusions and is synchronous with Grenville-age metamorphism (e.g. Jacobs et al., 1998, 2003a, 2003b; Marschall et al., 2013; Wang et al., 2020a), recorded as metamorphic zircon mantles overgrowing igneous zircon cores (e.g. Wang et al., 2020a). These were often themselves overgrown by a second generation of Pan-African (ca. 550 Ma) metamorphic zircon mantles, when the Kalahari Craton became part of Gondwana.

The period from 1060 to 980 Ma (n = 9) records continued minor magmatism as pegmatites, leucogranites and mafic dykes. Isotopic studies indicate that pre-Grenville crustal components were involved in the generation of Mesoproterozoic magmas and the spatial variation of Nd-Hf isotopes indicates an increasing juvenile input towards the proside of the continental arc, i.e. with increasing distance from the craton margin (Wang et al., 2020a). The Maud Belt more clearly developed on the substrate of the Proto-Kalahari Craton as a long-lived continental margin arc, and periodic magmatic influx is attributed to the switching between advancing and retreating subduction zone systems (Wang et al., 2020a). The Maud Belt differs from the Natal Belt by showing an opposite subduction polarity, facing the craton (e.g. Mendonidis et al. 2015; Wang et al., 2020a).

The eroded detritus from the early-stage magmatism in the Maud Belt was deposited at ca. 1130–1107 Ma near the eastern margin of the Grunehogna Craton, the remnants of which are preserved as the Ritscherflya Supergroup. Detrital zircon distribution in the Ritscherflya Supergroup shows a major age peak at ca. 1130 Ma, with minor Meso- and Paleoproterozoic as well as Archean components, presumably derived from the Grunehogna Craton (Perritt, 2001; Marschall et al., 2013). Some ca. 1130 Ma zircons rims surround older Archean-Paleoproterozoic cores, providing direct evidence that the Maud Belt was founded on the edge of the Proto-Kalahari Craton (Grunehogna part; Marschall et al., 2013). The Ritscherflya Supergroup was intruded by voluminous syn-sedimentary mafic sills at ca. 1107 Ma, known as the Borgmassivet intrusives, which have been interpreted as part of the Umkondo LIP (Moyes et al., 1995; Frimmel, 2004).

The Maud Belt can be traced into the Nampula Complex of northeast Mozambique, where almost identical magmatic pulses between ca. 1150 and 1050 Ma are also related to subduction-induced arc magmatism (Bingen et al., 2009; Macey et al., 2010) (n = 60; Fig. 10, Fig. 11). A further continuation into the Southern Irumide Belt of southern Tanzania and Malawi has also been reported (e.g. Kröner et al., 2003, Thomas et al., 2014, Manda et al., 2019).

Magmatism in the Maud Belt and its northwards Mozambiquan continuation had ceased by 1000 to 950 Ma (Fig. 11), but since it is flanked to the east (coordinates as seen in Fig. 10) by the 1000–900 Ma Tonian Oceanic Arc Super Terrane (Jacobs et al., 2015) it likely remained on the margin of Rodinia, unlike most of the other areas investigated in this study.

7. Western Australia data and results

7.1. Geological overview

The Australian continent comprises several ancient Archean crustal blocks (e.g. Yilgarn and Pilbara Cratons) bound together by a vast and potentially partially connected set of Proterozoic orogens (e.g. Albany-Fraser Orogen, Musgrave Province, Eucla Basement). Many of these Proterozoic orogens underwent protracted periods of repeated extension and compression which ultimately juxtaposed the crustal entities of Australia. The exact timing of amalgamation of the fundamental building blocks for the Australia continent (namely the North, West, and South Australian Cratons) is not fully resolved, though likely complete prior to or at 1.29 Ga (Gardiner et al., 2018). These Proterozoic orogens either reflect entirely new crustal additions or represent significant mantle additions into pre-existing Archean crust.

Relevant U-Pb ages from western Australia for this study, in total 199 ages, have been plotted in Fig. 12, relative probability curves are shown in Fig. 13A, and corresponding cumulative age diagrams in Fig. 13B. It should be stressed that this compilation only concerns data from the Albany-Fraser Orogen, Eucla Basement and Musgrave Province in western Australia; data from older Proterozoic orogens have not been included. The diagrams thus do not give a complete picture of the evolution of Australia during the Proterozoic, but only that of the aforementioned Grenville-age belts.

7.2. Albany-Fraser Orogen

The Albany–Fraser Orogen (AFO) is a partially covered Proterozoic crystalline basement block that wraps around the southern and southeastern edges of the Yilgarn Craton, Western Australia, for some 1200 km (Fig. 12). It represents the modification of the Archean craton margin during dominantly hyperextensional processes. The AFO is separated into several discrete lithotectonic domains — Northern Foreland, Biranup Zone, Nornalup Zone, and Fraser Zone. Each zone comprises rocks of Archean origin that have been variably modified by Paleoproterozoic and Mesoproterozoic magmatism (Smithies et al., 2015a). The Musgrave–Albany–Fraser Orogen extends westwards into the Bunger Hills and adjacent areas of Wilkes Land and Queen Mary Land in Antarctica where there is magmatism of similar age (Aitken et al., 2014).

Comparable with other orogenic belts that girdle the Yilgarn Craton (e.g. the Capricorn Orogen), the AFO is dominated by Paleoproterozoic to Mesoproterozoic intrusive rocks formed through a series of cryptic tectonomagmatic events (Smithies et al., 2015a; Spaggiari et al., 2011, 2015). These events involved variable recycling of a range of existing crustal elements and, importantly, also involved periods of refertilisation through juvenile mantle input (Kirkland et al., 2011). Models for the AFO originally inferred accretion of exotic terranes onto the eastern side of the Yilgarn Craton, with the development of a magmatic arc in the Fraser Zone during the Mesoproterozoic (Bodorkos and Clark, 2004). However, U–Pb geochronology, whole-rock geochemistry, isotope and crustal architectural studies have refined this model (Spaggiari et al., 2011, 2015). Current datasets indicate that the AFO contains no exotic lithological blocks (Smithies et al., 2015a). Rather, the orogen reflects the pronounced effects of juvenile mantle input into the Yilgarn Craton in a series of tectonomagmatic events that overprinted, but did not entirely obliterate the parental basement signature (Kirkland et al., 2011, 2015; Smithies et al., 2015a).

Whereas much of the magmatism in the AFO occurred during the main arc-accretion and subsequent reworking / delamination at 1.33 Ga and 1.20 Ga, during AFO Stages I and II, respectively, some igneous rocks in the Biranup and Nornalup Zones record an earlier period of magmatism from 1.81 Ga to 1.65 Ga (Smithies et al., 2015a). This earlier Paleoproterozoic magmatism is considered to have occurred in three discrete events — Salmon Gums Event (1.81–1.80 Ga, n = 3), Ngadju Event (1.77–1.75 Ga, n = 1), and Biranup Orogeny (1.71–1.65 Ga; Kirkland et al., 2011; Smithies et al., 2015a; n = 11, Fig. 13). Although no widespread magmatic rocks older than 1.81 Ga have yet been documented in the AFO, Hartnady et al. (2019) identified metasediments in the northern Biranup Zone containing detrital zircons with U-Pb ages between 1.91 and 1.85 Ga, indicating the presence of older magmatic rocks not currently exposed or recognized. The tectonic setting in which this Paleoproterozoic magmatism occurred has not yet been fully constrained, but it is generally understood to represent an extensional event (Hartnady et al., 2020b; Smits et al., 2014; Spaggiari et al., 2015), with short-lived pulses of compression (i.e. Zanthus Event; Kirkland et al., 2011; Smithies et al., 2015a), possibly reflecting processes similar to those observed in modern accretionary orogens (Hartnady et al., 2019).

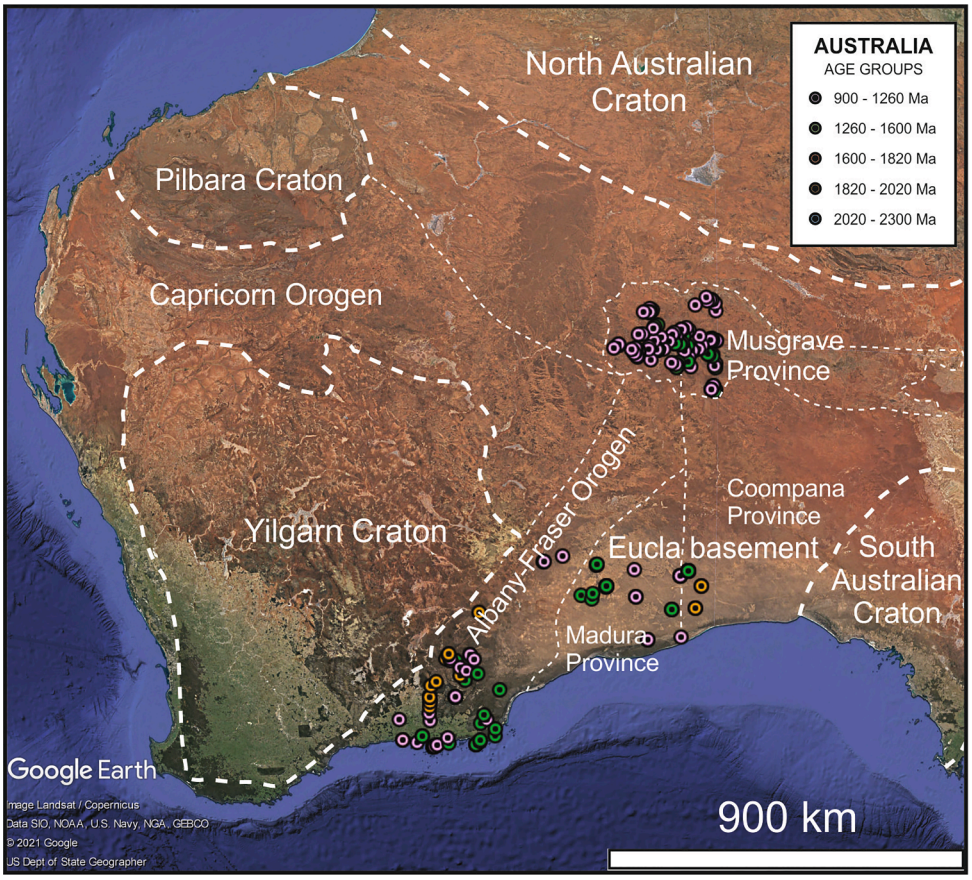

Fig. 12. Google Earth map of western Australia, with main geological provinces (white dashed lines) and magmatic U-Pb age data points indicated.

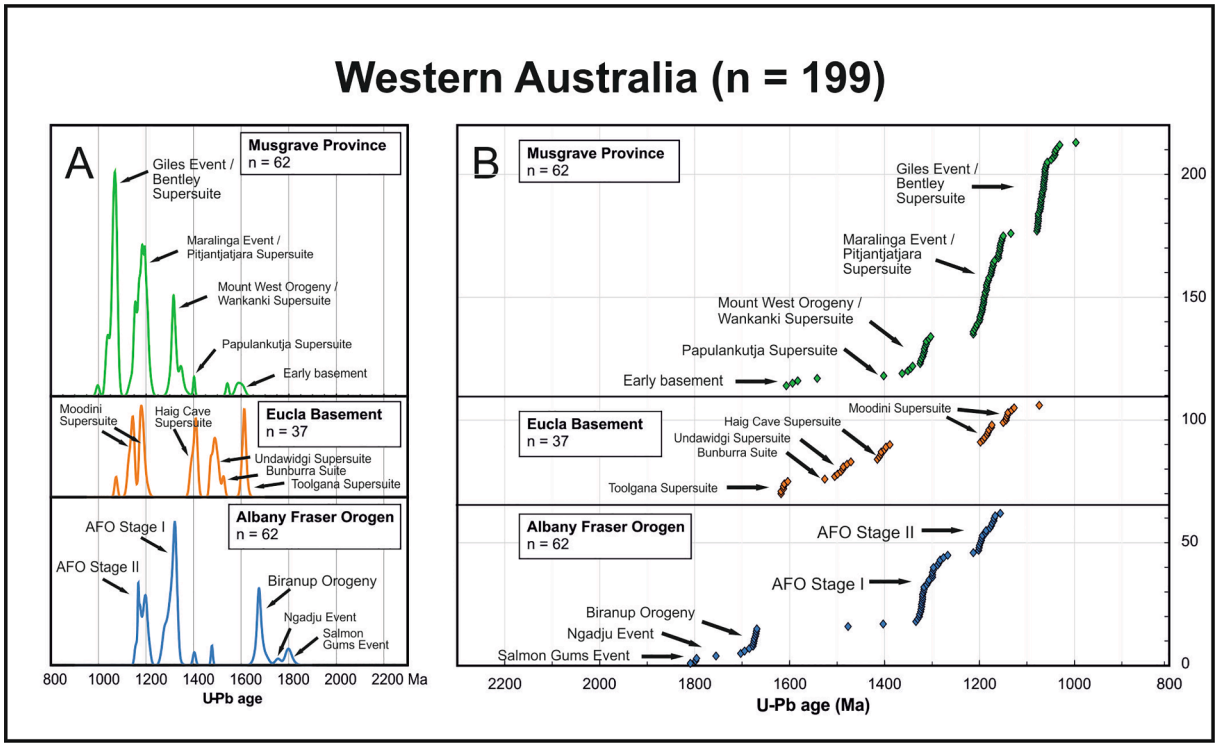

Fig. 13. A. Relative probability curves of magmatic U-Pb ages between 2300 and 800 Ma from the Musgrave Province, Eucla Basement and Albany-Fraser Orogen of western Australia. **B.** Cumulative age diagrams for the Musgrave Province, Eucla Basement and Albany-Fraser Orogen. Note that the age axis in panel B is reverse compared to panel A. For Australia, only age data from Grenville-age provinces were compiled, but not data from older Proterozoic provinces that would have yielded more Paleoproterozoic age peaks.

AFO Stage I at around 1300 Ma (n = 28; Fig. 13) involved the widespread emplacement of granites of the Recherche Supersuite. Magmatism of Stage I age is prolific in the northeasterly trending Fraser Zone, which contains the ca. 1300 Ma Fraser Range Metamorphics (Spaggiari et al., 2009), a series of gabbroic to granitic rocks with layers of migmatised garnet-bearing pelitic and calcic metasedimentary rocks. This lithological package is economically significant for Ni and was metamorphosed to high (granulite) temperatures closely after its formation. Myers (1985) interpreted the mafic rocks of the Fraser Zone as a large layered mafic intrusion, whereas Condie and Myers (1999) argued that it was a stack of accreted magmatic arcs. Metagranitic rocks of ca. 1300–1280 Ma age are also found in the Fraser Range Metamorphics along with the gabbros (De Waele and Pisarevsky, 2008). Initial interpretations of AFO Stage 1 included models of accretion or collision of exotic terranes, with northwest-directed convergence and subsequent collision of the Mawson Craton (Betts and Giles, 2006; Bodorkos and Clark, 2004; Clark et al., 2000; Myers et al., 1996; Spaggiari et al., 2009). Such models implied that the Fraser Zone was a magmatic or oceanic arc, produced through southeast-dipping subduction (Bodorkos and Clark, 2004; Condie and Myers, 1999). However, more recent U–Pb geochronology, whole-rock geochemistry, and Lu–Hf and Sm–Nd isotopic data do not support these interpretations — no exotic components, nor Mesoproterozoic magmatic or oceanic arcs, have been recognized within the orogen (Kirkland et al., 2011; Smithies et al., 2015a; Spaggiari et al., 2009). Moreover, thermodynamic modelling on metagabbroic rocks from the Fraser Zone and surrounding metasedimentary rocks indicate that they were metamorphosed along geothermal gradients in excess of 750 °C/GPa (Clark et al., 2014; Glasson et al., 2019). These recent results, including Archean inherited zircon crystals, support an intercontinental rift or back-arc setting for Stage I for much of the orogen (Kirkland et al., 2011; Spaggiari et al., 2011)

AFO Stage II at 1200 to 1150 Ma (Fig. 13; n = 17) is generally viewed in the context of intracratonic orogenesis, producing craton-directed thrust slices of high grade-rocks (Clark et al., 2000; Myers et al., 1996; Spaggiari et al., 2009). Stage II saw the emplacement of high-temperature A-type and charnockite magmas into the crust across a wide area extending into the Eucla Basement, east of the AFO, and north to the Musgrave Province. Stage II magmas are reflected in the Esperance magmatic supersuite of granites. Such widespread emplacement of high temperature rocks implies lithospheric delamination and appears to have been the process that reworked and stabilized a huge region of Proterozoic central and western Australia. Widespread metamorphic zircon growth throughout most components of the AFO traces Stage II fluid percolation. The exception to this widespread fluid flux was the Fraser Zone that retains little clear evidence of Stage II, with whatever evidence found being restricted to lower temperature thermochronometers within major shears in the Fraser Zone, implying this zone was transferred as a dissected block to the upper crust prior to Stage II (Kirkland et al., 2016).

7.3. Eucla basement

The Eucla Basement comprises the Madura and Coompana Provinces which resides on the eastern side of the AFO and encompasses a vast (ca. 1000 km wide) tract of Proterozoic crust that extends from the modified margin of the Yilgarn Craton to the Gawler Craton in South Australia (Fig. 12). The Coompana Province consists of Precambrian basement rocks to the west of the Jindargna Shear Zone (Dutch et al., 2015), and east of the Mundrabilla Shear Zone (Spaggiari and Smithies, 2015). The Madura Province lies to the west of the Mundrabilla Shear Zone, which in turn abuts the eastern AFO along the Rodona Shear Zone. Although these Proterozoic rocks are buried beneath younger Cenozoic sediments of the Eucla and Bight basins, they have been investigated by a series of drill holes across this region.

The Madura and Coompana Provinces consist of various igneous rocks, from oldest to youngest: The Toolgana Supersuite (1622–1610 Ma, n = 6; Fig. 13) consists of magnesian, calc-alkalic, high-K granitic to dioritic gneisses (Wingate et al., 2015), interpreted to be derived from a subduction-enriched mantle, compatible with a primitive arc setting (Smithies et al., 2015b, c). Rocks of the Bunburra Suite (ca. 1526 Ma; n = 1) and Undawidgi Supersuite (ca. 1490 Ma; n = 7) are metamorphosed syenogranite, monzogranite, tonalite, monzodiorite, syenite, and felsic volcanic rocks (Hartnady et al., 2020a; Jagodzinski et al., 2019; Wade et al., 2007), that reflect recycling of ca. 1600 Ma arc crust of the Toolgana Supersuite, with new mantle input (Smithies et al., 2015b, c). The Haig Cave Supersuite (ca. 1410 Ma, n = 7) comprises metamorphosed granites and gabbros, with adakitic signatures, holding inherited zircon crystals similar in age to the Undawidgi and Toolgana Supersuites (Kirkland et al., 2017). Lastly, the Moodini Supersuite (two pulses between 1200 and 1125 Ma; n = 15; Fig. 13) consists of high-K, Mg-rich shoshonitic rocks with smaller amounts of Fe-rich A-type varieties (Kirkland et al., 2017; Quentin de Gromad et al., 2017).

Distinct from the AFO, both the Madura and Coompana Province reveal Hf isotopic data that indicates a general lack of old evolved crust (Hartnady et al., 2020a; Kirkland et al., 2017). Instead magmatism appears to have been driven by repeated new mantle addition. In the Coompana Province crustal formation commenced by at least 1900 Ma (Hartnady et al., 2020a). Based on the lithological associations retrieved from drill cores, their geochemical affinities to oceanic crust, and the dominantly juvenile Hf isotopic character of the rocks (Kirkland et al., 2017), these provinces are interpreted to define the extent of a vast Proterozoic oceanic arc system that developed outboard of the western Gawler Craton, the eastern Yilgarn Craton and its modified margin (AFO), and the southern Arunta Orogen. This ocean, referred to as the Mirning Ocean, represents a significant volume of contiguous oceanic crust cratonized and frozen in place during injection of the 1220–1150 Ma Moodini buoyant felsic magmas (coeval with granite emplacement into the AFO and Musgrave Province) (Kirkland et al., 2017).

7.4. Musgrave Province

In central Australia, the Mesoproterozoic Musgrave Province defines an east–west-trending belt that is approximately 800 km by 400 km (Fig. 12). The province is bounded to the north and south by younger sedimentary rock basins. It lies where Australia's main Proterozoic structural trends converge and its structure reflects the amalgamation of the North, West (=Pilbara + Yilgarn), and South Australian Cratons. Camacho and Fanning (1995), Camacho et al. (2002), Clarke and Powell (1991), Evins et al. (2010), Glikson (1996), Gregory et al. (2009), Smithies et al. (2011), and White et al. (2002) all provide important contributions to understanding the orogen's basement, but its paleogeographic and tectonic evolution has only recently been synthesized (Howard et al., 2015). Nonetheless, the time of craton amalgamation that swept the Proterozoic orogens of Australia together is still uncertain (Aitken and Betts, 2009; Betts and Giles, 2006; Wade et al., 2006; Wade et al., 2008), although the current consensus is that it was complete by ca. 1290 Ma.

The Musgrave Province was tectonically active during at least five time periods: ca. 1600–1500 Ma, ca. 1350–1300 Ma, ca. 1220–1150 Ma, ca. 1080–1030 Ma (Fig. 13), and ca. 550 Ma. The former two events produced much of the crystalline basement to the Musgrave Province, while the last three occurred in an intracratonic setting likely after amalgamation of Proterozoic Australia.

An even earlier crust production event at 1950–1900 Ma is recorded in the Musgrave Province from Hf and Nd isotopic systematics and recently confirmed with dated juvenile inherited zircons and zircon Hf arrays with mantle oxygen isotopic signatures (Kirkland et al., 2013). This event is distinct from autochthonous processes recorded in the Albany-Fraser Orogen but comparable to the development of now cratonized oceanic crust in the Eucla Basement and potentially stretching towards the Proterozoic Rudall Province on the Pilbara Craton margin.

Additional juvenile material formed at 1600–1550 Ma (Fig. 13; n = 4) and was locally mixed with the 1950–1900 Ma component. In addition, transported unradiogenic Archean material was locally available to mix with 1600–1550 Ma magmas. Paragneiss, mainly included within granite, locally form a significant lithological component of the region (Gray, 1978; Gray and Compston, 1978). Evins et al. (2012) reported that the protoliths to these paragneisses (Wirku Metamorphics) had maximum depositional ages ≤ ca. 1400 Ma, and were derived from ca. 3200–2630 Ma, ca. 1790–1590 Ma, and ca. 1570–1470 Ma sources. Exposures of ca. 1600–1540 Ma orthogneiss also exist (e.g. Edgoose et al., 2004), although their extent and tectonic setting remain poorly understood.

The Papulankutja Supersuite (n = 1), consisting of calc-alkaline granitoids, represents ca. 1400 Ma igneous basement rocks, significantly older than the Wankanki Supersuite of the 1360–1300 Ma Mount West orogeny. A 1402 ± 4 Ma monzogranite has its foliation cross-cut by a 1318 ± 9 Ma granite dyke, indicating deformation and fabric formation prior the Mount West orogeny. The Papulankutja Supersuite may represent subduction-related magmatism associated with the beginning of South Australian Craton impingement on the North Australian Craton.

The Mount West orogeny saw the emplacement of metaluminous, calcic to alkali-calcic granitoids of the 1360–1300 Ma Wankanki Supersuite (Fig. 13; n = 16). These granitoids have geochemical similarities to Phanerozoic granites of the Andean continental arc (Smithies et al., 2010) and may reflect subduction as the North, West and South Australian Cratons finally amalgamated (Smithies et al., 2010; Smithies et al., 2009).

The Maralinga Event saw extensive emplacement of ferroan, alkali-calcic to calc-alkalic granites of the 1220–1150 Ma Pitjantjatjara Supersuite (n = 41). These rocks typically classify as within-plate and A-type and reflect extreme thermal perturbation of the lithosphere. Similar high temperature granitic rocks are found further south in the Madura Province (Moodini Supersuite) and penetrate the AFO (Esperance Supersuite). Such widespread magma bloom may be linked to lithospheric delamination which caused extensive lower crustal melting and effectively welded much of the Proterozoic regions to the adjoining Archean Yilgarn Craton and prevented their subduction.

Voluminous magmas intruded into and erupted across the Musgrave Province during the 1080–1030 Ma Giles Event (Howard et al., 2015); the magmatic expression of the east–west trending Ngaanyatjarra Rift (Evins et al., 2010). This event produced the Bentley Supersuite (n = 36), a sequence of bimodal volcanic rocks probably representing the world's largest accumulation of volcanic products, now located in Central Australia (Smithies et al., 2015d). The regional lithospheric architecture, including thin crust situated between the three cratonic masses of Australia (North, West and South) appears to have sustained a broad zone enriched in mantle-melts beneath the region for a protracted period (Smithies et al., 2015e).

7.5. Other Proterozoic components in Australia

Outside of the geographic area of Western Australia and the Wilkes Land – Albany Fraser Orogen – Madura and Coompana – Musgrave Province system there are other Protozoic orogens cropping out on the Australian continent. A brief discussion of some these components and relevant works is presented here, although no age data from these areas have been included in the present compilation. Further details are provided in the compilation of Neumann and Fraser (2007).

The Georgetown inlier region in northern Queensland consists largely of variably metamorphosed and deformed volcanosedimentary sequences of Palaeo- to Mesoproterozoic age, intruded by Mesoproterozoic granitoids. The eastern margin is in faulted contact with the Palaeozoic Tasman Orogen. The inlier preserves ca. 1700 Ma mafic and sedimentary sequences intruded by ca. 1600 Ma S-type granites (Volante et al., 2020). The Coen inlier, also in Queensland, spans 350 km north to south, 50 km east to west, and has similar ages of sedimentation and metamorphism as the Georgetown inlier (Neumann and Fraser, 2007).

The southern North Australian Craton, known as the Arunta region, consists of a range of individual Proterozoic terranes some of which may reflect rifted components of the same ancestral crustal block. In this region the 1690–1600 Warumpi Province forms the southernmost part of the Arunta region and is separated from an older, 1860–1700 Ma Aileron Province to the north by the Central Australian Suture. Both regions have been unified via their Hf isotopic signature in zircon (Hollis et al., 2013). The Pine Creek Orogen and Arnhem inlier form the northern margin of the North Australian Craton and consist of a sequence of rift sediments on Archean basement which were intruded by syn- to post orogenic granitoids and mafic bodies. This province was deformed and metamorphosed during two episodes of tectonism at ca. 1865–1850 Ma and ca. 1780–1770 Ma (Nixon et al., 2020). The connection, if any, of these other Proterozoic orogenic systems to the Wilkes Land – Albany Fraser Orogen – Madura and Coompana – Musgrave Province is currently unclear (Betts and Giles, 2006; Volante et al., 2020).

8. Discussion

8.1. Overview

The combined age-data of this compilation are shown in Fig. 14, first craton by craton (Fig. 14A), and then combined into one single relative probability curve (Fig. 14B). In these diagrams, data are both shown in unweighted (red curves) and weighted format, according to surface area of the geological provinces and cratonic regions sampled (black curves), to correct for uneven sampling density. The curves are largely similar, with the largest deviations being for the well-sampled 1990 and 1880 Ma peaks in Amazonia and the 1850 Ma peak in Laurentia, which become reduced in the weighted data. In the combined dataset, the largest deviation is in the large 1880 Ma peak, and to some extent also the 1440 Ma peak. For the latter, the weighted peak is instead more dominant.

When evaluating the combined data, it should be remembered that for Kalahari and western Australia, the data compilation was only focused on Grenville-age orogens, with only limited early Mesoproterozoic and Paleoproterozoic data from inliers within those belts included. Thus, the Kalahari and Australia data do not give the full picture of the Proterozoic evolution of those areas, and only the Grenville-age portion of those data are comparable with the Laurentia, Baltica and Amazonia data sets.

The combined diagram (Fig. 14B) shows some minor peaks prior to 2000 Ma, representing eastern Amazonia and the Karelian and Sarmatian parts of Baltica. This is followed by a larger peak at 1990 Ma, mostly reflecting Amazonian data, and the tallest peak centered at 1880 Ma, containing both Amazonian and Baltica (Svecofennian) data, as well as some Kalahari data, and reflecting an important step in the assembly of Columbia. The second tallest double-peak at 1800 to 1770 Ma contains a mixture of Amazonia, Baltica and Laurentia data, while the 1700 and 1660 Ma peaks are dominated by Laurentian data. At this time, the joint external Laurentia-Baltica-Amazonia margin had presumably been established. The Laurentian magmatic gap around 1550 Ma has no counterparts in Baltica or Amazonia; instead, Amazonia shows a broad magmatic peak around this age. The subsequent Mesoproterozoic activity, with a broad peak at 1470 to 1440 Ma and a much sharper peak at 1370 Ma, largely reflects the Laurentian evolution, but there is considerable magmatic activity in Amazonia as well during this period. Following Columbia break-up around 1250 Ma, mirrored by a Laurentian peak (Elzevirian and early Gardar magmatism), the subsequent Grenvillian evolution is seen as a very broad peak between 1200 and 1000 Ma, composed of overlapping more sharp peaks in the different cratons involved.

In Fig. 14A, the width of the panels is proportional to the surface area of the sampled part of each craton, rather than to the number of samples

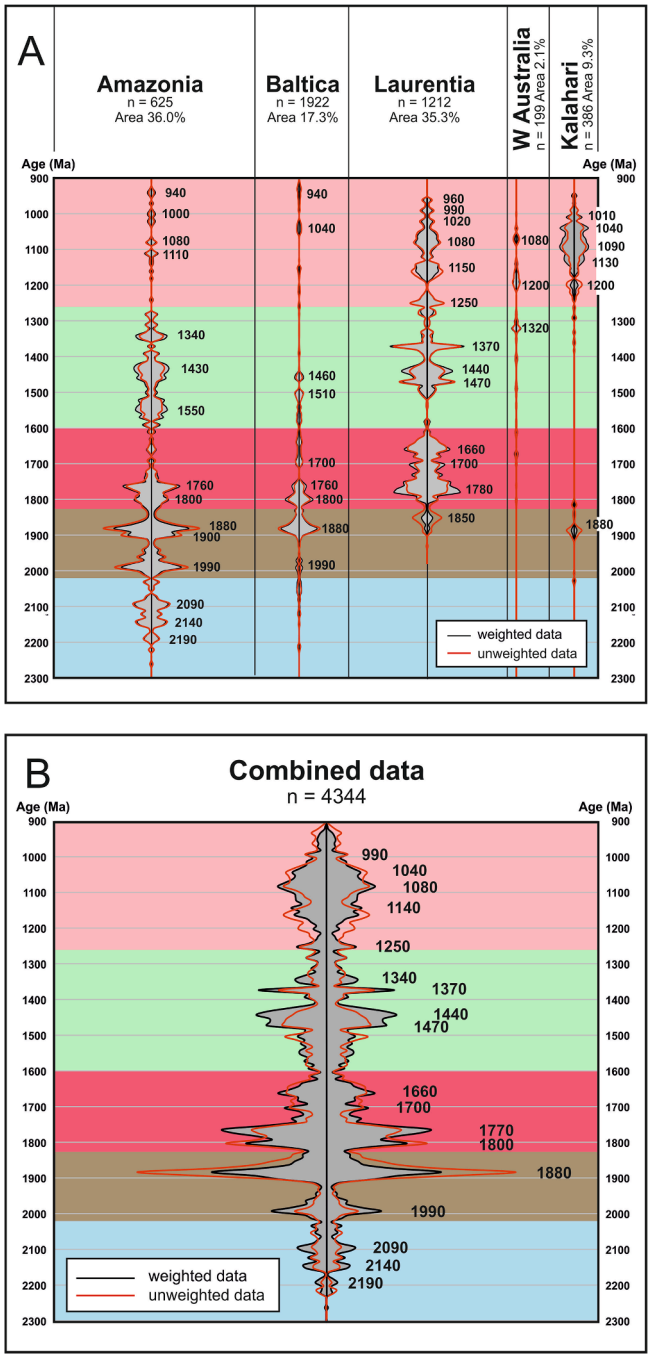

Fig. 14. A. Summary diagram with relative probability curves of U-Pb ages of proto- and syn-Columbian and proto-Rodinian magmatism from Laurentia, Baltica, Amazonia, western Australia and the Kalahari Craton in the time interval 2300 to 800 Ma. The cratons have been ordered according on how similar the curves are, with the width of each panel being proportional to the surface area of the studied parts of that craton. Both unweighted (red) and area weighted (black) curves are shown. n = number of data records from each craton represented by the curves. The area percentage is the surface area of the studied parts of each craton (Proterozoic accretionary orogens and subsequent Grenville-age orogens) as part of the combined area investigated. Background colours relate to the different time interval in which the samples have been subdivided on the Google Earth maps of each craton. Note that the Kalahari and Australia curves are incomplete, as our compilations from these areas only encompass Grenville-age orogens. **B.** Similar diagram as in A for the whole dataset combined. Note that it is not a complete global diagram, since only selected parts of selected cratons are shown.

included in that curve, unlike in the earlier diagrams. The panels representing different cratons have been organized in order of similarity. Table 1. shows correlation factors between the curves of the different cratons or continents. By far the best positive correlation, taking the whole time period 2300 to 900 Ma into consideration, is shown between Baltica and Amazonia, 0.617, whereas the other combinations show relatively low correlations. Western Australia and Kalahari show weak negative correlations to Baltica and Amazonia, and almost zero correlation to Laurentia, but the correlations involving those continents can not be taken at face value, since the Australian and Kalahari data records are very incomplete prior to 1.3 Ga.

The same relationships can be seen in Fig. 15, where the data for the different cratons are plotted as cumulative frequency plots. The Baltica and Amazonia curves are most similar, with a sharp increase prior to ca 1700 Ma. For the interval 2200–1900 Ma, the Amazonia curve shows a larger increase through time than Baltica, but if more data from the Sarmatian part of Baltica had been included, the Baltica curve may have shown a similar increase. The Laurentia curve has a more even slope, with a plateau during the Laurentian magmatic gap between 1600 and 1500 Ma. The Kalahari and western Australia curves, which represent far smaller number of samples (386 and 199, respectively), only from Grenville-age orogens, show a strong increase only after 1300 Ma, reflecting the limited input of older data from those cratons.

Table 1a
Correlation of magmatic ages between all cratons studied during the whole time period 2300 to 900 Ma.

	Laurentia	Baltica	Amazonia	Kalahari	W Australia
Laurentia	…	0.131	0.124	(0.032)	(0.017)
Baltica	0.131	…	0.617	(-0.101)	(-0.131)
Amazonia	0.124	0.617	…	(-0.194)	(-0.204)
Kalahari	(0.032)	(-0.101)	(-0.194)	…	0.119
W Australia	(0.017)	(-0.131)	(-0.204)	0.119	…

Gey values in brackets: Datasets are not really comparable, due to lack of compiled pre-Grenvillian data from Kalahari and western Australia.

Table 1b
Correlation of magmatic ages between Karelia, Sarmatia, and Amazonia from 2300 to 1820 Ma, prior to the full assembly of Columbia.

	Karelia	Sarmatia	Amazonia
Karelia	…	0.234	0.206
Sarmatia	0.234	…	0.369
Amazonia	0.206	0.369	…

Table 1c
Correlation of magmatic ages between Laurentia, Baltica, and Amazonia during the period of assumed Columbia existence, from 1900 to 1260 Ma.

	Laurentia	Baltica	Amazonia
Laurentia	…	−0.013	0.053
Baltica	−0.013	…	0.647
Amazonia	0.053	0.647	…

Table 1d
Correlation of magmatic ages between all cratons studied during Rodinia assembly, from 1260 to 900 Ma.

	Laurentia	Baltica	Amazonia	Kalahari	W Australia
Laurentia	…	−0.166	−0.028	0.297	0.103
Baltica	−0.166	…	−0.191	−0.137	−0.180
Amazonia	−0.028	−0.191	…	0.176	−0.194
Kalahari	0.297	−0.137	0.176	…	−0.004
W Australia	0.103	−0.180	−0.194	−0.004	…

Figs. 16–18 show more detailed comparisons of certain time intervals from certain cratons. Fig. 16 shows a comparison of 2300 to 1920 Ma magmatism in the Karelian and Sarmatian parts of Baltica, and in Amazonia, before the assembly of Columbia. Fig. 17 shows a comparison between the Sveconorwegian Province of Baltica and the Grenville Province of Laurentia from 2000 to 900 Ma. Fig. 18 shows a comparison of Grenville-age magmatism in all cratons involved in this study during the Proto-Rodinian to Rodinian stage from 1260 to 900 Ma.

It is obvious from the diagrams, and especially from Fig. 14, that magmatism did not proceed at an even pace, but that alternating periods of strong magmatic and/or orogenic activity were separated by quieter periods in all the continents studied. These observations provide important constraints on the hypothesis that Laurentia, Baltica and Amazonia formed one continuous accretionary orogen along the margin of Columbia (the GPAO of Condie, 2013), and that all five cratons subsequently became involved in the same collisional orogenic belt forming Rodinia, but they can not be used to prove or disprove any particular relationship.

An alternative possibility would be that the irregularities seen are largely a result of differential preservation of an originally more smooth magmatic record (cf. Hawkesworth et al., 2009). Whereas intra-plate magmatism and continental arc magmatism presumably would have similar, and rather high, preservation potentials, it is conceivable that rocks formed in oceanic arcs were rapidly recycled back into the mantle, and whole oceanic arcs may thus have been lost if they were never accreted to any continental margin. Moreover, older continental rocks may be recycled during younger orogenic events, such as the Grenville-Sveconorwegian, and thereby lost from the geological record. However, we find it unlikely that the large differences seen between magmatic peaks and troughs in most diagrams primarily are caused by differences in preservation, and instead chiefly attribute them to real local or regional differences in magmatic activity.

In a simplistic model, it could be assumed that magmatic and orogenic events along the GPAO were penecontemporaneous, reflecting periods of more or less intense subduction, or alternating advancing or retreating subduction zones. Such a relation would result in a strong positive correlation between magmatic events, as observed for Baltica and Amazonia. However, it is unlikely that one single continuous subduction zone ran along the whole Laurentia-Baltica-Amazonia margin, a distance of some 10 000 km (one quarter of the circumference of the Earth), and that the magmatic activity increased or decreased, or perhaps came to a complete stand-still, at the same time along the whole margin. Detailed studies of younger orogenes typically show complex behaviour in both space and time, e.g. in Paleozoic eastern Australia (Foster and Gray, 2000). Similar to the present-day Pacific margin, the Columbia margin would doubtless have shown large lateral variations, being fringed by several shorter subduction zones, continental and oceanic arcs, back-arc basins, rifted continental blocks, transform faults, etc, causing different geodynamic situations at different segments of this margin at the same time (c.f. Spencer et al., 2019). Slower subduction and less activity along one segment may have been compensated by faster subduction and more intense activity along another, leading to a negative correlation of events.

Similarly, collision between the different cratons would have proceeded at a different pace and at different angles, commencing and finishing at different times, leading to different sequences of magmatism. In particular, whether a continent formed the upper or lower plate in a continent collision scenario would have seriously affected the style, timing and intensity of the magmatism it underwent.

Although neither proving nor disproving any particular Proterozoic plate tectonic configuration or supercontinent reconstruction, this review may assist when discussing different scenarios. In the following sections, we discuss the data using the above diagrams along with a series of sketch maps (Fig. 19) depicting the magmatism and inferred plate tectonic situation during each of the time intervals in which the samples have been subdivided. Fig. 19 is also complemented by two animations of the data, available as supplementary electronic files.

8.2. 2300 – 2020 Ma period

During the first time period, 2300 to 2020 Ma, neither Columbia nor its constituents Laurentia and Baltica were assembled, but consisted of

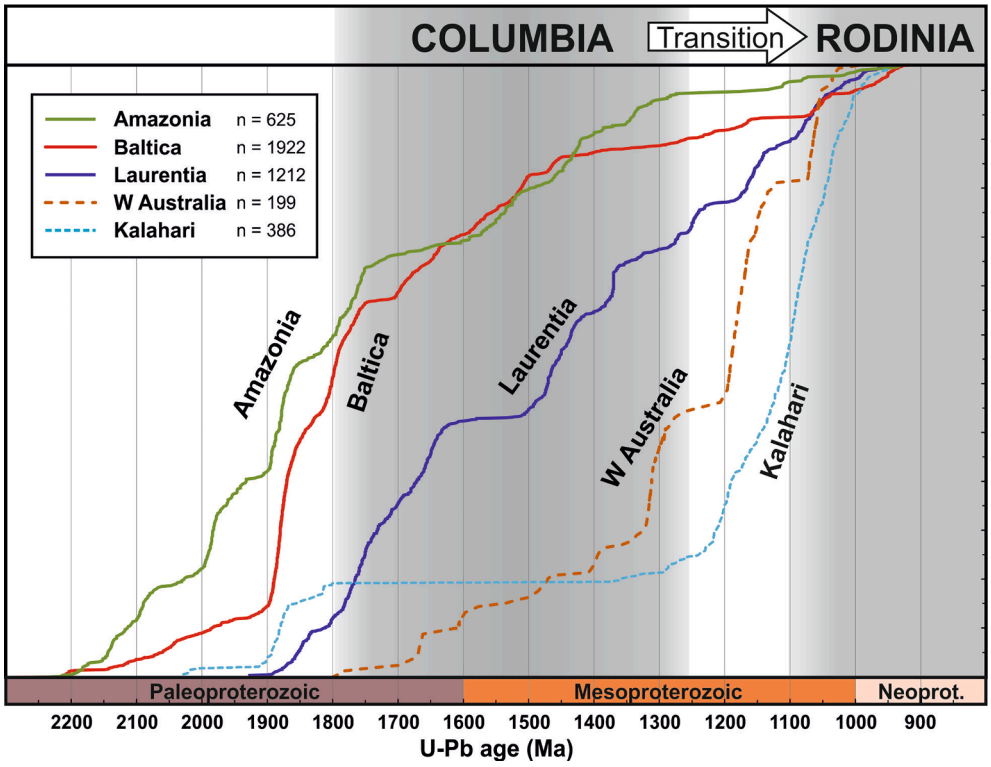

Fig. 15. Comparison of cumulative frequency plots for Amazonia, Baltica, Laurentia, W. Australia and Kalahari during the time interval 2300 to 800 Ma. n = number of data records from each craton represented by the curves. Since the cumulative frequency plots only cover the external proto- and syn-Columbian magmatism along the GPAO and penecontemporaneous intraplate magmatism, but not internal orogenic belts during the same period, and proto-Rodinian magmatism along subsequent Grenville-age belts, these curves do not show the full growth of the continents in question during the above period, but mainly their external growth. Note that the Kalahari and Australia curves are especially incomplete, as our compilations from these areas only encompass Grenville-age orogens, but not older Proterozoic provinces.

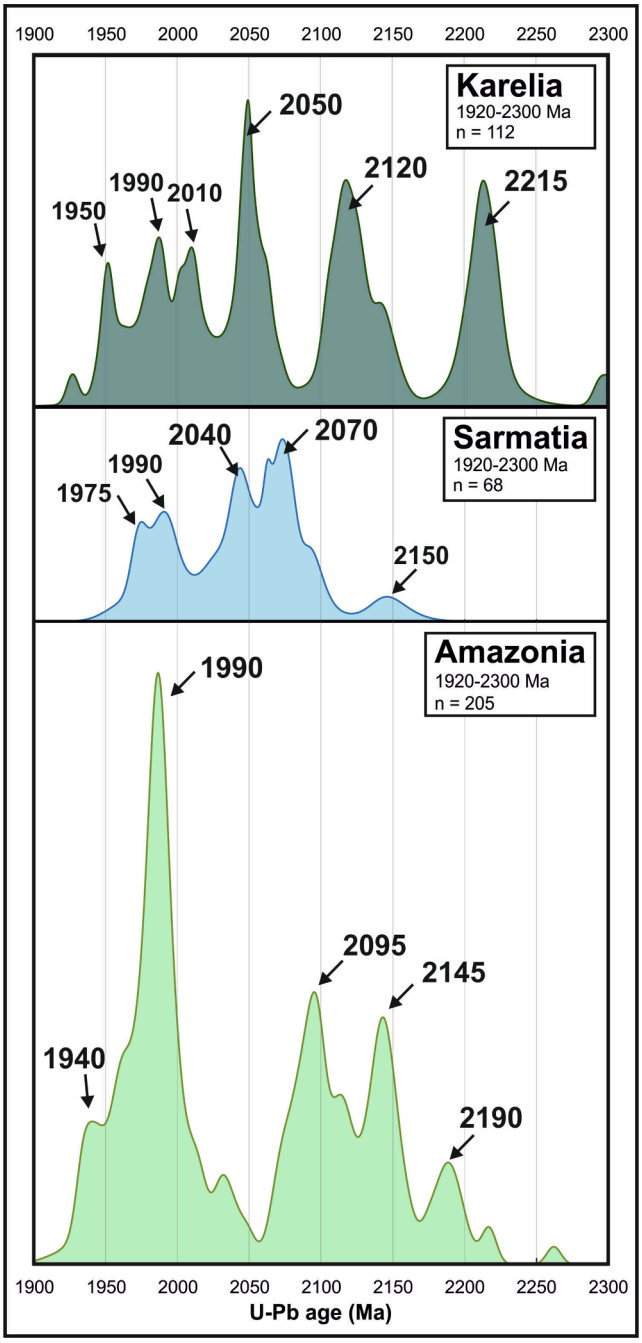

Fig. 16. Relative probability diagram giving a more detailed comparison of magmatic U-Pb ages in Karelia, Sarmatia and Amazonia in the time interval 1920–2300 Ma. No area correction (unweighted data). Height of panels is proportional to the number of sample records from each province during this time interval.

several separate proto-cratons. Within our area of interest, magmatic activity was largely restricted to the Karelian and Sarmatian proto-cratons of Baltica, and to eastern Amazonia (Fig. 16). Proterozoic magmatism within, or in between, the Archean cratons of northern Laurentia has not been included in our compilation. Magmatism within the Karelian proto-craton was largely mafic and extension-related, but also includes some intermediate and felsic rocks. Karelia (NE Fennoscandia) would have been separate from Sarmatia and Amazonia at this time, so its magmatism would have been unrelated to the magmatism in those proto-cratons.

Sarmatia and eastern Amazonia, however, could potentially have been united already at this stage (cf. Terentiev and Santosh, 2020). Both of them consist of a number of smaller Archean blocks, surrounded and intersected by early Paleoproterozoic magmatism. Our Sarmatia data have been restricted to orogenic belts in western Sarmatia, from which the two age peaks at 2070 and 2040 Ma are derived (Figs. 5, 6 and 16). Eastern Amazonia show peaks at 2190, 2145 and 2095 Ma that are broadly related to the Transamazonian orogeny. They have no obvious Sarmatian counterparts in Fig. 16, but it is conceivable that if we had included magmatism further east in Sarmatia, there would have been more ages above 2.1 Ga also from Sarmatia.

8.3. 2020 – 1820 Ma period

Magmatism during the first half of this period, 2020 to 1920 Ma, was still largely restricted to Karelia, Sarmatia and eastern Amazonia (Fig. 16). Leaving Karelia aside, Sarmatia and Amazonia both show a marked peak at 1990 Ma, but with a tail going down to ca. 1940 Ma. In Sarmatia, this magmatism is concentrated to the Osnitsk-Mikashevychi Igneous Belt along the western margin of the proto-craton. In Amazonia, the very marked 1990 Ma peak is a combination of magmatism related to the Tapajos orogeny, and magmatism related to the Orocaima SLIP and other nearby post-tectonic rocks. A possible interpretation, given the elongated shape of the Orocaima SLIP, wrapping around the older (Archean and Transamazonian) crust to the northeast, would be that the Orocaima rocks constitute a southwards (in present-day coordinates) continuation of the Osnitsk-Mikashevychi Belt in Sarmatia.

Correlation factors between magmatic ages in Karelia, western Sarmatia, and eastern Amazonia from 2300 to 1820 Ma, prior to and during Columbia assenbly, are shown in Table 1B. They are moderately positive (0.206, 0.234, 0.369), with the highest correlation between Sarmatia and Amazonia.

At ca 1900 Ma, magmatic activity increased considerably (Fig. 14). Along the western Sarmatian margin, activity continued along the Okolovo Belt and Belarus-Podlasie Granulite Belt (BPG, Fig. 5), although these are poorly represented in our database. Further northwest, in the Svecofennian Province of central Fennoscandia, there was a significant pulse of magmatic activity between 1910 and 1870 Ma, forming the bulk of the exposed crust in this area.

The Svecofennian Province consists of several lithotectonic units, separated by NW-trending dextral crustal-scale shear zones, where the bulk of the crust formed within a relatively short time interval of 1910 to 1870 Ma (cf. Stephens and Bergman Weihed, 2020; Figs. 6 and 14). These are often perceived as separate volcanic arcs which formed outboard of, and accreted to, the Karelian margin in the northeast (e.g. Korja et al., 2006; Lahtinen et al., 2005, 2008; Stephens and Bergman Weihed, 2020, and references therin). However, it is conceivable that much of this crust, especially in southern Finland and central Sweden (Bergslagen unit) formed along a more continuous elongated volcanic arc towards the southeast, outboard of western Sarmatia or in the closing gap between Sarmatia and Fennoscandia. As Sarmatia approached and eventually collided obliquely with Fennoscandia at 1800 to 1750 Ma (cf. Bogdanova et al., 2015, and references therein), it acted as a bulldozer that segmented the Svecofennian arc into several crustal blocks, which were transferred in a northwesterly direction and formed the large tract of 1910 to 1870 Ma crust in central Fennoscandia.

Magmatism of similar age in Amazonia is partly related to continued activity along a continental arc in the Ventuari-Tapajos Province and the Amoguijá arc in the Rio Apa Craton, but also to the intraplate Uatumã SLIP within the Central Amazonian and Ventuari-Tapajos Provinces (Fig. 8), which forms a marked peak at 1880 Ma (Figs. and 14).

Magmatism in the Ketilidian, Makkovikian and Penokean orogens of Laurentia is slightly younger, with a first peak at 1850 Ma. There is also some magmatism inside the Grenville Province and in the Mojave Province around 1850 Ma (Figs. 3, 4 and 14). The somewhat patchy distribution of magmatism of this age along the Laurentian margin may be due to the fact that Laurentia was not fully assembled at this time. The

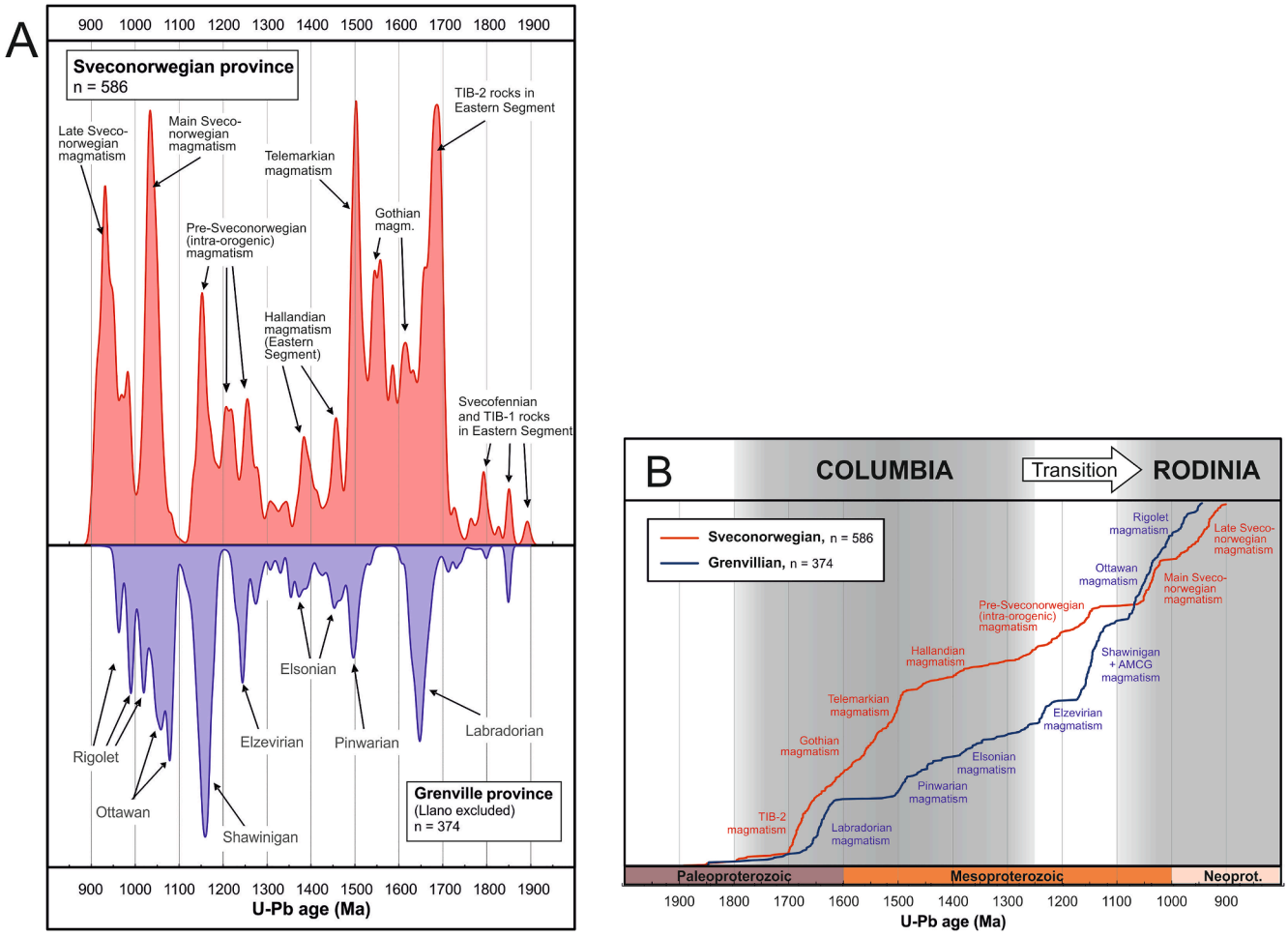

Fig. 17. A. Relative probability diagram giving a more detailed comparison of magmatic U-Pb ages in the Sveconorwegian Province in Baltica and the Grenville Province (Llano part excluded) in Laurentia during the time interval 2000 to 800 Ma. No area correction. Height of panels is proportional to the number of sample records from each province. **B.** The same data as a cumulative frequency plot comparing the Sveconorwegian and Grenville Provinces.

Ketilidian and Makkovikian Orogens formed outboard of the North Atlantic Craton, the Penokean Orogen and the early magmatism within the Grenville Province formed outboard of the Superior Craton, and early magmatism within Mojave Province close to the Wyoming Craton. However, it could also be a matter of preservation, since subsequent Grenvillian tectonism may have destroyed evidence for more extensive Paleoproterozoic magmatism along the Canadian Superior margin.

From Kalahari and western Australia, we only focused on the magmatism within the Grenville-age orogenic belts. Nevertheless, the Namaqua sector of the Namaqua-Natal Belt of Kalahari contains inliers with Paleoproterozoic magmatism at ca. 2000 Ma (Sperrgebiet Domain), ca. 1900 Ma (Richtersveld Magmatic Arc), and shortly before 1800 Ma (Steinkopf Domain; Fig. 11).

8.4. 1820 – 1600 Ma period

The beginning of this period saw the final assembly of at least the Laurentia-Baltica-Amazonia part of Columbia, depicted in the reconstruction in Fig. 1A (but cf. Pisarevsky et al., 2014, in Fig. 1B, where Amazonia was separate from Laurentia and Baltica), and thus the establishment of a long-lived continuous external Laurentia-Baltica-Amazonia active margin. The different parts of Australia may not have collided with western Laurentia until around 1600 Ma (e.g. Furlanetto et al., 2013, 2016; Pourteau et al., 2018; Nordsvan et al., 2018; Kirscher et al. 2019; Gibson and Champion, 2019; Gibson et al., 2020), and the position of Kalahari relatve to Columbia remains unconstrained.

There is an apparent lull in magmatic activity between ca. 1850 and 1820 Ma, possibly due to reorganization of subduction accompanying the assembly of Columbia. Magmatism, however, quickly resumed with a double peak at 1800 and 1760 Ma in Baltica and Amazonia, and a single peak at ca. 1780 Ma in Laurentia (Fig. 14). The 1800 Ma peak in Baltica is dominated by late- and post-orogenic magmatism within the Svecofennian Orogen, along with the TIB-1 phase of subduction-related magmatism in the Transscandinavian Igneous Belt and its continuation in the basement of Poland (Figs. 5 and 6). Both these types of magmatism continued until about 1750 Ma, overlapping with the intraplate AMCG magmatism of the Prutivka-Novogol LIP in Sarmatia that culminated around 1760 Ma (Figs. 5 and 6; Shumlyanskyy et al., 2021).

Magmatism in Amazonia between 1800 and 1750 Ma (with a peak at 1760 Ma) is dominated by activity related to the Juruena orogeny, such as the Alta Floresta SLIP that may represent peak magmatism previously attributed to the Colider volcanics and Teles Pires Suite. Much of this magmatism is similar in style and tectonic setting to the TIB-1 magmatism in Baltica, and occurs along the boundary between the Ventuari-Tapajos and Rio Negro-Juruena Provinces (Figs. 7, 8 and 14). In Laurentia, the dominant 1780 Ma peak mainly consists of rocks in the Yavapai and Mojave Provinces, with a smaller contribution from the Mazatzal Province, but also magmatic suites within the Penokean and Ketilidian Provinces (Figs. 3 and 4).

The magmatism in Laurentia continued until ca 1600 Ma, waning in the Mojave and Yavapai Provinces, but with strong peaks around 1650 Ma in the Mazatzal Province and in the Canadian Grenville Province,

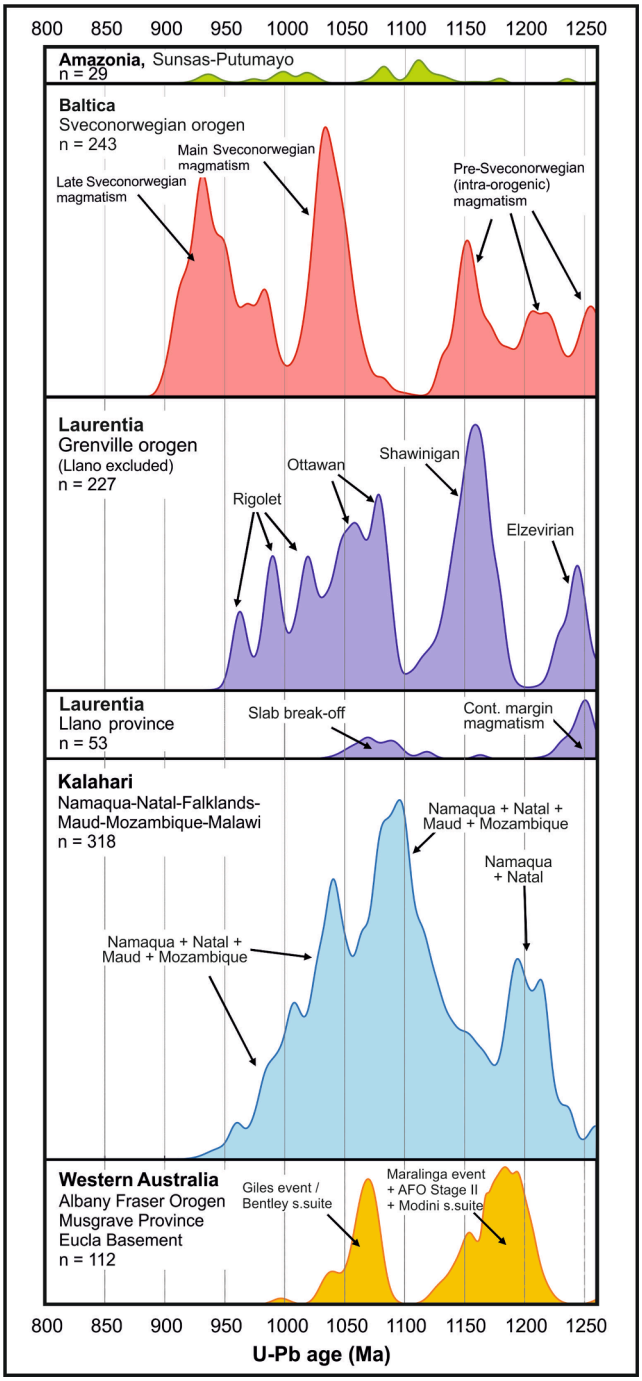

Fig. 18. Relative probability curves giving a more detailed comparison of U-Pb ages during the time interval 1260 to 900 Ma from the proto-Rodinian (Grenville-age) orogens in Laurentia, Baltica, Amazonia, Kalahari and western Australia. No area correction. The height of each panel is proportional to the number of sample records within the time-range in question from the respective area. The panels have been placed in an approximate order of neighbourhood for the cratons in question in Rodinia.

where it marks the Labradorian orogeny (Figs. 3, 4, 14 and 17). In contrast, Amazonia and Baltica showed a decline in magmatic activity after 1750 Ma. After an almost total magmatic lull, activity along the Transscandinavian Igneous Belt resumed around 1700 with the TIB-2 phase, followed by the double peaks of Gothian magmatism in the Sveconorwegian Province and intraplate rapakivi magmatism in the Svecofennian Province at around 1650 and 1550 Ma (Figs. 5, 6 and 17). Unlike the TIB-1 and TIB-2 magmatism, the Gothian magmatism in southwest Sweden and southern Norway, as well as subsequent Mesoproterozoic magmatism in the same areas, occurred further west or northwest compared to its present-day location, which results from large-scale Sveconorwegian crustal shortening.

A possible reason for the greater similarity between the Baltica and Amazonia magmatic record during this period, and in general, compared to between Baltica and Laurentia, could be if the Baltica and Amazonian margins were located inboard of a common subduction zone, whereas the Laurentian margin was located along a separate, independent, subduction zone, as depicted in Fig. 1A. This, however, is somewhat at odds with the model of Martin et al. (2020), who based on different Hf and Pb isotope signatures, suggested that Laurentia and Baltica formed a joint retreating accretionary orogenic system, and Amazonia and Kalahari a joint advancing orogenic system, along the margin of Columbia/Nuna, which then collapsed onto themselves to form the collisional Grenvillian orogen of Rodinia.

It appears that many Amazonian Proterozoic magmatic sequences, including SLIP activity, contain a higher proportion of older crustal components, as seen from Hf and Nd isotope data, compared to the largely juvenile Proterozoic crust in Baltica (Stephens and Bergman Weihed, 2020, and references therein). In Baltica, there is only very limited evidence of such older inheritance outside of the Archean Karelian craton margin, with most Hf and Nd data being near-chondritic or mildly depleted (weakly positive).

In western Australia, magmatic and orogenic activity occurred in pulses between 1800 and 1670 Ma within the Albany-Fraser Orogen; in the Eucla Basement and Musgrave Province magmatism started just before 1600 Ma (Fig. 13). Kalahari was quiet during this period.

8.5. 1600 – 1260 Ma period

After the final Mazatzal magmatism just after 1600 Ma, there is a distinct absence of magmatic activity in Laurentia that lasted to almost 1500 Ma (Figs. 4, 14A and 17). In Baltica, Gothian magmatism in the future Sveconorwegian Province continued, and was accompanied by the second pulse of intraplate rapakivi magmatism in central Fennoscandia around 1550 Ma (Figs. 6, 14A and 17). In Amazonia, magmatic activity between 1600 and 1500 Ma occured in the Cachoeirinha and Rio Alegre arcs of the Rondonian-San Ignacio Province, accompanied by the intraplate Serra da Providencia suite intruding the Jamari Complex in the same province (Figs. 9 and 14A).

In Laurentia, the magmatic lull is followed by Pinwarian magmatism in the Grenville Province around 1500 Ma and the intraplate magmatism of the Granite-Rhyolite Province in the central USA, along with similar types of A-type magmatism in adjacent provinces, divided into two sharp age peaks around 1460 Ma (dominating in the eastern part) and 1370 Ma (dominating in the southern part). In southern Greenland, the first phase of the intraplate Gardar magmatism took place between 1300 and 1260 Ma, heralding the break-up of Columbia. Within the Grenville Province, the sharp Pinwarian magmatic peak at 1500 Ma was followed by two more subdued peaks of Elsonian magmatism at ca 1470 to 1350 Ma (Fig. 17). This pattern is closely mimicked in the Sveconorwegian Province of Baltica by the sharp Telemarkian peak around 1500 (in the Telemarkia Terrane of southern Norway), followed by a less sharp Hallandian double-peak at 1460 and 1380 Ma (in the Eastern Segment of the Sveconorwegian Orogen in southern Sweden), posing the possibility of a strong geodynamic connection between the neighbouring Grenvillian and Sveconorwegian Provinces during this time period. The Telemarkian magmatism shows a volcanic arc signature in the west and a back-arc rift signature further east, but was originally located further to the west or northwest. The little understood Hallandian tectonomagmatic event, in contrast, occurred inboard of the Fennoscandian continental margin, and its early phase was accompanied by Dalopolonian A-type intraplate magmatism at around 1460 Ma in neighbouring southeast Sweden, Bornholm, and the basement of the southern Baltic Sea, Poland and Lithuania (the Southern Fennoscandia anorogenic

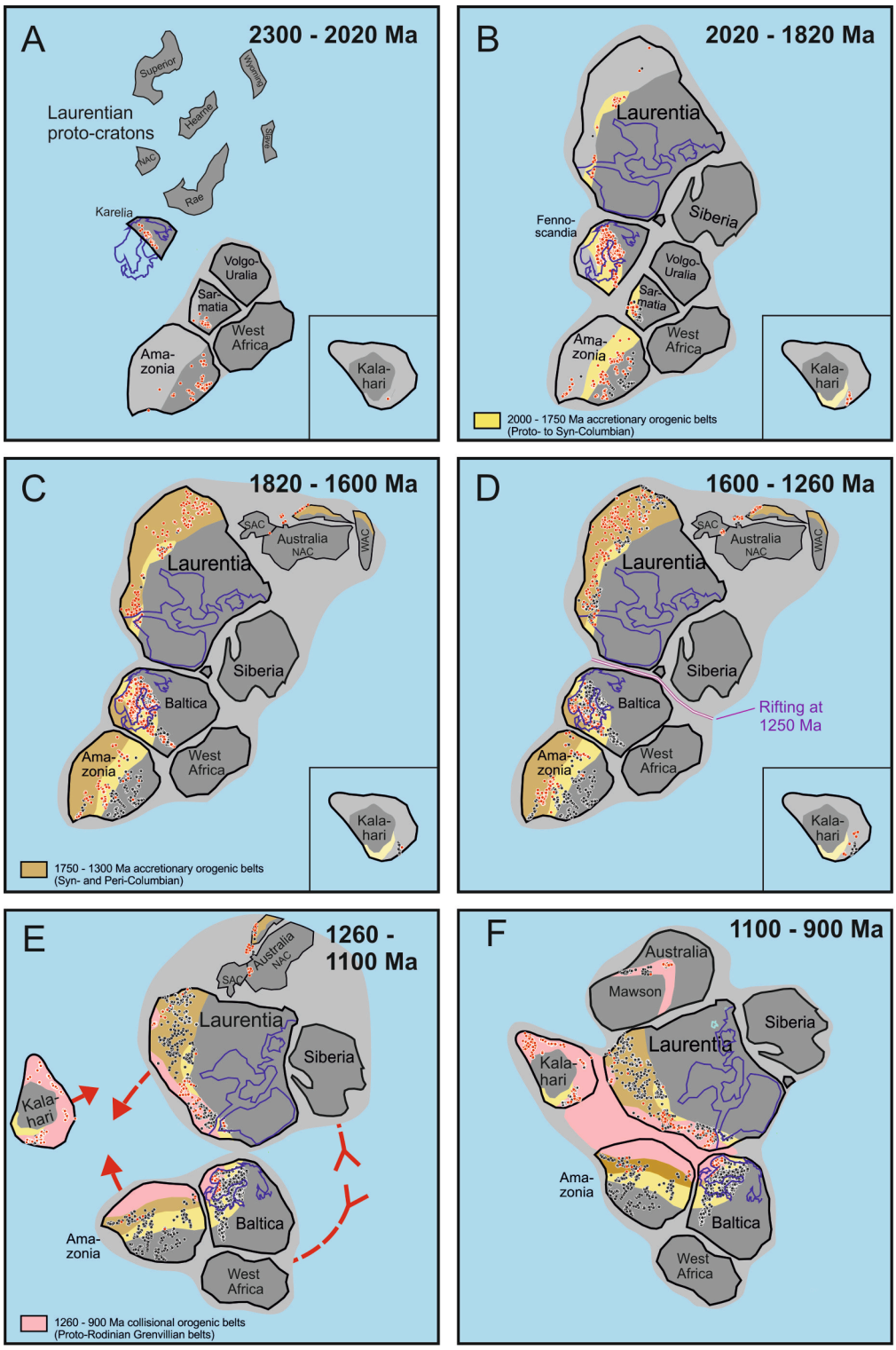

Fig. 19. A set of six maps, at 2020 Ma, 1820 Ma, 1600 Ma, 1260 Ma, 1100 Ma and 900 Ma, showing approximate relative positions of cratons at the end of each time interval, and active magmatism (red sample dots) in the studied parts of Laurentia, Baltica, Amazonia, Kalahari and western Australia during the preceding time interval (the first interval starting at 2300 Ma). Grey dots are samples from the earlier time intervals. Yellow areas: 2000–1750 Ma accretionary orogens along the margin of Columbia; Light brown areas: 1750–1300 Ma accretionary orogens along the margin of Columbia; Pink areas: 1260–900 Ma "Proto-Rodinian" collisional orogens. Rifting of Columbia and rotation to form Rodinia are shown schematically in panels D and E, respectively. In panel A, Volgo-Sarmatia is shown as one block together with West Africa and eastern Amazonia, separate from Karelia (northern Fennoscandia). As Laurentia was yet not united prior to 1850 Ma, it is shown as its constituent Archean cratons (drawn after figure 1 in St-Onge et al., 2009) in panel A, separated some random distance. Columbia is kept in the same position throughout its existence. Kalahari is shown as separate inset maps in panels A to D, since its location with respect to Columbia is highly uncertain. All magmatism is shown in its approximate present-day location relative to each craton, even though some of it probably occurred along island arcs or in microcontinental fragments outboard of the continental margin at that time. An animation (powerpoint file) using the same maps and data set is provided as an electronic supplement, showing the magmatism in 50 m.y. increments.

province in Fig. 5, which also includes the somewhat older (1500–1550 Ma) Mazury AMCG complex in northeast Poland).

In the Rondonian-San Ignacio Province in SW Amazonia, the Santa Helena and Alto Guaporé arc magmatism yields a strong peak around 1430, followed by another peak around 1340 Ma related to the accretion of the Paraguá Terrane that resulted in the formation of the Pensamiento granitoid complex (Bolivia), as well as the early phases of the Putumayo orogeny in NW Amazonia (Colombian part). It would appear that subduction-related magmatism continued more uninterrupted along the Amazonian margin during this period, compared to in Baltica and Laurentia, where magmatism was dominantly of intraplate type (possibly with the Grenville Province as an exception).

However, several intraplate AMCG suites also intruded in inboard positions in Amazonia during the same period, such as the Parguaza Suite in northern Amazonia (Venezuela). There has been much debate concerning the dominance and cause of intraplate rapakivi-type, anorogenic, A-type or AMCG-type magmatism within large parts of Columbia, both in Laurentia, Baltica, Amazonia and elsewhere, during the Mesoproterozoic. According to some models, this magmatism reflects a large mantle plume or superplume with attempted break-up of Columbia, or overheating and melting of the upper mantle, followed by magmatic underplating and melting of the overlying crust, due to the thermal insulation effect of a large and relatively stationary supercontinent (Anderson, 1983; Anderson and Bender, 1989; Hoffman, 1989; Windley, 1993; Anderson and Morrison, 2005; Frost and Frost, 2013). Other models see it as a distant inboard effect of contemporaneous subduction-related magmatism along the margin of Columbia (e.g. Åhäll et al., 2000; Nyman et al., 1994; Nyman and Karlstrom, 1997; Bickford et al., 2015). We hope that this geochronological overview may assist in future discussions.

In Kalahari, magmatism resumed at around 1360 Ma in the Namaqua Sector of the Namaqua-Natal Belt (Fig. 11). In western Australia, there are several pulses of magmatism in the Eucla Basement and Musgrave Province between 1820 and 1300 Ma. In the Albany-Fraser Orogen, magmatism resumed around 1330 Ma with AFO Stage 1, which ended at 1260 Ma (Fig. 13).

In Table 1C, correlation factors between magmatic ages along the GPAO in Laurentia, Baltica, and Amazonia during the time period of presumed Columbia assembly and existence, from 1900 to 1260 Ma, are shown. Correlation between Baltica and Amazonia is even higher for this time period, 0.647, compared to the whole 2300 to 900 Ma period (0.617, Table 1A), whereas Laurentia-Baltica and Laurentia-Amazonia correlations are virtually zero during the time of Columbia existence.

8.6. 1260–900 Ma period

The break-up of Columbia may have started already with the intraplate magmatism around 1450 Ma. However, the main phase of break-up is generally assumed to have started around 1260 Ma, marked by the intrusion of the giant Mackenzie dyke swarm in Canada and the Central Scandinavian Dolerite Group (CSDG) in Fennoscandia at this time (not included in our compilation). Break-up and separation, however, did not occur along the Mackenzie swarm or in central Scandinavia, but in between Fennoscandia and Greenland. The early pulse of Gardar alkaline magmatism in southernmost Greenland around 1270 Ma would have been closely related in time to this break-up.

In the Grenville Province of Laurentia, Elzevirian magmatism started at about the same time and peaked at 1250 or shortly thereafter (Figs. 17 and 18). The same magmatism is also seen in the Llano segment and other uplifts in Texas (Mosher, 1998; Bickford et al., 2000). This magmatism is normally assumed to have originated in a magmatic arc outboard of the Laurentian margin (Mosher, 1998), which accreted to Laurentia during the subsequent orogeny. This would suggest that subduction, at least initially, occurred on the Laurentian side of the closing Grenville ocean. On the Baltica side, so called Pre-Sveconorwegian or Intra-orogenic magmatism occurred in three pulses at around 1260, 1220 and 1150 Ma (Figs. 17 and 18). This magmatism is often bimodal, and may be considered to be extension- rather than subduction-related. The marked gap in the magmatic record seen in the Grenville Province around 1200 Ma is not observed in the Sveconorwegian Province of Baltica (Figs. 17 and 18).

Magmatism in Amazonia around this time appears rather scattered and less intense, but this is probably due to limited sampling (Figs. 9 and 18). In Kalahari, magmatism was underway both in the Namaqua and Natal Sectors by 1200 Ma, with a marked peak in the Namaqua Sector at this age. It started slightly later in the Maud Belt of Antarctica and its northwards continuation into northern Mozambique and Malawi at around 1150 Ma (Figs. 11 and 18). In western Australia, a magmatic gap is seen around 1250 Ma, followed by intense magmatic activity both in the Albany-Fraser Orogen (AFO Stage II), the Eucla Basement (Moodini Supersuite), and the Musgrave Province (Maralinga Event) from 1210 to 1120 Ma, when another magmatic gap followed (Figs. 13 and 18).

The main phase of Grenville orogenic activity in Laurentia is often taken to have commenced after the Elzevirian orogenic pulse, and is comprised of three orogenic and magmatic phases, the Shawinigan, the Ottowan and Rigolet, clearly seen in Figs. 4, 17 and 18. The Shawinigan phase, with a strong peak around 1170 Ma, largely consists of AMCG magmatism, but is also accompanied by orogenic deformation. Prior to the main collisional Ottawan phase at 1090 to 1050 Ma, there is another gap at 1100 Ma seen in our data, which is also seen in Baltica, Amazonia and western Australia, but not in Kalahari (Fig. 18). However, this gap coincides with the strong extension-related mafic magmatism within the Mid-Continent Rift System (Keweenawan rift) in Laurentia, as well as the Umkondo mafic LIP in Kalahari (Hanson et al., 1998, 2004; de Kock et al., 2014; Choudhary et al., 2019), neither of which were included in our compilation. Possibly, subduction-related magmatism was shutting down on all continents except Kalahari in connection with these mantle-generated LIP events.

The collisional Ottawan phase, with a double-peak at 1080 and 1060 Ma, is followed by the post-collisional Rigolet phase in the Canadian Grenville Province, with three magmatic subpeaks at 1020, 990 and 960 Ma (Fig. 18). In the Sveconorwegian Province, the early Sveconorwegian syn-orogenic magmatism of the Sirdal belt in western Norway is slightly younger than the Ottowan phase, starting at 1065 Ma, peaking around 1040 Ma and continuing to 1010 Ma. The late Sveconorwegian post-orogenic magmatism, consisting of the ferroan hornblende-biotite granite suite and the Rogaland AMCG complex, commenced at 1000 Ma, peaked around 930 Ma, and ended with late-stage pegmatites at 900 Ma, about 50 million years later than the end of the Rigolet phase in Canada (Fig. 18). Thus, even though the Sveconorwegian Orogen is dominantly considered the opposing collisional margin of the northern Grenville Province in Labrador, it seems that the evolution on the Sveconorwegian side lagged behind by some tens of million years. One reason for such a diachronous evolution could be the asymmetry caused by Baltica being the upper plate and Laurentia the lower plate during final collision. Another reason could be that the (now missing) outer margin of Baltica may have collided with the Laurentia side, or intervening magmatic arcs, at a relatively earlier age, whereas the more inboard parts of the Sveconorwegian Orogen preserved in SW Fennoscandia were more affected by late-stage collisional and post-collisional processes.

In SW Amazonia, the Sunsas syn-orogenic magmatism appears to have continued up to around 1000 Ma, with post-orogenic magmatism as young as 990–970 Ma (Rondonian Tin Granites), and other minor activity until ca 930 Ma (Figs. 9 and 18). However, the small number of data records makes it difficult to evaluate the evidence. It should also be remembered that while the Putumayo Orogen in NW Amazonia would have had a close spatial relation both to Baltica and Laurentia, the classical Sunsas Orogen in SW Amazonia was located further away from Baltica, and probably not in direct contact with the Laurentian Grenville margin, since smaller blocks such as the Arequipa-Antofalla Basement block (AAB in Fig. 2; cf. Loewy et al., 2004; Johansson, 2014) may have

occupied the intervening space.

In western Australia, magmatism after the 1100 Ma lull is restricted to the Musgrave Province, with magmatism related to the Giles Event / Bentley Supersuite peaking at ca 1070 and continuing until around 1020 Ma (Figs. 13, 18). This makes the Australian age pattern slightly more like that of the Laurentian Grenville Province, rather than the Baltica-Amazonia pattern. However, in a Rodinia configuration like that in Fig. 2, the Australian proto-Rodinian orogens would have been facing the Mawson continent of East Antarctica, and may not have been a direct continuation of the Laurentian Grenville (Llano) Orogen.

The Namaqua-Natal Belt of the Kalahari craton would have been the opposing margin of the Llano segment of the Grenville Orogen, with which it collided, according to current Rodinia models (e.g. Li et al., 2008; Jacobs et al., 2008; Fig. 2). Prior to collision, the Laurentian side probably acted as the pro-side whilst Kalahari represented the retro-side of the developing orogenic system, consistent with the observation that there was never subduction underneath Proto-Kalahari. The 1400–1200 Ma continental arc magmatism of the Llano segment (Figs. 4 and 18) broadly overlaps in time with the early phases of magmatism in the Namaqua sector (Figs. 11 and 18), but since these were on separate plates, presumably still approaching each other prior to collision, no close relationship can be anticipated. The main Namaqua-Natal tectono-metamorphism recorded at ca. 1100 – 1050 Ma is roughly coeval with the Ottawan cycle in Laurentia and with the 1100 to 1050 Ma "slab break-off phase" in the Llano segment. Kalahari has a particular strong igneous pulse at 1100 Ma, which at this stage is poorly understood. It may immediately precede the final juxtaposition of Kalahari and Laurentia and is largely coeval with the Umkondo-Borg LIP in Kalahari, as well as the magmatism of the Mid-Continental Rift System (e.g. Hanson et al., 1998, 2004; de Kock et al., 2014; Choudhary et al., 2019).

In Table 1D, correlation factors for magmatism between all the five cratons during the time interval for Rodinia assembly (1260-900 Ma) illustrated in Fig. 18 are shown. They range from moderately positive to moderately negative, the highest correlations beings shown between Laurentia and Kalahari (0.297), and Amazonia and Kalahari (0.176). Correlation between Amazonia and Baltica is negative during this period (−0.191), but based on relatively limited data from Amazonia (n = 29). The correlation between Laurentia and Baltica is also negative (−0.166). The correlation factor for magmatism in the Grenville Province of Laurentia compared to the Sveconorwegian Province of Baltica during the whole time period 1900 to 900 Ma, however, is on the positive side (0.222; cf. Fig. 17).

After 900 Ma, magmatism completely ceased in all studied areas, attesting to the position of at least most of them within the stable interior of the Rodinia supercontinent following the proto-Rodinian Grenville orogeny. Instead, magmatism would have resumed around the exterior margin of Rodinia or in oceanic arcs within its exterior ocean.

9. Summary and conclusions

In total 4344 magmatic U-Pb ages in the range 2300 to 800 Ma, mostly on zircon but some on other minerals, with an uncertainty of ≤±20 million years, have been compiled from the Great Proterozoic Accretionary Orogen along the margin of the Columbia / Nuna supercontinent and from the subsequent Grenvillian collisional orogens forming the core of Rodinia. The age data are derived from rocks from Laurentia (North America and Greenland, n = 1212), Baltica (northeast Europe, n = 1922), Amazonia (central South America, n = 625), the Kalahari craton (southern Africa and Dronning Maud Land in East Antarctica, n = 386) and western Australia (n = 199). At least Laurentia, Baltica and Amazonia most likely formed a ca. 10 000 km long continuous external active continental margin of Columbia from ca. 1800 Ma until Columbia break-up at ca. 1260 Ma, after which all of these cratons were involved in the Rodinia-forming Grenvillian orogeny. However, the magmatic record is not smooth and continuous but highly irregular, with marked peaks and troughs, both on the individual cratons and when combined. The magmatic peaks typically range in duration from a few tens of million years up to around hundred million years, with intervening troughs of comparable length. These patterns may reflect real local or regional variations in magmatic activity and intensity, or variations in preservation of an original smoother magmatic record. However, it appears unlikely that the preservation of magmatic rocks should vary by several orders of magnitude within a few tens of million years along the same continental margin. Instead this variation is attributed to differences in the rate and direction of subduction, accretion of oceanic arcs or microcontinents along the continental margin, lower/upper plate asymmetry during continent collision, or, when it comes to intraplate magmatism, to irregular events of mantle upwelling and magmatic underplating.

Some magmatic peaks coincide from one craton to another, whether by coincidence or because of paleogeographic proximity and common geodynamic setting, while others do not. The best overall correlation, 0.617, is shown between Baltica and Amazonia, suggesting that they may have been close neighbours in a SAMBA-like configuration, and perhaps shared the same peri-Columbian subduction system for a considerable time. Available paleomagnetic poles for Amazonia are roughly consistent with this model. Correlation factors between Laurentia and Baltica, or Laurentia and Amazonia, are below 0.14 (correlations involving Australia or Kalahari are unreliable, due to the much smaller data record compiled from these cratons). Comparison between the Grenville Province in northeastern Laurentia and the Sveconorwegian Province in southwestern Fennoscandia (Baltica) shows some striking similarities, especially in the Mesoproterozoic (Pinwarian and Elsonian magmatism in the Grenville Province versus Telemarkian and Hallandian magmatism in the Sveconorwegian Province), but also differences in the timing of events, especially during the final Grenville-Sveconorwegian collision, when the Sveconorwegian evolution seems to lag behind some tens of million years. Also between the other cratons, the evolution before and during the final Grenvillian collision is largely diachronous. After 900 Ma, magmatic activity had ceased in all areas investigated, attesting to the position of at least most of them within the stable interior of Rodinia.

We hope that the data compilation presented here provides impetus and inspiration for present and future geologists and geochronologists to acquire more data and provide more detailed investigations of the geological relationships between all the Proterozoic cratonic blocks. In addition to more geochronological data, multidisciplinary studies incorporating geophysical and geochemical data, and paleomagnetic studies, will be needed to test and expand our observations and hypotheses.

CRediT authorship contribution statement

Åke Johansson: Conceptualization, Data curation, Project administration, Writing. **Bernard Bingen:** Data curation, Writing. **Hannu Huhma:** Data curation, Writing. **Tod Waight:** Data curation, Writing. **Rikke Vestergaard:** Data curation, Writing. **Alvar Soesoo:** Data curation, Writing. **Grazina Skridlaite:** Data curation, Writing. **Ewa Krzeminska:** Data curation, Writing. **Leonid Shumlyanskyy:** Data curation, Writing. **Mark E. Holland:** Data curation, Writing. **Christopher Holm-Denoma:** Data curation, Writing. **Wilson Teixeira:** Data curation, Writing. **Frederico M. Faleiros:** Data curation, Writing. **Bruno V. Ribeiro:** Data curation, Writing. **Joachim Jacobs:** Data curation, Writing. **Chengcheng Wang:** Data curation, Writing. **Robert J. Thomas:** Data curation, Writing. **Paul H. Macey:** Data curation, Writing. **Christopher L. Kirkland:** Data curation, Writing. **Michael I.H. Hartnady:** Data curation, Writing. **Bruce M. Eglington:** Data curation, Animation. **Stephen J. Puetz:** Data curation, Maps, Statistics. **Kent C. Condie:** Senior adviser.

Declaration of Competing Interest

The authors declare that they have no known competing financial interests or personal relationships that could have appeared to influence the work reported in this paper.

Acknowledgements

This study was done as a multi-national and multi-continental side-project by many persons, largely from home, during the Covid-19 pandemic. The work of Bruno Ribeiro was supported by the Australian Research Council (FL160100168). It is a contribution to IGCP-project 648 “Supercontinent Cycles and Global Geodynamics”. It is also a contribution to the memory of Russian-Swedish geologist Svetlana Bogdanova (1937-2019), who from her base at Lund University in southernmost Sweden with great enthusiasm led many studies on the geology of southern Sweden, Bornholm and the concealed basement of the East European Platform, especially in her Russian homeland, and not the least co-directed the preceding IGCP 440 project “Rodinia Assembly and Breakup”. This paper benefitted from the comments and suggestions by journal reviewers William Collins and Ross Mitchell, as well as an internal USGS review by Jamey Jones, USGS Alaska Science Center. Any use of trade, firm, or product names is for descriptive purposes only and does not imply endorsement by the U.S. Government.

Appendix. Supplementary data

Supplementary data to this article can be found online at https://doi.org/10.1016/j.precamres.2021.106463.

References

Åhäll, K.-I., Connelly, J., Brewer, T.S., 2000. Episodic rapakivi magmatism due to distal orogenesis? Correlation of 1.69–1.50 Ga orogenic and inboard “anorogenic’’ events in the Baltic Shield. Geology 28, 823–826.

Aitken, A.R.A., Betts, P.G., 2009. Constraints on the Proterozoic supercontinent cycle from the structural evolution of the south-central Musgrave Province, central Australia. Precambr. Res. 168, 284–300.

Aitken, A.R.A., Young, D.A., Ferraccioli, F., Betts, P.G., Greenbaum, J.S., Richter, T.G., Roberts, J.L., Blankenship, D.D., Siegert, M.J., 2014. The subglacial geology of Wilkes Land, East Antarctica. Geophys. Res. Lett. 41, 2390–2400. https://doi.org/10.1002/2014GL059405.

Almeida, J.A.C., Dall’Agnol, R., Rocha, M.C., 2017. Tonalite–trondhjemite and leuco-granodiorite–granite suites from the Rio Maria domain, Carajás province, Brazil: implications for discrimination and origin of the Archean Na-granitoids. Can. Mineral. 55, 437–456.

Amato, J.M., Boullion, A.O., Serna, A.M., Sanders, A.E., Farmer, G.L., Gehrels, G.E., Wooden, J.L., 2008. Evolution of the Mazatzal province and the timing of the Mazatzal orogeny: Insights from U-Pb geochronology and geochemistry of igneous and metasedimentary rocks in southern New Mexico. Geological Society of America Bulletin 120, 328–346. https://doi.org/10.1130/B26200.1.

Andersen, T., Griffin, W.L., Sylvester, A.G., 2007. Sveconorwegian crustal underplating in southwestern Fennoscandia: LAM-ICPMS U-Pb and Lu-Hf isotope evidence from granites and gneisses in Telemark, southern Norway. Lithos 93, 273–287.

Anderson, J.L., 1983. Proterozoic anorogenic granite plutonism of North America. Geol. Soc. Am. Mem. 161, 133–154.

Anderson, J.L., Bender, E.E., 1989. Nature and origin of Proterozoic A-type granitic magmatism in the southwestern United States. Lithos 23, 19–52.

Anderson, J.L., Morrison, J., 2005. Ilmenite, magnetite, and peraluminous Mesoproterozoic anorogenic granites of Laurentia and Baltica. Lithos 80, 45–60.

Andersson, U.B., Neymark, L.A., Billström, K., 2002. Petrogenesis of Mesoproterozoic (Subjotnian) rapakivi complexes of central Sweden: implications from U-Pb zircon ages, Nd, Sr, and Pb isotopes. Trans. R. Society of Edinburgh: Earth Sci. 92, 201–228.

Antonio, P.Y.J., D’Agrella-Filho, M.S., Trindade, R.I.F., Nédélec, A., Oliveira, D.C., Silva, F.F., Roverato, M., Lana, C., 2017. Turmoil before the boring billion: paleomagnetism of the 1880–1860 Ma Uatumã event in the Amazonian craton. Gondwana Res. 49, 106–129. https://doi.org/10.1016/j.gr.2017.05.006.

Antonio, P.Y.J., D’Agrella-Filho, M.S., Nedelec, A., Poujol, M., Sanchez, C., Dantas, E.L., Dall’Agnol, R., Teixeira, M.F.B., Proietti, A., Martinez-Dopico, C.I., Oliveira, D., Silva, F., Marangoanha, B., Trindade, R., 2021. New constraints for paleogeographic reconstructions at ca. 1.88 Ga from geochronology and paleomagnetism of the Carajás dyke swarm (eastern Amazonia). Precambr. Res. 353 https://doi.org/10.1016/j.precamres.2020.106039.

Appelquist, K., Brander, L., Johansson, Å., Andersson, U.B., Cornell, D., 2011. Character and origin of variably deformed granitoids in central southern Sweden: implications from geochemistry and Nd isotopes. Geol. J. 46, 597–618. https://doi.org/10.1002/gj.1303.

Arndt, N., Davaille, A., 2013. Episodic earth evolution. Tectonophysics 609, 661–674. https://doi.org/10.1016/j.tecto.2013.07.002.

Aronoff, R.F., Andronicos, C.L., Vervoort, J.D., Hunter, R.A., 2016. Redefining the metamorphic history of the oldest rocks in the southern Rocky Mountains. Bull. Geol. Society America 128, 1207–1227. https://doi.org/10.1130/B31455.1.

Bailie, R., Macey, P.H., Nethenzheni, S., Frei, D., le Roux, P., 2017. The Keimoes Suite redefined: the geochronological and geochemical characteristics of the ferroan granites of the eastern Namaqua Sector, Mesoproterozoic Namaqua-Natal Metamorphic Province, southern Africa. J. Afr. Earth Sc. 134, 737–765.

Barnes, M.A., Anthony, E.Y., Williams, I., Asquith, G.B., 2002. Architecture of a 1.38-1.34 Ga granite-rhyolite complex as revealed by geochronology and isotopic and elemental geochemistry of subsurface samples from west Texas, USA. Precambr. Res. 119, 9–43. https://doi.org/10.1016/S0301-9268(02)00116-X.

Barr, S.M., White, C.E., Culshaw, N.G., Ketchum, J.W.F., 2001. Geology and tectonic setting of Paleoproterozoic granitoid suites in the Island Harbour Bay area, Makkovik Province. Labrador. Can. J. Earth Sci. 38, 441–463.

Bartels, A., Nielsen, T.F.D., Lee, W.R., Upton, B.G.J., 2015. Petrological and geochemical characteristics of Mesoproterozoic dyke swarms in the Gardar Province, South Greenland: evidence for a major sub-continental lithospheric mantle component in the generation of the magmas. Mineral. Mag. 79, 909–939.

Barth, A.P., Wooden, J.L., Coleman, D.S., Vogel, M.B., 2009. Assembling and disassembling California: A zircon and monazite geochronologic framework for Proterozoic crustal evolution in southern California. The Journal of Geology 117, 221–239. https://doi.org/10.1086/597515.

Bauer, W., Fielitz, W., Jacobs, J., Fanning, C.M., Spaeth, G., 2003. Mafic dykes from Heimefrontfjella and implications for the post-Grenvillian to pre-Pan-African geological evolution of western Dronning Maud Land, Antarctica. Antarct. Sci. 15, 379–391.

Bauer, W., Jacobs, J., Thomas, R.J., Spaeth, G., Weber, K., 2009. Geology of the Vardeklettane Terrane, Heimefrontfjella (East Antarctica). Polarforschung 79, 29–32.

Bennett, V.C., DePaolo, D.J., 1987. Proterozoic crustal history of the western United States as determined by neodymium isotopic mapping. Bull. Geol. Society America 99, 674–685. https://doi.org/10.1130/0016-7606(1987)99<674:PCHOTW>2.0.CO;2.

Bergman, S., Stephens, M.B., Andersson, J., Kathol, B., Bergman, T., 2012. Bedrock map of Sweden, scale 1:1 million. Sveriges Geologiska Undersökning K 423.

Bergström, U., Stephens, M.B., Wahlgren, C.-H., 2020. Polyphase (1.6-1.5 and 1.1-0.9 Ga) deformation and metamorphism of Proterozoic (1.7 Ga) continental crust, Idefjorden terrane, Sveconorwegian orogen. Chapter 16 in Stephens, M.B., Bergman Weihed, J. (eds.), 2020. Sweden: Lithotectonic Framework, Tectonic Evolution and Mineral Resources. Geological Society Memoir 50, Geological Society of London, 397-434.

Bettencourt, J.S., Tosdal, R.M., Leite Jr., W.B., Payolla, B.L., 1999. Mesoproterozoic rapakivi granites of the Rondônia Tin Province, southwestern border of the Amazonian craton, Brazil – I. Reconnaissance U-Pb geochronology and regional implications. Precambr. Res. 95, 41–67. https://doi.org/10.1016/S0301-9268(98)00126-0.

Bettencourt, J.S., Leite Jr, W., Payolla, B., Ruiz, A.S., Matos, R.S., Tosdal, R.M., 2010. The Rondonian-San Ignacio Province in the SW Amazonian Craton: an overview. J. S. Am. Earth Sci. 29, 28–46.

Bettencourt, J.S., Juliani, C., Xavier, R.P., Monteiro, L.V.S., Bastos Neto, A.C., Klein, E.L., Assis, R., Leite Jr., W.B., Moreto, C.P.N., Fernandes, C.M.D., Pereira, V.P., 2016. Metallogenetic systems associated with granitoid magmatism in the Amazonian Craton: an overview of the present level of understanding and exploration significance. J. S. Am. Earth Sci. 68, 22–49.

Betts, P.G., Giles, D., 2006. The 1800–1100 Ma tectonic evolution of Australia. Precambr. Res. 144, 92–125.

Bial, J., Buettner, S.H., Schenk, V., Appel, P., 2015. The long-term high-temperature history of the central Namaqua Metamorphic Complex: evidence for a Mesoproterozoic continental back-arc in southern Africa. Precambr. Res. 268, 243–278.

Bibikova, E.V., Bogdanova, S.V., Postnikov, A.V., Popova, L.P., Kirnozova, T.I., Fugzan, M.M., Glushchenko, V.V., 2009. Sarmatia–Volgo-Uralia junction zone: isotopic-geochronologic characteristic of supracrustal rocks and granitoids. Stratigr. Geol. Correl. 17, 561–573.

Bickford, M.E., Hill, B.M., 2007. Does the arc accretion model adequately explain the Paleoproterozoic evolution of southern Laurentia? An expanded interpretation. Geology 35, 167–170. https://doi.org/10.1130/G23174A.1.

Bickford, M.E., Shuster, R.D., Boardman, S.J., 1989. U/Pb geochronology of the Proterozoic volcano-plutonic terrane in the Gunnison and Salida areas, Colorado. In: Grambling, J.A., Tewksbury, B.J. (Eds.), Proterozoic geology of the southern Rocky Mountains. Geological Society of America Special Paper 235, 33–48.

Bickford, M.E., Soegaard, K., Nielsen, K.C., McLelland, J.M., 2000. Geology and geochronology of Grenville-age rocks in the Van Horn and Franklin Mountains area, west Texas: Implications for the tectonic evolution of Laurentia during the Grenville. Geological Society of America Bulletin 112 (7), 1134–1148. https://doi.org/10.1130/0016-7606(2000)112<1134:GAGOGR>2.0.CO;2.

Bickford, M.E., Mueller, P.A., Condie, K.C., Hanan, B.B., Kamenov, G.D., 2019. Ages and Hf isotopic compositions of detrital zircons in the Pinal schist, southern Arizona, USA: Provenance, tectonic setting, and evidence for pre-1.7 Ga crust in SW Laurentia. Precambrian Research 331, 105374. https://doi.org/10.1016/j.precamres.2019.105374.

Bickford, M.E., Van Schmus, W.R., Karlstrom, K.E., Mueller, P.A., Kamenov, G.D., 2015. Mesoproterozoic-trans-Laurentian magmatism: a synthesis of continent-wide age distributions, new SIMS U-Pb ages, zircon saturation temperatures, and Hf and Nd isotopic compositions. Precambr. Res. 265, 286–312. https://doi.org/10.1016/j.precamres.2014.11.024.

Bingen, B., Viola, G., 2018. The early-Sveconorwegian orogeny in southern Norway: tectonic model involving delamination of the sub-continental lithospheric mantle. Precambr. Res. 313, 170–204.

Bingen, B., Nordgulen, Ø., Sigmond, E.M.O., Tucker, R.D., Mansfeld, J., Högdahl, K., 2003. Relations between 1.19-1.13 Ga continental magmatism, sedimentation and metamorphism, Sveconorwegian province, S Norway. Precambr. Res. 124, 215–241.

Bingen, B., Skår, Ø., Marker, M., Sigmond, E.M.O., Nordgulen, Ø., Ragnhildstveit, J., Mansfeld, J., Tucker, R.D., Liégeois, J.P., 2005. Timing of continental building in the Sveconorwegian orogen, SW Scandinavia. Norw. J. Geol. 85, 87–116.

Bingen, B., Davis, W.J., Hamilton, M.A., Engvik, A., Stein, H., Skår, Ö., Nordgulen, Ø., 2008a. Geochronology of high-grade metamorphism in the Sveconorwegian belt, S. Norway: U-Pb, Th-Pb and Re-Os data. Norw. J. Geol. 88, 13–42.

Bingen, B., Nordgulen, Ø., Viola, G., 2008b. A four-phase model for the Sveconorwegian orogeny, SW Scandinavia. Norw. J. Geol. 88, 43–72.

Bingen, B., Jacobs, J., Viola, G., Henderson, I.H.C., Skår, Ø., Boyd, R., Thomas, R.J., Solli, A., Key, R.M., Daudi, E.X.F., 2009. Geochronology of the Precambrian crust in the Mozambique belt in NE Mozambique, and implications for Gondwana assembly. Precambr. Res. 170, 231–255.

Bingen, B., Viola, G., Möller, C., Vander Auwera, J., Laurent, A., Yi, K., 2021. The Sveconorwegian orogeny. Gondwana Res. 90, 273–313.

Bispo-Santos, F., D'Agrella-Filho, M.S., Trindade, R.I.F., Janikian, L., Reis, N.J., 2014. Was there SAMBA in Columbia? Paleomagnetic evidence from 1790 Ma Avanavero mafic sills (Northern Amazonian craton). Precambr. Res. 244, 139–155. https://doi.org/10.1016/j.precamres. 2013.11.002.

Bleeker, W., 2003. The late Archean record: a puzzle in ca. 35 pieces. Lithos 71, 99–134. https://doi.org/10.1016/j.lithos.2003.07.003.

Blignault, H.J., Van Aswegen, G., Van der Merwe, S.W., Colliston, W.P., 1983. The Namaqualand Geotraverse and environs: part of the Proterozoic mobile belt. In: Botha, B.J.V. (Ed.), Namaqualand Metamorphic Complex. Special Publication of the Geological Society of South Africa, 1–29.

Bodorkos, S. and Clark, D.J., 2004. Evolution of a crustal-scale transpressive shear zone in the Albany–Fraser Orogen, SW Australia: 2. Tectonic history of the Coramup Gneiss and a kinematic framework for Mesoproterozoic collision of the West Australian and Mawson cratons. Journal of Metamorphic Geology 22, 713-731.

Bogdanova, S.V., 2001. Tectonic setting of 1.65-1.4 Ga AMCG magmatism in the Western East European Craton (Western Baltica). EUG 11 Abstracts, Strasbourg, France, p. 769.

Bogdanova, S.V., Bingen, B., Gorbatschev, R., Kheraskova, T., Kozlov, V., Puchkov, V., Volozh, Y., 2008. The East European Craton (Baltica) before and during the assembly of Rodinia. Precambr. Res. 160, 23–45.

Bogdanova, S.V., De Waele, B., Bibikova, E.V., Belousova, E.A., Postnikov, A.V., Fedotova, A.A., Popova, L.P., 2010. Volgo-Uralia: the first U-Pb, Lu-Hf and Sm-Nd isotopic evidence of preserved Paleoarchean crust. Am. J. Sci. 310, 1345–1383.

Bogdanova, S.V., Gorbatschev, R., Garetsky, R.G., 2016. Europe/East European Craton. Reference Module in Earth Systems and Environmental Sciences, Elsevier, pp. 1-18.

Bogdanova, S.V., Gintov, O.B., Kurlovich, D., Lubnina, N.V., Nilsson, M., Orlyuk, M.I., Pashkevich, I.K., Shumlyanskyy, L.V., Starostenko, V.I., 2013. Late Palaeoproterozoic mafic dyking in the Ukrainian Shield (Volgo-Sarmatia) caused by rotations during the assembly of supercontinent Columbia. Lithos 174, 196–216.

Bogdanova, S.V., Gorbatschev, R., Skridlaite, G., Soesoo, A., Taran, L., Kurlovich, D., 2015. Trans-Baltic Palaeoproterozoic correlations towards the reconstruction of supercontinent Columbia/Nuna. Precambr. Res. 259, 5–33.

Boger, S.D., Raetz, M., Giles, D., Etchart, E., Fanning, C.M., 2005. U-Pb age from the Sunsás region of Eastern Bolivia, evidence for allochtonous origin of the Paragua Block. Precambrian Res. 139, 121–146.

Bonilla, A., Frantz, J.C., Charão-Marques, J., Cramer, T., Franco, J.A., Amaya, Z., 2016. Magmatismo Rapakivi em la cuenca media del rio Inírida, departamento de Guainía, Colombia. Boletin de Geologia, 38(1). https://doi.org/10.18273/revbol.v38n1-2016001.

Borghetti, C., Philipp, R.P., Mandetta, P., Hoffmann, I.B., 2018. Geochronology of the Archean Tumucumaque Complex, Amapá Terrane, Amazonian Craton, Brazil. J. S. Am. Earth Sci. 88, 294–311.

Brewer, T.S., Åhäll, K.I., Menuge, J.F., Storey, C.D., Parrish, R.R., 2004. Mesoproterozoic bimodal volcanism in SW Norway, evidence for recurring pre-Sveconorwegian continental margin tectonism. Precambr. Res. 134, 249–273.

Camacho, A., Fanning, C., 1995. Some isotopic constraints on the evolution of the granulite and upper amphibolite facies terranes in the eastern Musgrave Block, central Australia. Precambr. Res. 71, 155–181.

Camacho, A., Hensen, B., Armstrong, R., 2002. Isotopic test of a thermally driven intraplate orogenic model, Australia. Geology 30, 887–890.

Cavosie, A., Selverstone, J., 2003. Early Proterozoic oceanic crust in the northern Colorado Front Range: Implications for crustal growth and initiation of basement faults. Tectonics 22, 1–23. https://doi.org/10.1029/2001TC001325.

Cawood, P.A., Pisarevsky, S.A., 2017. Laurentia-Baltica-Amazonia relations during Rodinia assembly. Precambr. Res. 292, 386–397.

Cawood, P.A., Strachan, R., Cutts, K., Kinny, P.D., Hand, M., Pisarevsky, S., 2010. Neoproterozoic orogeny along the margin of Rodinia: Valhalla orogen, North Atlantic. Geology 38, 99–102.

Cawood, P.A., Hawkesworth, C.J., Dhuime, B., 2013. The continental record and the generation of continental crust. Geol. Soc. Am. Bull. 125, 14–32. https://doi.org/10.1130/B30722.1.

Chadwick, B., Garde, A.A., 1996. Palaeoproterozoic oblique plate convergence in South Greenland: a reappraisal of the Ketilidian Orogen. Geol. Soc., London, Special Publ. 112, 179–196.

Chamberlain, K.R., 1998. Medicine Bow orogeny: timing of deformation and model of crustal structure produced during continent-arc collision, ca. 1.78 Ga, southeastern Wyoming. Rocky Mt Geol. 33, 259–277. https://doi.org/10.2113/33.2.259.

Chamberlain, K.R., Bowring, S.A., 1990. Proterozoic geochronologic and isotopic boundary in NW Arizona. J. Geol. 98, 399–416.

Chichester, B., Rychert, C., Harmon, N., van der Lee, S., Frederiksen, A., Zhang, H., 2018. Seismic imaging of the North American midcontinent rift using S-to-P receiver functions. J. Geophys. Res: Solid Earth 123. https://doi.org/10.1029/2018JB015771.

Choudhary, B.R., Ernst, R.E., Xua, Y.-G., Evans, D.A.D., de Kock, M.O., Meert, J.G., Ruiz, A.S., Lima, G.A., 2019. Geochemical characterization of a reconstructed 1110 Ma Large Igneous Province. Precambr. Res. 332 (105382), 1–22. https://doi.org/10.1016/j.precamres.2019.105382.

Clark, D., Hensen, B., Kinny, P., 2000. Geochronological constraints for a two-stage history of the Albany-Fraser Orogen, Western Australia. Precambr. Res. 102, 155–183.

Clark, C., Kirkland, C.L., Spaggiari, C.V., Oorschot, C., Wingate, M.T.D., Taylor, R.J., 2014. Proterozoic granulite formation driven by mafic magmatism: an example from the Fraser Range Metamorphics, Western Australia. Precambr. Res. 240, 1–21.

Clarke, G., Powell, R., 1991. Decompressional coronas and symplectites in granulites of the Musgrave Complex, central Australia. J. Metamorph. Geol. 9, 441–450.

Clifford, T.N., Barton, E.S., Stern, R.A., Duchesne, J.C., 2004. U-Pb zircon calendar for Namaquan (Grenville) crustal events in the granulite-facies terrane of the O'okiep copper district of South Africa. J. Petrol. 45, 669–691.

Coint, N., Slagstad, T., Roberts, N.M.W., Marker, M., Røhr, T., Sørensen, B.E., 2015. The late Mesoproterozoic Sirdal Magmatic Belt, SW Norway: relationships between magmatism and metamorphism and implications for Sveconorwegian orogenesis. Precambr. Res. 265, 57–77.

Condie, K.C., 1982. Plate-tectonics model for Proterozoic continental accretion in the southwestern United States. Geology 10, 37–42. https://doi.org/10.1130/0091-7613(1982)10<37:PMFPCA>2.0.CO;2.

Condie, K.C., 1998. Episodic continental growth and supercontinents: A mantle avalanche connection? Earth and Planetary Science Letters 163, 97–108. https://doi.org/10.1016/S0012-821X(98)00178-2.

Condie, K.C., 2013. Preservation and recycling of crust during accretionary and collisional phases of Proterozoic orogens: a bumpy road from Nuna to Rodinia. Geosciences 2013, 240–261. https://doi.org/10.3390/geosciences3020240.

Condie, K., Myers, J., 1999. Mesoproterozoic Fraser Complex: Geochemical evidence for multiple subduction-related sources of lower crustal rocks in the Albany-Fraser Orogen, Western Australia. Aust. J. Earth Sci. 46, 875–882.

Condie, K.C., Davaille, A., Aster, R.C., Arndt, N., 2015. Upstairs-downstairs: Supercontinents and large igneous provinces, are they related? Int. Geol. Rev. 57, 1341–1348. https://doi.org/10.1080/00206814.2014.963170.

Condie, K.C., Arndt, N., Davaille, A., Puetz, S.J., 2017. Zircon age peaks: production or preservation of continental crust? Geosphere 13, 227–234. https://doi.org/10.1130/ges01361.1.

Condie, K.C., Puetz, S.J., Davaille, A., 2018. Episodic Crustal Production before 2.7 Ga. Precambr. Res. 312, 16–22. https://doi.org/10.1016/j.precamres.2018.05.005.

Cordani, U.G., Teixeira, W., 2007. Proterozoic accretionary belts in the Amazonian Craton. In: Hatcher Jr. R.D., Carlson M.P., McBride J.H., Martinez Catalán J.R. (eds.). The 4D Framework of Continental Crust. GSA Memoir. Boulder, Colorado: Geological Society of America 200, 297–320.

Cordani, U.G., Teixeira, W., D'Agrella-Filho, M.S., Trindade, R.I., 2009. The position of the Amazonian Craton in supercontinents. Gondwana Res. 15, 396–407.

Cordani, U.G., Sato, K., Sproensser, W., Fernandes, F.S., 2016. U-Pb zircon ages of rocks from the Amazonas Territory of Colombia and their bearing on the tectonic history of the NW sector of the Amazonian Craton. Braz. J. Geol. 46, 5–35.

Cornell, D.H., Pettersson, Å., 2007. Ion probe dating of the Achab Gneiss, a young basement to the central Bushmanland ore district? J. Afr. Earth Sc. 47, 112–116.

Cornell, D.H. Thomas, R.J., Gibson, R. Moen, H.F.G. Moore J.M. and Reid, D.L., 2006. Namaqua-Natal Province. In: Johnson, M.R., Anhauesser, C.R., Thomas, R.J (eds.): The Geology of South Africa. Geological Society of South Africa, Johannesburg/ Council for Geoscience, Pretoria, 325–379.

Cornell, D.H., Pettersson, Å., Whitehouse, M.J., Scherstén, A., 2009. A new chronostratigraphic paradigm for the age and tectonic history of the Mesoproterozoic Bushmanland ore district, South Africa. Econ. Geol. 104, 385–404.

Cornell, D.H., Pettersson, Å., Simonsen, S.L., 2012. Zircon U-Pb emplacement and Nd-Hf crustal residence ages of the Straussburg granite and Friersdale charnockite in the Namaqua-Natal Province, South Africa. S. Afr. J. Geol. 115, 465–484.

Cornell, D.H., van Schijndel, V., Simonsen, S.L., Frei, D., 2015. Geochronology of Mesoproterozoic hybrid intrusions in the Konkiep Terrane, Namibia, from passive to active continental margin in the Namaqua-Natal Wilson Cycle. Precambr. Res. 265, 166–188.

Corrigan, D., Hajnal, Z., Németh, B., Lucas, S.B., 2005. Tectonic framework of a Paleoproterozoic arc– continent to continent–continent collisional zone, Trans-Hudson Orogen, from geological and seismic reflection studies. Can. J. Earth Sci. 42, 421–434.

Corrigan, D., Pehrsson, S., Wodicka, N., de Kemp, E., 2009. The Palaeoproterozoic Trans-Hudson Orogen: A prototype of modern accretionary processes. Geol. Soc. Spec. Pub. 327, 457–479. https://doi.org/10.1144/SP327.19.

D'Agrella-Filho, M.S., Bispo-Santos, F., Trindade, R.I.F., Antonio, P.Y.J., 2016. Paleomagnetism of the Amazonian Craton and its role in paleocontinents. Braz. J. Geol. 46, 275–299.

D'Agrella-Filho, M.S., Antonio, P.Y.J., Trindade, R.I.F., Teixeira, W., Bispo-Santos, F., 2020. The Precambrian Drift History and Paleogeography of Amazonia. In: L.P. Pesonen, J. Salminen, D.A.D. Evans, S.-Å Elming, T. Veikkolainen (eds.). Ancient Supercontinents and the Paleogeography of the Earth. Elsevier, Chapter 6, p. 207-243.

Dalziel, I.W., Mosher, S., Gahagan, L.M., 2000. Laurentia-Kalahari collision and the assembly of Rodinia. J. Geol. 108, 499–513.

Daniel, C.G., Pfeifer, L.S., Jones, J.V., McFarlane, C.M., 2013. Detrital zircon evidence for non-Laurentian provenance, Mesoproterozoic (ca. 1490–1450 Ma) deposition and orogenesis in a reconstructed orogenic belt, northern New Mexico, USA: Defining the Picuris orogeny. Bull. Geol. Society America 125, 1423–1441. https://doi.org/10.1130/B30804.1.

de Kock, M.O., Ernst, R., Söderlund, U., Jourdan, F., Hofmann, A., Le Gall, B., Berrand, H., Chisonga, B.C., Beukes, N., Rajesh, H.M., Moseki, L.M., Fuchs, R., 2014. Dykes of the 1.11 Ga Umkondo LIP, Southern Africa: Clues to a complex plumbing system. Precambr. Res. 249, 129–143. https://doi.org/10.1016/j.precamres.2014.05.006.

De Waele, B., Pisarevsky, S., 2008. Geochronology, paleomagnetism and magnetic fabric of metamorphic rocks in the northeast Fraser Belt, Western Australia. Aust. J. Earth Sci. 55, 605–621.

Delor, C., De Roever, E.W.F., Lafon, J.M., Lahondère, D., Rossi, P., Cocherie, A., Guerrot, C., Potrel, A., 2003. The Bakhuis ultrahigh-temperature granulite belt (Suriname): II. Implications for late Transamazonian crustal stretching in a revised Guiana Shield framework. Géol. Fr. 2–4, 207–230.

Dhuime, B., Hawkesworth, C.J., Storey, C.D., Cawood, P.A., 2011. From sediments to their source rocks: Hf and Nd isotopes in recent river sediments. Geology 39, 407–410. https://doi.org/10.1130/G31785.1.

Dickin, A.P., 2000. Crustal formation in the Grenville province: Nd-isotope evidence. Canadian Journal of Earth Sciences 37, 165–181. https://doi.org/10.1139/cjes-37-2-3-165.

Dickin, A., 2021. Comment on Hinchey (2021): "Lithogeochemical and Nd isotopic constraints on felsic magmatism in the Makkovik Orogen, Labrador, Canada: Implications for assembly of the supercontinent Nuna". Lithos 392-393, 106903. https://doi.org/10.1016/j.lithos.2021.106093.

Doe, M.F., Jones, J.V., Karlstrom, K.E., Thrane, K., Frei, D., Gehrels, G., Pecha, M., 2012. Basin formation near the end of the 1.60–1.45 Ga tectonic gap in southern Laurentia: Mesoproterozoic Hess Canyon Group of Arizona and implications for ca. 1.5 Ga supercontinent configurations. Lithosphere 4, 77–88. https://doi.org/10.1130/L160.1.

Doggart, S.W., 2019. Geochronology and isotopic characterisation of LCT pegmatites from the Orange River Pegmatite Province (Doctoral dissertation, Stellenbosch: Stellenbosch University), 234p.

Dörr, W., Belka, Z., Marheine, D., Schastok, J., Valverde-Vaquero, P., Wiszniewska, J., 2002. U-Pb and Ar–Ar geochronology of anorogenic granite magmatism of the Mazury Complex, NE Poland. Precambr. Res. 119, 101–120.

du Bray, E.A., Holm-Denoma, C.S., Lund, K., Premo, W.R., 2018. Review of the geochemistry and metallogeny of approximately 1.4 Ga granitoid intrusions of the conterminous United States. U.S. Geological Survey Scientific Investigations Report 2017–5111, 34 p., https://doi.org/10.3133/sir20175111.

Duebendorfer, E.M., Chamberlain, K.R., Jones, C.S., 2001. Paleoproterozoic tectonic history of the Cerbat Mountains, northwestern Arizona: Implications for crustal assembly in the southwestern United States. Bulletin of the Geological Society of America 113, 575–590. https://doi.org/10.1130/0016-7606(2001)113<0575:PTHOTC>2.0.CO;2.

Duebendorfer, E.M., Williams, M.L., Chamberlain, K.R., 2015. Case for a temporally and spatially expanded Mazatzal orogeny. Lithosphere 7, 603–610. https://doi.org/10.1130/L412.1.

Dutch, R.A., Doublier, M.P., Pawley, M.J., Wise, T.W., Reid, A.J., Clark, D.J., Kennett, B. L.N., Fraser, G., Thiel, S., van der Wielen, S., 2015. Geological and geodynamic implications of the western Gawler Craton section of seismic line 13GA-EG1. What lies beneath the western Gawler Craton 59–75.

Edgoose, C., Close, D., Scrimgeour, I., 2004. Geology of the Musgrave Block, Northern Territory. Government Printer of the Northern Territory.

Eglington, B.M., 2006. Evolution of the Namaqua-Natal Belt, southern Africa–A geochronological and isotope geochemical review. J. Afr. Earth Sc. 46, 93–111.

Eglington, B.M., Thomas, R.J., Armstrong, R.A., Walraven, F., 2003. Zircon geochronology of the Oribi Gorge Suite, KwaZulu-Natal, South Africa: constraints on the timing of trans-current shearing in the Namaqua-Natal Belt. Precambr. Res. 123, 29–46.

Emslie, R.F., Hamilton, M.A., Thriault, R.J., 1994. Petrogenesis of a mid-Proterozoic anorthositic mangerite charnockite granite (AMCG) complex: isotopic and chemical evidence from the Nain Plutonic Suite. J. Geol. 102, 539–558. https://doi.org/10.1086/629697.

Ernst, R.E., Bleeker, W., Söderlund, U., Kerr, A.C., 2013. Large Igneous Provinces and supercontinents: toward completing the plate tectonic revolution. Lithos 174, 1–14.

Evans, D.A.D., 2009. The palaeomagnetically viable, long-lived and all-inclusive Rodinia supercontinent reconstruction. Geol. Society, London, Special Publ. 327, 371–404. https://doi.org/10.1144/SP327.16.

Evans, D.A.D., 2013. Reconstructing pre-Pangean supercontinents. GSA. Bulletin 125 (11–12), 1735–1751. https://doi.org/10.1130/B30950.1.

Evans, D.A.D., Mitchell, R.N., 2011. Assembly and breakup of the core of Paleoproterozoic-Mesoproterozoic supercontinent Nuna. Geology 39, 443–446. https://doi.org/10.1130/G31654.1.

Evins, P., Kirkland, C., Wingate, M., Smithies, R., Howard, H., Bodorkos, S., 2012. Provenance of the 1340–1270 Ma Ramarama Basin in the west Musgrave Province, central Australia. Geol. Survey of Western Australia, Report 116, 39.

Evins, P.M., Smithies, R.H., Howard, H.M., Kirkland, C.L., Wingate, M.T.D., Bodorkos, S., 2010. Devil in the detail; The 1150–1000 Ma magmatic and structural evolution of the Ngaanyatjarra Rift, west Musgrave Province, Central Australia. Precambr. Res. 183, 572–588.

Faleiros, F.M., Pavan, M., Reḿedio, M.J., Rodrigues, J.B., Almeida, V.V., Caltabeloti, F. P., Pinto, L.G.R., Oliveira, A.A., Pinto de Azevedo, E.J., Costa, V.S., 2016. Zircon U-Pb ages of rocks from the Rio Apa cratonic terrane (Mato Grosso do Sul, Brazil): new insights for its connection with the Amazonian craton in pre-Gondwana times. Gondwana Res. 34, 187–204.

Fernandes, C.M.D., Juliani, C., Monteiro, L.V.S., Lagler, B., Echeverri-Misas, C.M., 2011. High-K calc-alkaline to A-type fissure-controlled volcano-plutonism of the São Felix do Xingu region, Amazonian craton, Brazil: exclusively crustal sources or only mixed Nd model ages? J. S. Am. Earth Sci. 32, 351–368.

Fisher, C.M., Loewy, S.L., Miller, C.F., Berquist, P., Van Schmus, W.R., Hatcher, R.D., Wooden, J.L., Fullagar, P.D., 2010. Whole-rock Pb and Sm-Nd isotopic constraints on the growth of southeastern Laurentia during Grenvillian orogenesis. Bull. Geol. Society America 122, 1646–1659. https://doi.org/10.1130/B30116.1.

Foster, D.A., Gray, D.R., 2000. Evolution and Structure of the Lachlan Fold Belt (Orogen) of Eastern Australia. Annu. Rev. Earth Planet. Sci. 28, 47–80. https://doi.org/10.1146/annurev.earth.28.1.47.

Fraga, L.M.B., Cordani, U.G., 2019. Early Orosirian tectonic evolution of the Central Guiana Shield: insights from new U-Pb SHRIMP data. In: 11th Inter-Guiana Geological Conference: Tectonics and Metallogenesis of NE South America. Paramaribo, Suriname, Geologisch Mijnbouwkundige Dienst Suriname. Mededeling 29, 59–62.

Fraga, L.M.B., Dall'Agnol, R., Costa, J.B.S., Macambira, M.J.B., 2009a. The Mesoproterozoic Mucajaí anorthosite-mangerite-rapakivi granite complex, Amazonian craton, Brazil. Can. Mineral. 47, 1469–1492.

Fraga, L.M., Macambira, M.J.B., Dall'Agnol, R., Costa, J.B.S., 2009b. 1.94–1.93 Ga charnockitic magmatism from the central part of the Guiana Shield, Roraima, Brazil: single zircon evaporation data and tectonic implications. J. S. Am. Earth Sci. 27, 247–257.

Fraga, L.M., Lafon, J-M., Tassinari, C.C.G., 2020. Geologia e evolução tectônica das porções central e nordeste do Escudo das Guianas e sua estrutura ção em cinturões eo-orosirianos. In: Bartorelli, A., Teixeira, W., de Neves, B.B.B. (Eds.), Geocronologia e Evolução Tectônica do Continente Sul-Americano: A Contribuição de Umberto Giuseppe Cordani. Solaris Edições Culturais publishers, São Paulo, pp. 92–110.

Frimmel, H.E. 2004. Formation of a late Mesoproterozoic supercontinent: the South Africa–East Antarctica connection. In Eriksson, P.G., Altermann, W., Nelson, D.R., Mueller, W.U., Catuneanu, O.,(eds.): The Precambrian Earth: Tempos and Events. Amsterdam: Elsevier, 240–255.

Frost, C.D., Frost, B.R., 2013. Proterozoic ferroan feldspathic magmatism. Precambr. Res. 228, 151–163. https://doi.org/10.1016/j.precamres.2013.01.016.

Furlanetto, F., Thorkelson, D.J., Gibson, H.D., Marshall, D.D., Rainbird, R.H., Davis, W. J., Crowley, J.L., Vervoort, J.D., 2013. Late Paleoproterozoic terrane accretion in northwestern Canada and the case for circum-Columbian orogenesis. Precambr. Res. 224, 512–528. https://doi.org/10.1016/j.precamres.2012.10.010.

Furlanetto, F., Thorkelson, D.J., Rainbird, R.H., Davis, W.J., Gibson, H.D., Marshall, D. D., 2016. The Paleoproterozoic Wernecke Supergroup of Yukon, Canada: Relationships to orogeny in northwestern Laurentia and basins in North America, East Australia, and China. Gondwana Res. 39, 14–40. https://doi.org/10.1016/j.gr.2016.06.007.

Garde, A.A., Hamilton, M.A., Chadwick, B., Grocott, J., McCaffrey, K.J.W., 2002. The Ketilidian orogen of South Greenland: geochronology, tectonics, magmatism and fore-arc accretion during Palaeoproterozoic oblique convergence. Can. J. Earth Sci. 39, 765–793.

Gardiner, N.J., Maidment, D.W., Kirkland, C.L., Bodorkos, S., Smithies, D., Jeon, H., 2018. Isotopic insight into the Proterozoic crustal evolution of the Rudall Province, Western Australia. Precambr. Res. 313, 31–50.

Gee, D.G., Andréasson, P.-G., Lorenz, H., Frei, D., Majka, J., 2015. Detrital zircon signatures of the Baltoscandian margin along the Arctic Circle Caledonides in Sweden: the Sveconorwegian connection. Precambr. Res. 265, 40–56.

Geraldes, M.C., Van Schmus, W.R., Condie, K.C., Bell, S., Teixeira, W., Babinski, M., 2001. Proterozoic geologic evolution of the SW part of the Amazonian craton in Mato Grosso state, Brazil. Precambr. Res. 111, 91–128.

Geraldes, M.C., Teixeira, W., Heilbron, M., 2004. Lithospheric versus asthenospheric source of the SW Amazonian Craton A-type granites: the role of the Paleo- and Mesoproterozoic accretionary belts for their coeval continental suite. Episodes 27 (3), 185–189.

Gibson, G.M., Champion, D.C., 2019. Antipodean fugitive terranes in southern Laurentia: How Proterozoic Australia built the American West. Lithosphere 11 (4), 551–559. https://doi.org/10.1130/L1072.1.

Gibson, G.M., Champion, D.C., Huston, D.L., Whitnall, I.W., 2020. Orogenesis in Paleo-Mesoproterozoic eastern Australia: a response to arc-continent and continent-continent collision during assembly of the Nuna supercontinent. Tectonics 24, pp. https://doi.org/10.1029/2019TC005717.

Giovanardi, T., Girardi, V.A.V., Teixeira, W., Mazzucchelli, M., 2019. Mafic dyke swarms at 1882, 535 and 200 Ma in the Carajás region, Amazonian Craton: Sr-Nd isotopy, trace element geochemistry and inferences on their origin and geological settings. J. S. Am. Earth Sci. 92, 197–208.

Glasson, K.J., Johnson, T.E., Kirkland, C.L., Gardiner, N.J., Clark, C., Blereau, E., Hartnady, M., Spaggiari, C., Smithies, H., 2019. A window into an ancient backarc? The magmatic and metamorphic history of the Fraser Zone, Western Australia. Precambr. Res. 323, 55–69.

Glikson, A., 1996. Geology of the western Musgrave Block, central Australia, with particular reference to the mafic-ultramafic Giles Complex. Australian Government Publishing Service.

Gonzales, D.A., Van Schmus, W.R., 2007. Proterozoic history and crustal evolution in southwestern Colorado: insight from U/Pb and Sm/Nd data. Precambr. Res. 154, 31–70. https://doi.org/10.1016/j.precamres.2006.12.001.

Goodge, J.W., Vervoort, J.D., 2006. Origin of Mesoproterozoic A-type granites in Laurentia: Hf isotope evidence. Earth Planet. Sci. Lett. 243, 711–731. https://doi.org/10.1016/j.epsl.2006.01.040.

Goodge, J.W., Vervoort, J.D., Fanning, C.M., Brecke, D.M., Farmer, G.L., Williams, I.S., Myrow, P.M., DePaolo, D.J., 2008. A positive test of East Antarctica-Laurentia juxtaposition within the Rodinia supercontinent. Science 321, 235–240. https://doi.org/10.1126/science.1159189.

Gorbatschev, R., Bogdanova, S., 1993. Frontiers in the Baltic Shield. Precambr. Res. 64, 3–21.

Gower, C., Krogh, T.E., 2002. A U-Pb geochronological review of the Proterozoic history of the eastern Grenville Province. Can. J. Earth Sci. 39, 795–829. https://doi.org/10.1139/e01-090.

Gower, C.F., Ryan, A.B., Rivers, T., 1990. Mid-Proterozoic Laurentia-Baltica: an overview of its geological evolution and a summary of the contributions made by this volume. In Gower, C.F., Rivers, T., Ryan, A.B. (eds.). Mid-Proterozoic Laurentia-Baltica. GAC Special Paper 38, Geological Association of Canada, 1-20.

Gower, C., Schärer, U., Heaman, L., 1992. The Labradorian orogeny in the Grenville Province, eastern Labrador, Canada. Can. J. Earth Sci. 29, 1944–1957.

Gower, C., Kamo, S., Kwok, K., Krogh, T., 2008. Proterozoic southward accretion and Grenvillian orogenesis in the interior Grenville Province in eastern Labrador: Evidence from U-Pb geochronological investigations. Precambr. Res. 165, 61–95.

Grambling, J.A., 1986. Crustal thickening during Proterozoic metamorphism and deformation in New Mexico (USA). Geology 14, 149–152. https://doi.org/10.1130/0091-7613(1986)14<149:CTDPMA>2.0.CO;2.

Granseth, A., Slagstad, T., Coint, N., Roberts, N.M.W., Røhr, T.S., Sørensen, B.E., 2020. Tectonomagmatic evolution of the Sveconorwegian orogen recorded in the chemical and isotopic compositions of 1070–920 Ma granitoids. Precambr. Res. 340, 105527.

Gray, C., 1978. Geochronology of granulite-facies gneisses in the western Musgrave Block, Central Australia. J. Geol. Soc. Aust. 25, 403–414.

Gray, C., Compston, W., 1978. A rubidium-strontium chronology of the metamorphism and prehistory of central Australian granulites. Geochim. Cosmochim. Acta 42, 1735–1747.

Gregory, C.J., Buick, I.S., Hermann, J., Rubatto, D., 2009. Mineral-scale trace element and U-Th–Pb age constraints on metamorphism and melting during the Petermann Orogeny (central Australia). J. Petrol. 50, 251–287.

Grenholm, M., 2019. The global tectonic context of the ca. 2.27–1.96 Ga Birimian Orogen – insights from comparative studies, with implications for supercontinent cycles. Earth-Sci. Rev. 193, 260–298.

Grenholm, M., Jessell, M., Thébaud, N., 2019. A geodynamic model for the Paleoproterozoic (ca. 2.27–1.96 Ga) Birimian Orogen of the southern West African Craton – Insights into an evolving accretionary-collisional orogenic system. Earth Sci. Rev. 192, 138–193.

Groenewald, C.A., Macey, P.H., 2020. Lithostratigraphy of the Mesoproterozoic Yas-Schuitdrift Batholith, South Africa and Namibia. S. Afr. J. Geol. 123, 431–440.

Groenewald, P.B., Moyes, A.B., Grantham, G.H., Krynauw, J.R., 1995. East Antarctic crustal evolution: geological constraints and modelling in western Dronning Maud Land. Precambr. Res. 75, 231–250.

Halama, R., Vennemann, T., Siebel, W., Markl, W., 2005. The Grønnedal-Ika Carbonatite-Syenite Complex, South Greenland: Carbonatite Formation by Liquid Immiscibility. J. Petrol. 46, 191–217.

Hanski E., 2015. Synthesis of the geological evolution and metallogeny of Finland. Chapter 2 in Maier, W.D., Lahtinen, R., O'Brien, H. (eds.). Mineral Deposits of Finland. Elsevier B.V., Amsterdam, 39-71.

Hanson, R.E., Martin, M.W., Bowring, S.A., Munyanyiwa, H., 1998. U-Pb zircon age for the Umkondo dolerites, eastern Zimbabwe: 1.1 Ga large igneous province in southern Africa-East Antarctica and possible Rodinia correlations. Geology 26, 1143–1146.

Hanson, R.E., Crowley, J.L., Bowring, S.A., Ramezani, J., Gose, W.A., Dalziel, I.W.D., Pancake, J.A., Seidel, E.K., Blenkinsop, T.G., Mukwakwami, J., 2004. Coeval large-scale magmatism in the Kalahari and Laurentian cratons during Rodinia assembly. Science 304, 1126–1129.

Hartnady, C.J.H., Joubert, P., Stowe, C.W., 1985. Proterozoic crustal evolution in southwestern Africa. Episodes 8, 236–244.

Hartnady, M.I.H., Kirkland, C.L., Smithies, R.H., Poujol, M., Clark, C., 2019. Periodic Paleoproterozoic calc-alkaline magmatism at the south eastern margin of the Yilgarn Craton; implications for Nuna configuration. Precambr. Res. 332, 105400.

Hartnady, M.I.H., Kirkland, C., Dutch, R., Bodorkos, S., Jagodzinski, E., 2020a. Evaluating zircon initial Hf isotopic composition using a combined SIMS–MC-LASS-ICP-MS approach: A case study from the Coompana Province in South Australia. Chem. Geol. 558, 119870.

Hartnady, M.I.H., Kirkland, C.L., Martin, L., Clark, C., Smithies, R.H., Spaggiari, C.V., 2020b. Zircon oxygen and hafnium isotope decoupling during regional metamorphism: implications for the generation of low $\delta^{18}O$ magmas. Contrib. Miner. Petrol. 175, 9.

Hawkesworth, C.J., Cawood, P.A., Kemp, T., Storey, C., Dhuime, B., 2009. A matter of preservation. Science 323, 49–50. https://doi.org/10.1126/science.1168549.

Hawkesworth, C.J., Dhuime, B., Pietranik, A.B., Cawood, P.A., Kemp, A.I.S., Storey, C.D., 2010. The generation and evolution of the continental crust. J. Geol. Society 167, 229–248. https://doi.org/10.1144/0016-76492009-072.

Hawkesworth, C.J., Cawood, P.A., Dhuime, B., 2019. Rates of generation and growth of the continental crust. Geosci. Front. 10, 165–173. https://doi.org/10.1016/j.gsf.2018.02.004.

Hawkins, D.P., Bowring, S.A., Ilg, B.R., Karlstrom, K.E., Williams, M.L., 1996. U-Pb geochronologic constraints on the Paleoproterozoic crustal evolution of the Upper Granite Gorge, Grand Canyon, Arizona. Bulletin of the Geological Society of America 108, 1167–1181. https://doi.org/10.1130/0016-7606(1996)108<1167:UPGCOT>2.3.CO;2.

Heinonen, A.P., Fraga, L.M., Rämö, O.T., Dall'Agnol, R., Mänttäri, I., Andersen, T., 2012. Petrogenesis of the igneous Mucajaí AMG complex, northern Amazonian craton, U-Pb geochronological, and Nd–Hf–O isotopic constraints. Lithos 151, 17–34.

Hermansson, T., Stephens, M.B., Corfu, F., Page, L., Andersson, J., 2008. Migratory tectonic switching, western Svecofennian orogen, central Sweden: Constraints from U/Pb zircon and titanite geochronology. Precambr. Res. 161, 250–278.

Hinchey, A.M., 2021a. Lithogeochemical and Nd isotopic constraints on felsic magmatism in the Makkovik Orogen, Labrador, Canada: implications for assembly of the supercontinent Nuna. Lithos 382–383, 105917.

Hinchey, A.M. 2021b. Localized backarc extension in an overall compressional setting during the assembly of Nuna: Geochemical and isotopic evidence from Orosirian (1883–1848 Ma) mafic magmatism of the Aillik Group, Labrador, Canada. Earth and Space Science 8, https://doi.org/10.1029/2020EA001489.

Hinchey, A.M., 2021c. Lithofacies architecture and paleoenvironment of a Paleoproterozoic volcano-sedimentary sequence: Insight into rift-related volcanism during supercontinent assembly. Precambrian Res 367, 106443. https://doi.org/10.1016/j.precamres.2021.106443.

Hinchey, A.M., 2021d. Reply to Dickin (2021) comment(s) on Hinchey (2021): "Lithogeochemical and Nd isotopic constraints on felsic magmatism in the Makkovik Orogen, Labrador, Canada: Implications for assembly of the supercontinent Nuna. Lithos 392–393, 106158. https://doi.org/10.1016/j.lithos.2021.106158.

Hinchey, A.M., Rayner, N., Davis, W.J., 2020. Episodic Paleoproterozoic crustal growth preserved in the Aillik Domain, Makkovik Province, Labrador. Precambr. Res. 337, 105526.

Hoffman, P.F., 1989. Speculations on Laurentia's first gigayear (2.0 to 1.0 Ga). Geology 17, 135–138.

Högdahl, K., Andersson, U.B., Eklund, O. (eds.), 2004. The Transscandinavian Igneous Belt (TIB) in Sweden: a review of its character and evolution. Geological Survey of Finland, Special Paper 37, 125 pp.

Holland, M.E., Karlstrom, K.E., Doe, M.F., Gehrels, G.E., Pecha, M., Shufeldt, O.P., Begg, G., Griffin, W.L., Belousova, E., 2015. An imbricate midcrustal suture zone: The Mojave-Yavapai province boundary in Grand Canyon, Arizona. Bull. Geol. Society America 127, 1391–1410. https://doi.org/10.1130/B31232.1.

Holland, M.E., Karlstrom, K.E., Gehrels, G., Shufeldt, O.P., Begg, G., Griffin, W., Belousova, E., 2018. The Paleoproterozoic Vishnu basin in southwestern Laurentia: implications for supercontinent reconstructions, crustal growth, and the origin of the Mojave crustal province. Precambr. Res. 308, 1–17. https://doi.org/10.1016/j.precamres.2018.02.001.

Holland, M.E., Grambling, T.A., Karlstrom, K.E., Jones, J.V., Nagotko, K.N., Daniel, C.G., 2020. Geochronologic and Hf-isotope framework of Proterozoic rocks from central New Mexico, USA: Formation of the Mazatzal crustal province in an extended continental margin arc. Precambr. Res. 347, 105820 https://doi.org/10.1016/j.precamres.2020.105820.

Hollis, J.A., Kirkland, C.L., Spaggiari, C.V., Tyler, I.M., Haines, P.W., Wingate, M.T.D., Belousova, E.A., Murphy, R.C., 2013. Zircon U-Pb–Hf isotope evidence for links between the Warumpi and Aileron Provinces, West Arunta region. Geol. Survey Western Australia, Record 2013 (9), 30p.

Holm, D., Medaris, L.G., McDannell, K.T., Schneider, D.A., Schulz, K., Singer, B.S., Jicha, B.R., 2020. Growth, overprinting, and stabilization of Proterozoic provinces in the southern Lake Superior region. Precambr. Res. 339, 105587 https://doi.org/10.1016/j.precamres.2019.105587.

Holm, D.K., Van Schmus, W.R., Mac Neil, L.C., Boerboom, T.J., Schweitzer, D., Schneider, D.A., 2005. U-Pb zircon geochronology of Paleoproterozoic plutons from the northern mid-continent, U.S.A.: evidence for subduction flip and continued convergence after geon 18 Penokean orogenesis. Geol. Soc. Am. Bull. 117, 259–275.

Howard, H.M., Smithies, R.H., Kirkland, C.L., Kelsey, D.E., Aitken, A.R.A., Wingate, M.T.D., de Gromard, R.Q., Spaggiari, C.V., Maier, W.D., 2015. The burning heart—the Proterozoic geology and geological evolution of the west Musgrave Region, central Australia. Gondwana Res. 27, 64–94.

Huhma, H., O'Brien, H., Lahaye, Y., Mänttäri, I., 2011. Isotope geology and Fennoscandian lithosphere evolution. Geol. Surv. Finland Spec. Pap. 49, 35–48.

Ibañez–Mejia, M., 2020. The Putumayo Orogen of Amazonia: a synthesis. In: Gómez, J. and Mateus–Zabala, D. (eds), The Geology of Colombia, Volume 1 Proterozoic-Paleozoic. Servicio Geológico Colombiano, Publicaciones Geológicas Especiales 35, 101-131. Bogotá. https://doi.org/10.32685/pub.esp.35.2019.06.

Ibañez–Mejia, M., Cordani, U.G., 2020. Zircon U–Pb geochronology and Hf–Nd–O isotope geochemistry of the Paleo- to Mesoproterozoic basement in the westernmost Guiana Shield. In: Gómez, J. and Mateus–Zabala, D. (eds), The Geology of Colombia, Volume 1 Proterozoic-Paleozoic. Servicio Geológico Colombiano, Publicaciones Geológicas Especiales 35, 65–90. Bogotá. https://doi.org/10.32685/pub.esp35.2019.04.

Ilg, B.R., Karlstrom, K.E., Hawkins, D.P., Williams, M.L., 1996. Tectonic evolution of Paleoproterozoic rocks in the Grand Canyon: Insights into middle-crustal processes. Bulletin of the Geological Society of America 108, 1149–1166. https://doi.org/10.1130/0016-7606(1996)108<1149:TEOPRI>2.3.CO;2.

Jacobs, J., Thomas, R.J., 2004. Himalayan-type indenter-escape tectonics model for the southern part of the late Neoproterozoic–early Paleozoic East African-Antarctic orogen. Geology 32, 721–724.

Jacobs, J., Thomas, R.J., Weber, K., 1993. Accretion and indentation tectonics at the southern edge of the Kaapvaal craton during the Kibaran (Grenville) orogeny. Geology 21, 203–206.
Jacobs, J., Fanning, C.M., Henjes-Kunst, F., Olesch, M., Paech, H.J., 1998. Continuation of the Mozambique Belt into East Antarctica: Grenville-age metamorphism and polyphase Pan-African high-grade events in central Dronning Maud Land. J. Geol. 106, 385–406.
Jacobs, J., Thomas, R.J., Armstrong, R.A., Henjes-Kunst, F., 1999. Age and thermal evolution of the Mesoproterozoic Cape Meredith Complex, West Falkland. J. Geol. Soc. Lond. 156, 917–928.
Jacobs, J., Bauer, W., Fanning, C.M., 2003a. New age constraints for Grenville-age metamorphism in western central Dronning Maud Land (East Antarctica), and implications for the palaeogeography of Kalahari in Rodinia. Int. J. Earth Sci. 92, 301–315.
Jacobs, J., Fanning, C.M., Bauer, W., 2003b. Timing of Grenville-age vs. Pan-African medium-to high grade metamorphism in western Dronning Maud Land (East Antarctica) and significance for correlations in Rodinia and Gondwana. Precambr. Res. 125, 1–20.
Jacobs, J., Pisarevsky, S., Thomas, R.J., Becker, T., 2008. The Kalahari Craton during the assembly and dispersal of Rodinia. Precambr. Res. 160, 142–158.
Jacobs, J., Elburg, M., Läufer, A., Kleinhanns, I.C., Henjes-Kunst, F., Estrada, S., Ruppel, A.S., Damaske, D., Montero, P., Bea, F., 2015. Two distinct late Mesoproterozoic/early Neoproterozoic basement provinces in central/eastern Dronning Maud Land, East Antarctica: The missing link, 15–21° E. Precambr. Res. 265, 249–272.
Jagodzinski, E.A., Bodorkos, S., Crowley, J.L., Pawley, M.J., Wise, T.W., 2019. PACE Copper Coompana Drilling Project: U-Pb dating of basement and cover rocks. Geol. Survey of South Australia Report - Book 2018 (00028), 211.
Jessup, M.J., Jones, J.V., Karlstrom, K.E., Williams, M.L., Connelly, J.N., Heizler, M.T., 2006. Three Proterozoic orogenic episodes and an intervening exhumation event in the Black Canyon of the Gunnison Region, Colorado. J. Geol. 114, 555–576. https://doi.org/10.1086/506160.
Johansson, Å., 2009. Baltica, Amazonia and the SAMBA connection – 1000 million years of neighbourhood during the Proterozoic? Precambr. Res. 175, 221–234.
Johansson, Å., 2014. From Rodinia to Gondwana with the 'SAMBA' model – A distant view from Baltica towards Amazonia and beyond. Precambr. Res. 244, 226–235.
Johansson, Å., 2016. Comments to "Detrital zircon signatures of the Baltoscandian margin along the Arctic Circle Caledonides in Sweden: The Sveconorwegian connection" by Gee et al. (2015). Letter to the Editor. Precambrian Research 276, 233-235.
Johansson, Å., Bogdanova, S., Cecys, A., 2006. A revised geochronology for the Blekinge Province, southern Sweden. GFF 128, 287–302.
Johansson, Å., Waight, T., Andersen, T., Simonsen, S.L., 2016. Geochemistry and petrogenesis of Mesoproterozoic A-type granitoids from the Danish island of Bornholm, southern Fennoscandia. Lithos 244, 94–108.
Johnston, S.T., Armstrong, R., Heaman, L., McCourt, S., Mitchell, A., Bisnath, A., Arima, M., 2001. Preliminary U-Pb Geochronology of the Tugela Terrane, Natal Belt, Eastern South Africa. Memoir of the National Institute for Polar Research Special Issue, vol. 55, National Institute Polar Research, Tokyo (2001), 40–58.
Jones, D.S., Snoke, A.W., Premo, W.R., Chamberlain, K.R., 2010. New models for Paleoproterozoic orogenesis in the Cheyenne belt region: evidence from the geology and U-Pb geochronology of the Big Creek Gneiss, southeastern Wyoming. Bull. Geol. Society of America 122, 1877–1898. https://doi.org/10.1130/B30164.1.
Karlstrom, K.E., Bowring, S.A., 1988. Early Proterozoic Assembly of Tectonostratigraphic Terranes in Southwestern North America. J. Geol. 96, 561–576.
Karlstrom, K.E., Åhäll, K.-I., Harlan, S.S., Williams, M.L., McLelland, J., Geissman, J.W., 2001. Long-lived (1.8 – 1.0 Ga) convergent orogen in southern Laurentia, its extension to Australia and Baltica, and implications for refining Rodinia. Precambr. Res. 111, 5–30. https://doi.org/10.1016/S0301-9268(01)00154-1.
Karlstrom, K.E., Bowring, S.A., Conway, C.M., 1987. Tectonic significance of an Early Proterozoic two-province boundary in central Arizona. Bulletin of the Geological Society of America 99, 529–538. https://doi.org/10.1130/0016-7606(1987)99<529:TSOAEP>2.0.CO;2.
Kerr, A., 1989. Geochemistry of the Trans-Labrador Granitoid Belt, Canada: A quantitative comparative study of a Proterozoic batholith and possible Phanerozoic counterparts. Precambrian Research 45, 1–17. https://doi.org/10.1016/0301-9268(89)90027-2.
Kerr, A., Krogh, T.E., Corfu, F., Scharer, U., Gandhi, S.S., Kwok, Y.Y., 1992. Episodic early Proterozoic granitoid plutonism in the Makkovik Province, Labrador: U-Pb geochronological data and geological implications. Canadian Journal of Earth Sciences 29, 1166–1179.
Kerr, A., Ryan, B., Gower, C.F., Wardle, R.J., 1996. The Makkovik Province: extension of the Ketilidian Mobile Belt in mainland North America. Geol. Soc. London Spec. Publ. 112, 155–177. https://doi.org/10.1144/GSL.SP.1996.112.01.09.
Ketchum, J.W.F., Culshaw, N.G., Barr, S.M., 2002. Anatomy and orogenic history of a Paleoproterozoic accretionary belt: the Makkovik Province, Labrador, Canada. Can. J. Earth Sci. 39, 711–730.
Kirkland, C.L., Smithies, R.H., Woodhouse, A.J., Howard, H.M., Wingate, M.T.D., Belousova, E.A., Cliff, J.B., Murphy, R.C., Spaggiari, C.V., 2013. Constraints and deception in the isotopic record; the crustal evolution of the west Musgrave Province, central Australia. Gondwana Res. 23, 759–781.
Kirkland, C.L., Smithies, R.H., Spaggiari, C.V., 2015. Foreign contemporaries - Unravelling disparate isotopic signatures from Mesoproterozoic Central and Western Australia. Precambr. Res. 265, 218–231.
Kirkland, C.L., Smithies, R.H., Spaggiari, C.V., Wingate, M.T.D., de Gromard, R.Q., Clark, C., Gardiner, N.J., Belousova, E.A., 2017. Proterozoic crustal evolution of the Eucla basement, Australia: Implications for destruction of oceanic crust during emergence of Nuna. Lithos 278, 427–444.
Kirkland, C., Spaggiari, C., Pawley, M., Wingate, M., Smithies, R., Howard, H., Tyler, I., Belousova, E.A., Poujol, M., 2011. On the edge: U-Pb, Lu–Hf, and Sm–Nd data suggests reworking of the Yilgarn craton margin during formation of the Albany-Fraser Orogen. Precambr. Res. 187, 223–247.
Kirkland, C.L., Spaggiari, C.V., Johnson, T.E., Smithies, R.H., Danišík, M., Evans, N.J., Wingate, M.T.D., Clark, C., Spencer, C.J., Mikucki, E., 2016. Grain size matters: implications for element and isotopic mobility in titanite. Precambr. Res. 278, 283–302.
Kirscher, U., Liu, Y., Li, Z.X., Mitchell, R.N., Pisarevsky, S.A., Denyszyn, S.W., Nordsvan, A., 2019. Paleomagnetism of the Hart Dolerite (Kimberley, Western Australia) – a two-stage assembly of the supercontinent Nuna? Precambr. Res. 329, 170–181. https://doi.org/10.1016/j.precamres.2018.12.026.
Kirscher, U., Mitchell, R.N., Liu, Y., Nordsvan, A.R., Cox, G.M., Pisarevsky, S.A., Wang, C., Wu, L., Murphy, J.B., Li, Z.-X., 2021. Paleomagnetic constraints on the duration of the Australia-Laurentia connection in the core of the Nuna supercontinent. Geology 49, 174–179. https://doi.org/10.1130/G47823.1.
Klein, E.L., Almeida, M.E., Rosa-Costa, L.T., 2012. The 1.89-1.87 Ga Uatumã Silicic Large Igneous Province, northern South America. Large Igneous Provinces Commission, International Association of Volcanology and Chemistry of the Earth's Interior. http://www.largeigneousprovinces.org/12nov.
Korja, A., Lahtinen, R., Nironen, M., 2006. The Svecofennian orogen: a collage of microcontinents and island arcs. In: Gee, D.G. & Stephenson, R.A. (eds.). European Lithosphere Dynamics. Geological Society, London, Memoir 32, 561–578.
Kröner, A., Muhongo, S., Hegner, E., Wingate, M.T.D., 2003. Single zircon geochronology and Nd isotopic systematics of Proterozoic high grade rocks from the Mozambique belt of southern Tanzania (Masasi area): implications for Rodinia and Gondwana assembly. J. Geol. Society 160, 745–757.
Kroonenberg, S.B., De Roever, E.W.F., Fraga, L.M., Reis, N.J., Faraco, T., Lafon, J.-M., Cordani, U., Wong, T.E., 2016. Paleoproterozoic evolution of the Guiana Shield in Suriname: a revised model. Neth. J. Geosci. 95, 491–522.
Krzeminska, E., Krzemiński, L., Petecki, Z., Wiszniewska, J., Salwa, S., Żaba, J., Gaidzik, K., Williams, I.S., Rosowiecka, O., Taran, L., Johansson, Å., Pécskay, Z., Demaiffe, D., Grabowski, J., Zieliński, G., 2017. Geological Map of Crystalline Basement in the Polish Part of the East European Platform 1:1000000. Państwowy Instytut Geologiczny, Warszawa.
Krzeminska, E., Johansson, Å., Krzeminski, L., Wiszniewska, J., Williams, I.S., Petecki, Z., Salwa, S., 2021. Basement correlation across the southernmost Baltic Sea: Geochemical and geochronological evidence from onshore and offshore deep drill cores, northern Poland. Precambr. Res. 362, 106300 https://doi.org/10.1016/j.precamres.2021.106300.
Ksienzyk, A.K., Jacobs, J., 2015. Western Australia-Kalahari (WAlahari) connection in Rodinia: Not supported by U/Pb detrital zircon data from the Maud Belt (East Antarctica) and the Northampton Complex (Western Australia). Precambr. Res. 259, 207–221.
Lahtinen, R., Korja, A., Nironen, M., 2005. Paleoproterozoic tectonic evolution. In: Lehtinen, M., Nurmi, P.A., Rämö, O.T. (eds.). Precambrian Geology of Finland – Key to the Evolution of the Fennoscandian Shield. Elsevier B.V., Amsterdam, 481–532.
Lahtinen, R., Garde, A.A., Melezhik, V.A., 2008. Paleoproterozoic evolution of Fennoscandia and Greenland. Episodes 31, 20–28.
Lahtinen, R., Huhma, H., Lahaye, Y., Jonsson, E., Manninen, T., Lauri, L., Bergman, S., Hellström, F., Niiranen, T., Nironen, M., 2015a. New geochronological and Sm-Nd constraints across the Pajala shear zone of northern Fennoscandia: reactivation of a Paleoproterozoic suture. Precambr. Res. 256, 10–119.
Lahtinen, R., Huhma, H., Lahaye, Y., Kousa, J., Luukas, J., 2015b. Archean-Proterozoic collision boundary in central Fennoscandia: Revisited. Precambr. Res. 261, 127–165.
Lahtinen, R., Huhma, H., Lahaye, Y., Lode, S., Heinonen, S., Sayab, M., Whitehouse, M.J., 2016. Paleoproterozoic magmatism across the Archean-Proterozoic boundary in central Fennoscandia: geochronology, geochemistry and isotopic data (Sm-Nd, Lu-Hf, O). Lithos 262, 507–525.
Lamarão, C.N., Dall'Agnol, R., Pimentel, M.M., 2005. Nd isotopic composition of Paleoproterozoic volcanic and granitoid rocks of Vila Riozinho: implications for the crustal evolution of the Tapajós gold province, Amazon craton. Journal South America Earth Science, 18, 277-292. https://doi:10.1016/j.jsames.2004.11.005.
Lambert, C.W., 2013. Granitic melt transport and emplacement along transcurrent shear zones: Case study of the Pofadder Shear Zone in South Africa and Namibia. (Thesis, Stellenbosch University) (128 pp.). http://scholar.sun.ac.za/handle/10019.1/85682.
Larson, S.Å., Berglund, J., 1992. A chronological subdivision of the Transscandinavian Igneous Belt – three magmatic episodes? Geologiska Föreningen i Stockholm Förhandlingar 114, 459–461.
Laurent, A.T., Duchene, S., Bingen, B., Bosse, V., Seydoux-Guillaume, A.M., 2018. Two successive phases of ultrahigh temperature metamorphism in Rogaland, S. Norway: evidence from Y-in-monazite thermometry. J. Metamorph. Geol. 36, 1009–1037.
Leal, R.E., Lafon, J.M., Rosa-Costa, L.T., Dantas, E.L., 2018. Orosirian magmatic episodes in the Erepecuru - Trombetas Domain (Southeastern Guyana Shield): implications for the crustal evolution of the Amazonian Craton. J. S. Am. Earth Sci. 85, 278–297.
Lee, C.T., Yin, Q., Rudnick, R.L., Jacobsen, S.B., 2001. Preservation of ancient and fertile lithospheric mantle beneath the southwestern United States. Nature 411, 69–73. https://doi.org/10.1038/35075048.
Lehtinen, M., Nurmi, P.A., Rämö, O.T. (eds.), 2005. Precambrian Geology of Finland – Key to the Evolution of the Fennoscandian Shield. Developments in Precambrian Geology 14. Elsevier B.V., Amsterdam, 736 pp.
Li, Z.X., Bogdanova, S.V., Collins, A.S., Davidson, A., De Waele, B., Ernst, R.E., Fitzsimons, I.C.W., Fuck, R.A., Gladkochub, D.P., Jacobs, J., Karlstrom, K.E., Lu, S.,

Natapov, L.M., Pease, V., Pisarevsky, S.A., Thrane, K., Vernikovsky, V., 2008. Assembly, configuration, and break-up history of Rodinia: a synthesis. Precambrian Research 160, 179-210.

Litherland, M., Annells, R.N., Appleton, J.D., Berrange, J.P., Bloomfield, K., Burton, C.C. I., Darbyshire, D.P.F., Fletcher, C.J.N., Hawkins, M.P., Klinck, B.A., Llanos, A., Mitchell, W.I., O'Connor, E.A., Pitfield, P.E.J., Power, G., Webb, B.C., 1986. The geology and mineral resources of the Bolivian Precambrian shield. British Geological Survey, Overseas Memoir 9, 153.

Litherland, M., Annels, R.N., Hawkins, M.P., Klinck, B.A., O'Connor, E.A., Pitfield, P.E.J., Power, G., Darbyshire, D.P.F., Fletcher, C.N.J., Mitchell, W.I., Webb, B.C., 1989. The Proterozoic of eastern Bolivia and its relationships to the Andean mobile belt. Precambr. Res. 43, 157–174.

Liu, Y., Mitchell, R.N., Li, Z.-X., Kirscher, U., Pisarevsky, S.A., Wang, C., 2021. Archean geodynamics: ephemeral supercontinents or long-lived supercratons. Geology 49, 794–798. https://doi.org/10.1130/G48575.1.

Loewy, S.L., Connelly, J.N., Dalziel, I.W.D., Gower, C., 2003. Eastern Laurentia in Rodinia: Constraints from whole-rock Pb and U/Pb geochronology. Tectonophysics 375, 169–197. https://doi.org/10.1016/S0040-1951(03)00338-X.

Loewy, S.L., Connelly, J.N., Dalziel, I.W.D., 2004. An orphaned basement block: the Arequipa-Antofalla Basement of the central Andean margin of South America. Geol. America Bulletin 116, 171–187.

Loewy, S.L., Dalziel, I.W.D., Pisarevsky, S., Connelly, J.N., Tait, J., Hanson, R.E., Bullen, D., 2011. Coats Land crustal block, East Antarctica: A tectonic tracer for Laurentia? Geology 39, 859–862.

Lorenz, H., Gee, D.G., Larionov, A., Majka, J., 2012. The Grenville-Sveconorwegian orogen in the High Arctic. Geol. Mag. 149, 875–891.

Lundqvist, Th., Persson, P.-O., 1999. Geochronology of porphyries and related rocks in northern and western Dalarna, south-central Sweden. GFF 121, 307–322.

Macambira, M.J.B., Teixeira, W., Vasquez, M.L., 2020. O Cráton Amazônico e suas províncias geocronológicas: o legado de Umberto Cordani. In: Bartorelli, A., Teixeira, W., Brito Neves, B.B. (eds.) Geocronologia e Evolução Tectônica do Continente Sul-Americano: a Contribuição de Umberto Giuseppe Cordani. 1ª edição. São Paulo, Solares Edições Culturais. p. 47-62.

Macambira, M.J.B., Vasquez, M.L., Silva, D.C.C., Galarza, M.A., Barros, C.E.M., Camelo, J.F., 2009. Crustal growth of the central-eastern Paleoproterozoic domain, SE Amazonian craton: Juvenile accretion vs. reworking. J. South America Earth Sci. 27, 235–246. https://doi.org/10.1016/j. jsames.2009.02.001.

Macey, P.H., Thomas, R.J., Grantham, G.H., Ingram, B.A., Jacobs, J., Armstrong, R.A., Roberts, M.P., Bingen, B., Hollick, L., De Kock, G.S., Viola, G., 2010. Mesoproterozoic geology of the Nampula Block, northern Mozambique: Tracing fragments of Mesoproterozoic crust in the heart of Gondwana. Precambr. Res. 182, 124–148.

Macey, P.H., Thomas, R.J., Minnaar, H.M., Gresse, P.G., Lambert, C.W., Groenewald, C. A., Miller, J.A., Indongo, J., Angombe, M., Shifotoka, G., Frei, D., 2017. Origin and evolution of the ~1.9 Ga Richtersveld magmatic arc, SW Africa. Precambr. Res. 292, 417–451.

Macey, P.H., Abrahams, Y., Miller, J.A., 2018a. Lithostratigraphy of the Mesoproterozoic Stolzenfels Enderbite (Komsberg Suite), South Africa and Namibia. S. Afr. J. Geol. 121, 217–226.

Macey, P.H., Bailie, R.H., Miller, J.A., Thomas, R.J., De Beer, C., Frei, D., Le Roux, P.J., 2018b. Implications of the distribution, age and origins of the granites of the Mesoproterozoic Spektakel Suite for the timing of the Namaqua Orogeny in the Bushmanland Subprovince of the Namaqua-Natal Metamorphic Province, South Africa. Precambr. Res. 312, 68–98.

Mako, C.A., Williams, M.L., Karlstrom, K.E., Doe, M.F., Powicki, D., Holland, M.E., Gehrels, G., Pecha, M., 2015. Polyphase Proterozoic deformation in the Four Peaks area, central Arizona, and relevance for the Mazatzal orogeny. Geosphere 11, 1975–1995. https://doi.org/10.1130/GES01196.1.

Manda, B.W.C., Cawood, P.A., Spencer, C.J., Prave, A., Robinson, R., Roberts, N.M.W., 2019. Evolution of the Mozambique Belt in Malawi constrained by granitoid U-Pb, Sm-Nd and Lu-Hf isotopic data. Gondwana Res. 68, 93–107.

Marschall, H.R., Hawkesworth, C.J., Leat, P.T., 2013. Mesoproterozoic subduction under the eastern edge of the Kalahari-Grunehogna Craton preceding Rodinia assembly: the Ritscherflya detrital zircon record, Ahlmannryggen (Dronning Maud Land, Antarctica). Precambr. Res. 236, 31–45.

Martin, E.L., Spencer, C.J., Collins, W.J., Thomas, R.J., Macey, P.H., Roberts, N.M.W., 2020. The core of Rodinia formed by the juxtaposition of opposed retreating and advancing accretionary orogens. Earth Sci. Rev. 211 (103413), 1–17.

Matos, R., Teixeira, W., Geraldes, M.C., Bettencourt, J.S., 2009. Geochemistry and isotopic evidence of the Pensamiento Granitoid Complex, Rondonian-San Ignacio province, eastern Precambrian Shield of Bolivia: petrogenetic constraints for a Mesoproterozoic magmatic arc setting. Rev. Geol. USP Sér. Científ. 9 (2), 89–117.

Matthews, P.E., 1972. Possible Precambrian obduction and plate tectonics in southeastern Africa. Nature 240, 37–39.

McClung, C.R., 2006. Basin analysis of the Mesoproterozoic Bushmanland Group of the Namaqua metamorphic province, South Africa (Doctoral dissertation, University of Johannesburg), 509p.

McLelland, J.M., 1989. Crustal growth associated with anorogenic, mid-Proterozoic anorthosite massifs in northeastern North America. Tectonophysics 161, 331–341. https://doi.org/10.1016/0040-1951(89)90163-7.

McLelland, J., Daly, S., McLelland, J.M., 1996. The Grenville orogenic cycle (ca. 1350–1000 Ma): an Adirondack perspective. Tectonophysics 265, 1–28.

Meert, J.G., Santosh, M., 2017. The Columbia supercontinent revisited. Gondwana Res. 50, 67–83.

Melcher, F., Graupner, T., Oberthür, T., Schütte, P., 2017. Tantalum-(niobium-tin) mineralisation in pegmatites and rare-metal granites of Africa. S. Afr. J. Geol. 120, 77–100.

Mendonidis, P., Armstrong, R.A., 2009. A new U-Pb zircon age for the Portobello granite from the southern part of the Natal Metamorphic Belt. South African Journal of Geology 112 (2), 197–208.

Mendonidis, P., Thomas, R.J., Grantham, G.H., Armstrong, R.A., 2015. Geochronology of emplacement and charnockite formation of the Margate Granite Suite, Natal Metamorphic Province, South Africa: implications for Natal-Maud belt correlations. Precambr. Res. 265, 189–202.

Mertanen, S., Pesonen, L.J., 2012. Paleo-Mesoproterozoic assemblages of continents: paleomagnetic evidence for near equatorial supercontinents. In: Haapala, I. (ed.), From the Earth's Core to Outer Space. Lecture Notes in Earth Sciences 137. Springer, Berlin, Heidelberg.

Milhomem Neto, J.M., Lafon, J.M., 2019. Zircon U-Pb and Lu-Hf isotope constraints on Archean crustal evolution in southeastern Guyana Shield. Geosci. Front. 10, 1477–1506.

Milhomem Neto, J.M., Lafon, J.M., 2020. Crustal growth and reworking of Archean crust within the Rhyacian domains of the southeastern Guiana Shield, Brazil: Evidence from zircon U-Pb–Hf and whole-rock Sm–Nd geochronology. J. S. Am. Earth Sci. 103, 102740 https://doi.org/10.1016/j.jsames.2020.102740.

Miller, R.M.G., 2008. The Geology of Namibia, 1. Archaean to Mesoproterozoic, Geological Survey, Windhoek, Namibia.

Mitchell, R.N., Zhang, N., Salminen, J., Liu, Y., Spencer, C.J., Steinberger, B., Murphy, J. B., Li, Z.-X., 2021. The supercontinent cycle. Nature Rev. Earth Environ. 2, 358–374. https://doi.org/10.1038/s43017-021-00160-0.

Möller, C., Andersson, J., 2018. Metamorphic zoning and behaviour of an underthrusting continental plate. J. Metamorph. Geol. 36, 567–589.

Möller, C., Andersson, J., Dyck, B., Antal Lundin, I., 2015. Exhumation of an eclogite terrane as a hot migmatitic nappe, Sveconorwegian orogen. Lithos 226, 147–168.

Morgan, J.W., Stein, H.J., Hannah, J.L., Markey, R.J., Wiszniewska, J., 2000. Re-Os study of Fe-Ti-V oxide and Fe-Cu-Ni sulfide deposits, Suwałki Anorthosite Massif, northeast Poland. Miner. Deposita 35, 391–401.

Moscati, R.J., Premo, W.R., DeWitt, E.H., Wooden, J.L., 2017. U-Pb ages and geochemistry of zircon from Proterozoic plutons of the Sawatch and Mosquito ranges, Colorado, U.S.A.: implications for crustal growth of the central Colorado province. Rocky Mt Geol. 52, 17–106. https://doi.org/10.24872/rmgjournal.52.1.17.

Mosher, S., 1998. Tectonic evolution of the southern Laurentian Grenville orogenic belt. Geological Society of America Bulletin 110, 1357–1375. https://doi.org/10.1130/0016–7606(1998)110<1357:TEOTSL>2.3.CO;2.

Mosher, S., Levine, J.S.F., Carlson, W.D., 2008. Mesoproterozoic plate tectonics: A collisional model for the Grenville-aged orogenic belt in the Llano Uplift, central Texas. Geology 36, 55–58. https://doi.org/10.1130/G24049A.1.

Moyes, A.B., Krynauw, J.R., Barton, J.M., 1995. The age of the Ritscherflya Supergroup and Borgmassivet Intrusions, Dronning Maud Land, Antarctica. Antarct. Sci. 7, 87–97.

Myers, J.S., 1985. The Fraser Complex—a major layered intrusion in Western Australia. Geol. Survey Western Australia Report 14, 57–66.

Myers, J.S., Shaw, R.D., Tyler, I.M., 1996. Tectonic evolution of Proterozoic Australia. Tectonics 15, 1431–1446.

Nedel, I.M., Ruiz, A.S., Matos-Salinas, G., Sousa, M.Z.A., Pimentel, M.M., Pavaneto, P., 2017. Front San Diablo na região de Miraflores, Faixa Sunsás, Bolívia: implicações tectônicas e estratigráficas. Geol. USP Sér. Científ. 17 (3), 125–147.

Nedel, I.M., Fuck, R.A., Ruiz, A.S., Matos, R., Ferreira, A.C.D., 2020. U-Pb geochronology and geochemistry of Grenville-age plutons in the Sunsas Belt - Bolivia, SW Amazonian Craton: Tectonic and magmatic implications. J. S. Am. Earth Sci. 104, 102845 https://doi.org/10.1016/j.jsames.2020.102845.

Neder, R.D., Leite, J.A.D., Figueiredo, B.R., McNaughton, N.J., 2002. 1.76 Ga volcano-plutonism in the southwestern Amazonian Craton, Aripuanã-MT, Brazil: Tectono-stratigraphic implications from SHRIMP U-Pb zircon data and rock geochemistry. Precambr. Res. 119, 171–187. https://doi.org/10.1016/S0301-9268(02)00122-5.

Neumann, N., Fraser, G. (eds.), 2007. Geochronological synthesis and time-space plots for Proterozoic Australia. Geoscience Australia Record 2007/06.

NICE Working Group, 2007. Reinterpretation of Paleoproterozoic accretionary boundaries of the north-central United States based on a new aeromagnetic-geologic compilation. Precambrian Research 157, 71–79.

Nironen, M., 1997. The Svecofennian Orogen: a tectonic model. Precambr. Res. 86, 21–44.

Nixon, A.L., Glorie, S., Collins, A.S., Whelan, J.A., Reno, B.L., Danišík, M., Wade, B.P., Fraser, G., 2020. Footprints of the Alice Springs Orogeny preserved in far northern Australia: an application of multi-kinetic thermochronology in the Pine Creek Orogen and Arnhem Province. Journal of the Geological Society 178 (2), jgs2020–173. https://doi.org/10.1144/jgs2020-173.

Nke, A.Y., Bailie, R.H., Macey, P.H., Thomas, R.J., Frei, D., Le Roux, P., Spencer, C.J., 2020. The 1.8 Ga Gladkop Suite: The youngest Palaeoproterozoic domain in the Namaqua-Natal Metamorphic Province, South Africa. Precambr. Res. 350, 105941.

Nomade, S., Chen, Y., Pouclet, A., Féraud, G., Théveniaut, H., Daouda, B.Y., Vidal, M., Rigolet, C., 2003. The Guiana and West African Shield Palaeoproterozoic grouping: new palaeomagnetic data for French Guiana and Ivory Coast. Geophys. J. Int. 154, 677–694.

Nordsvan, A.R., Collins, W.J., Li, Z.-X., Spencer, C.J., Pourteau, A., Withnall, I.W., Betts, P.G., Volante, S., 2018. Laurentian crust in northeast Australia: implications for the assembly of the supercontinent Nuna. Geology 46, 251–254. https://doi.org/10.1130/G39980.1.

Nyman, M.W., Karlstrom, K.E., 1997. Pluton emplacement processes and tectonic setting of the 1.42 Ga Signal batholith, SW USA: important role of crustal anisotropy during regional shortening. Precambr. Res. 82, 237–263.
Nyman, M.W., Karlstrom, K.E., Kirby, E., Graubard, C.M., 1994. Mesoproterozoic contractional orogeny in western North America: Evidence from 1.4 Ga plutons. Geology 22, 901–904.
Olivarius, M., Friis, H., Kokfelt, T.F., Wilson, J.R., 2015. Proterozoic basement and Palaeozoic sediments in the Ringkøbing-Fyn High characterized by zircon U-Pb ages and heavy minerals from Danish onshore wells. Bull. Geol. Soc. Den. 63, 29–44.
Oliveira, M.A., Dall' Agnol, R., Almeida, J.A.C., 2011. Petrology of the Mesoarchean Rio Maria suite: implications for the genesis of sanukitoid rocks. J. Petrol. 51, 2121–2148.
Papapavlou, K., Darling, J.R., Storey, C.D., Lightfoot, P.C., Moser, D.E., Lasalle, S., 2017. Dating shear zones with plastically deformed titanite: new insights into the orogenic evolution of the Sudbury impact structure (Ontario, Canada). Precambr. Res. 291, 220–235. https://doi.org/10.1016/j.precamres.2017.01.007.
Parman, S.W., 2015. Time-lapse zirconography: Imaging punctuated continental evolution. Geochem. Perspect. Lett. 1, 43–52. https://doi.org/10.7185/geochemlet.1505.
Pastor-Galán, D., Nance, R.D., Murphy, J.B., Spencer, C.J. 2019. Supercontinents: myths, mysteries, and milestones. In Wilson, R.W., Houseman, G.A., McCaffrey, K.J.W., Doré, A.G., Buiter, S.J.H. (eds). Fifty Years of the Wilson Cycle Concept in Plate Tectonics. Geological Society, London, Special Publications 470, 39–64.
Payolla, B.L., Bettencourt, J.S., Kozuch, M., Leite Jr., W.B., Fetter, A.H., Van Schmus, W. R., 2002. Geological evolution of the basement rocks in the east-central part of the Rondônia Tin Province, SW Amazonian Craton, Brazil: U-Pb and Sm–Nd isotopic constraints. Precambr. Res. 119, 141–169.
Perritt, S., 2001. The Ahlmannryggen group, western Dronning Maud Land, Antarctica (Doctoral dissertation), 153p.
Persson, A.I., 1999. Absolute (U–Pb) and relative age determinations of intrusive rocks in the Ragunda rapakivi complex, central Sweden. Precambr. Res. 95, 109–127.
Pesonen, L.J., Mertanen, S., Veikkolainen, T., 2012. Paleo-Mesoproterozoic supercontinents – a paleomagnetic view. Geophysica 48, 5–48.
Petersson, A., Scherstén, A., Bingen, B., Gerdes, A., Whitehouse, M.J., 2015. Mesoproterozoic continental growth: U-Pb-Hf-O zircon record in the Idefjorden Terrane, Sveconorwegian Orogen. Precambr. Res. 261, 75–95.
Pettersson, Å., 2008. Mesoproterozoic crustal evolution in Southern Africa, PhD thesis, Gothenburg University, A117; http://gupea.ub.gu.se/handle/2077/17269.
Pettersson, Å., Cornell, D.H., Moen, H.F., Reddy, S., Evans, D., 2007. Ion-probe dating of 1.2 Ga collision and crustal architecture in the Namaqua-Natal Province of southern Africa. Precambr. Res. 158, 79–92.
Pisarevsky, S.A., Elming, S.-Å., Pesonen, L.J., Li, Z.-X., 2014. Mesoproterozoic paleogeography: supercontinent and beyond. Precambr. Res. 244, 207–225.
Pourteau, A., Smit, M.A., Li, Z.-X., Collins, W.J., Nordsvan, A.R., Volante, S., Li, J., 2018. 1.6 Ga crustal thickening along the final Nuna suture. Geology 46, 959–962. https://doi.org/10.1130/G45198.1.
Premo, W.R., Van Schmus, W.R., 1989. Zircon geochronology of Precambrian rocks in southeastern Wyoming and northern Colorado. In: Grambling, J.A., Tewksbury, B.J. (Eds.), Proterozoic Geology of the Southern Rocky Mountains. Geological Society of America Special Paper 235, p. 13-32.
Puetz, S.J., Condie, K.C., 2020. Applying Popperian falsifiability to geodynamic hypotheses: empirical testing of the episodic crustal/zircon production hypothesis and selective preservation hypothesis. Int. Geol. Rev. 63, 1920–1950. https://doi.org/10.1080/00206814.2020.1818143.
Quentin de Gromad, R., Spaggiari, C.V., Munro, M., Sakota, J., DePaoli, M., 2017. SGTSG 2017 Albany-Fraser Orogen pre-conference fieldtrip: transect across an Archean craton margin to a Proterozoic ophiolite. Geological Survey of Western Australia.
Raith, J.G., Cornell, D.H., Frimmel, H.E., De Beer, C.H., 2003. New insights into the geology of the Namaqua tectonic province, South Africa, from ion probe dating of detrital and metamorphic zircon. J. Geol. 111, 347–366.
Ramberg, I.B., Bryhni, I., Nöttvedt, A., Rangnes, K. (eds.), 2008. The Making of a Land. Geology of Norway. Geological Society of Norway, Trondheim, 624 pp.
Rämö, O.T., Haapala, I., 2005. Rapakivi granites. In: Lehtinen, M., Nurmi, P.A., Rämö, O. T. (eds.). Precambrian Geology of Finland – Key to the Evolution of the Fennoscandian Shield. Elsevier B.V., Amsterdam, 533–562.
Rämo, T., Huhma, H., Kirs, J., 1996. Radiogenic isotopes of the Estonian and Latvian rapakivi granite suites: new data from the concealed Precambrian of the East European Craton. Precambr. Res. 79, 209–226.
Reed, J.C., Bickford, M.E., Premo, W.R., Aleinikoff, J.N., Pallister, J.S., 1987. Evolution of the Early Proterozoic Colorado province: Constraints from U-Pb geochronology. Geology 15, 861–865. https://doi.org/10.1130/0091-7613(1987)15<861:EOTEPC>2.0.CO;2.
Reid, D.L., 1979. Total rock Rb-Sr and U-Th-Pb isotopic study of Precambrian metavolcanic rocks in the lower Orange River region, southern Africa. Earth Planet. Sci. Lett. 42, 368–378.
Reis, N.J., Fraga, L.M., Faria, M.S.G. de, Almeida, M.E., 2003. Geologia do Estado de Roraima, Brasil. In: Rossi P., Lafon J-M, Vasquez M.L. (eds.). Geology of France and Surrounding Areas – Special Guiana Shield. No. 2-3-4, BRGM, p. 121-134.
Reis, N.J., Teixeira, W., Hamilton, M.A., Bispo-Santos, F., Almeida, M.E., D'Agrella-Filho, M.S., 2013. Avanavero mafic magmatism, a late Paleoproterozoic LIP in the Guiana Shield, Amazonian Craton: U-Pb ID-TIMS baddeleyite, geochemical and paleomagnetic evidence. Lithos 174, 175–195.
Reis, N.J., Teixeira, W., Bettencourt, J.S., D'Agrella-Filho, M.S., Ernst, R.E., Goulart, L.E., 2021. Large Igneous Provinces of the Amazonian Craton and their Metallogenic Potential in Proterozoic Times. In R. K. Srivastava et al, (eds.). Large Igneous Provinces and their Plumbing Systems. Special Publication of Geological Society of London 518, 37pp. doi: https://doi.org/10.1144/SP518-2021-7.
Ribeiro, B.V., Cawood, P.A., Faleiros, F.M., Mulder, J.A., Martin, E., Finch, M.A., Raveggi, M., Teixeira, W., Cordani, U.G., Pavan, M., 2020. A long-lived active margin revealed by zircon U-Pb-Hf data from the Rio Apa Terrane (Brazil): new insights into the Paleoproterozoic evolution of the Amazonian Craton. Precambr. Res. 350, 105919.
Riley, T.R., Flowerdew, M.J., Pankhurst, R.J., Millar, I.L., Whitehouse, M.J., 2020. U-Pb zircon geochronology from Haag Nunataks, Coats Land and Shackleton Range (Antarctica): constraining the extent of juvenile Late Mesoproterozoic arc terranes. Precambr. Res. 340, 105646.
Ripa, M., Stephens, M.B., 2020a. Continental magmatic arc and siliciclastic sedimentation in the far-field part of a 1.7 Ga accretionary orogen. Chapter 9 in Stephens, M.B., Bergman Weihed, J. (eds.), 2020. Sweden: Lithotectonic Framework, Tectonic Evolution and Mineral Resources. Geological Society Memoir 50, Geological Society of London, 253-268.
Ripa, M., Stephens, M.B., 2020b. Magmatism (1.6-1.4 Ga) and Mesoproterozoic sedimentation related to intracratonic rifting coeval with distal accretionary orogenesis. Chapter 10 in Stephens, M.B., Bergman Weihed, J. (eds.), 2020. Sweden: Lithotectonic Framework, Tectonic Evolution and Mineral Resources. Geological Society Memoir 50, Geological Society of London, 269-288.
Rivers, T., 1997. Lithotectonic elements of the Grenville Province: Review and tectonic implications. Precambr. Res. 86, 117–154.
Rivers, T., 2008. Assembly and preservation of lower, mid, and upper orogenic crust in the Grenville Province-Implications for the evolution of large hot long-duration orogens. Precambr. Res. 167, 237–259. https://doi.org/10.1016/j.precamres.2008.08.005.
Rivers, T., Corrigan, D., 2000. Convergent margin on southeastern Laurentia during the Mesoproterozoic: tectonic implications. Canadian Journal of Earth Sciences 37, 359–383.
Rivers, T., Ketchum, J., Indares, A., Hynes, A., 2002. The High Pressure belt in the Grenville Province: Architecture, timing, and exhumation. Can. J. Earth Sci. 39, 867–893.
Rizzotto, G.J., Hartmann, L.A., 2012. Geological and geochemical evolution of the Trincheira Complex, a Mesoproterozoic ophiolite in the southwestern Amazon craton, Brazil. Lithos 148, 277–295.
Rizzotto, G.J., Santos, J.O.S., Hartmann, L.A., Tohver, E., Pimentel, M.M., Mcnaughton, N.J., 2013. The Mesoproterozoic Guaporé suture in the SW Amazonian Craton: geotectonic implications based on field geology, zircon geochronology and Nd-Sr isotope geochemistry. J. S. Am. Earth Sci. 48, 271–295.
Rizzotto, G.J., Hartmann, L.A., Santos, J.O.S., McNaughton, N.J., 2014. Tectonic evolution of the southern margin of the Amazonian craton in the late Mesoproterozoic based on field relationships and zircon U-Pb geochronology. An Acad. Bras Ciências 86, 57–84.
Rizzotto, G.J., Alves, C.L., Rios, F.S., Barros, M.A.S., 2019. The Western Amazonia Igneous Belt. J. S. Am. Earth Sci. 96, 102326 https://doi.org/10.1016/j.jsames.2019.102326.
Robb, L.J., Armstrong, R.A., Waters, D.J., 1998. Nature and duration of mid-crustal granulite facies metamorphism and crustal growth: evidence from single zircon U-Pb geochronology in Namaqualand, South Africa. Economic Geology Research Unit, University of the Witwatersrand, No. 323.
Roberts, N.M.W., Slagstad, T., 2015. Continental growth and reworking on the edge of the Columbia and Rodinia supercontinents; 1.86-0.9 Ga accretionary orogeny in southwest Fennoscandia. Int. Geol. Rev. 57, 1582–1606.
Roberts, N.M.W., Slagstad, T., Parrish, R.R., Norry, M.J., Marker, M., Horstwood, M.S.A., 2013. Sedimentary recycling in arc magmas: geochemical and U-Pb-Hf-O constraints on the Mesoproterozoic Suldal Arc, SW Norway. Contrib. Miner. Petrol. 165, 507–523.
Rogers, J.J.W., Santosh, M., 2002. Configuration of Columbia, a Mesoproterozoic supercontinent. Gondwana Res. 5, 5–22.
Rollinson, H., 2017. There were no large volumes of felsic continental crust in the early Earth. Geosphere 13, 235–246. https://doi.org/10.1130/GES01437.1.
Saar de Almeida, B., Geraldes, M.C., Sommer, C.A., Corrales, F., Paes de Barros, A.J., 2021. The Colider and Roosevelt volcanic rocks (SW Amazonian Craton): geochemistry and Sm-Nd characteristics of a silicic large igneous province. Acta Geochimica 40, 1023–1049. https://doi.org/10.1007/s11631-021-00490-2.
Sadowski, G.R., Bettencourt, J.S., 1996. Mesoproterozoic tectonic correlations between eastern Laurentia and the western border of the Amazon Craton. Precambr. Res. 76, 213–227.
Santos, J.O.S., Groves, D.I., Hartmann, L.A., Moura, M.A., Mcnaughton, N.J. 2001. Gold deposits of the Tapajós and Alta Floresta Domains, Tapajós-Parima orogenic belt, Amazon Craton, Brazil. Mineralium Deposita 36, 278-299. https://doi.org/10.1007/s001260100172.
Santos, J.O.S., Pinto, V., McNaughton, N.J., Silva, L.C., 2011. Magmatismo Serra Grande em Roraima: formação cogenética de granito rapakivi e charnockito em ca. 1430 Ma [Serra Grande anorogenic suite (Roraima state, Brazil): coeval rapakavi granite and charnockite at ca. 1430 Ma. In: Simpósio de Geologia da Amazônia, Brazil. CDROM.
Santos, J.O.S., Hartmann, L.A., Gaudette, H.E., Groves, D.I., McNaughton, N.J., Fletcher, I.R., 2000. A new understanding of the Amazon Craton provinces based on integration of field mapping and U-Pb and Sm-Nd geochronology. Gondwana Res. 3, 453–488.
Santos, J.O.S., Van Breemen, O.B., Groves, D.I., Hartmann, L.A., Almeida, M.E., Mcnaughton, N.J., Fletcher, I.R., 2004. Timing and evolution of multiple Paleoproterozoic magmatic arcs in the Tapajós Domain, Amazon Craton: constraints from SHRIMP and TIMS zircon, baddeleyite and titanite U-Pb geochronology. Precambr. Res. 131, 73–109. https://doi.org/10.1016/j.precamres.

Santos, J.O.S., Rizzotto, G.J., Potter, P.E., McNaughton, N.J., Matos, R.S., Hartmann, L. A., Chemale Jr., F., Quadros, M.S., 2008. Age and autochthonous evolution of the Sunsás orogen in West Amazon Craton based on mapping and U-Pb geochronology. Precambr. Res. 165, 120–152.

Sato, K. and Tassinari, C.C.G., 1997. Principais eventos de acresção continental no Cráton Amazônico, baseados em idade modelo Sm-Nd, calculadas em evoluções de estágio único e estágio duplo. In: Costa M.L. and Angélica R.S. (eds.). Contribuições à Geologia da Amazônia. Belém, SBG, 1, 91-142.

Scandolara, J.E., Fuck, R.A., Dall'Agnol, R., Dantas, E.L., 2013. Geochemistry and origin of the early Mesoproterozoic mangerite-charnockite-rapakivi granite association of the Serra da Providência suite and associated gabbros, central-eastern Rondônia, SW Amazonian Craton, Brazil. J. S. Am. Earth Sci. 4, 166–193.

Scandolara, J.E., Correa, R.T., Fuck, R.A., Souza, V.S., Rodrigues, J.B., Ribeiro, P.S.E., Frasca, A.A.S., Saboia, A.M., Lacerda Filho, J.V., 2017. Paleo-Mesoproterozoic arc-accretion along the southwestern margin of the Amazonian craton: the Juruena accretionary orogen and possible implications for Columbia supercontinente. J. S. Am. Earth Sci. 73, 223–247.

Schulz, K.J., Cannon, W.F., 2007. The Penokean orogeny in the Lake Superior region. Precambr. Res. 157, 4–25.

Selverstone, J., Hodgins, M., Aleinikoff, J.N., Fanning, C.M., 2000. Mesoproterozoic reactivation of a Paleoproterozoic transcurrent boundary in the northern Colorado Front Range: Implications for ~ 1.7- and 1.4-Ga tectonism. Rocky Mt Geol. 35, 139–162. https://doi.org/10.2113/35.2.139.

Semblano, F.R.D., Macambira, M.J.B., Vasquez, M.L., 2016a. Petrography, geochemistry and Sm-Nd isotopes of the granites from eastern of the Tapajós Domain, Pará state. Braz. J. Geol. 46, 509–529. https://doi.org/10.1590/2317-4889201620160059.

Semblano, F.R.D., Pereira, N.C.S., Vasquez, M.L., Macambira, M.J.B., 2016b. Novos dados geológicos e isotópicos para o Domínio Iriri-Xingu, Província Amazônia Central; implicações para a idade do Grupo Iriri, Geologia USP. Série Científica 16 (3), 19–38. https://doi.org/10.11606/issn.2316-9095.v16i3p19-38.

Shaw, C.A., Karlstrom, K.E., 1999. The Yavapai-Mazatzal crustal boundary in the Southern Rocky Mountains. Rocky Mt Geol. 34, 37–52. https://doi.org/10.2113/34.1.37.

Shchipansky, A.A., Samsonov, A.V., Petrova, A.Yu., Larionova, Y.U., 2007. Geodynamics of the Eastern Margin of Sarmatia in the Paleoproterozoic. Geotecton 41, 38–62.

Shumlyanskyy, L., 2014. Geochemistry of the Osnitsk-Mikashevichy volcanoplutonic complex of the Ukrainian shield. Geochem. Int. 52, 912–924.

Shumlyanskyy, L., Billström, K., Hawkesworth, C., Elming, S.-Å., 2013. U-Pb age and Hf isotope compositions of zircons from the northwestern region of the Ukrainian shield: mantle melting in response to post-collision extension. Terra Nova 24, 373–379.

Shumlyanskyy, L., Ernst, R., Söderlund, U., Billström, K., Mitrokhin, O., Tsymbal, S., 2016a. New U-Pb ages for mafic dykes in the Northwestern region of the Ukrainian shield: coeval tholeiitic and jotunitic magmatism. GFF 138, 79–85.

Shumlyanskyy, L., Mitrokhin, O., Billström, K., Ernst, R., Vishnevska, E., Tsymbal, S., Cuney, M., Soesoo, A., 2016b. The ca. 1.8 Ga mantle plume-related magmatism of the central part of the Ukrainian shield. GFF 138, 86–101.

Shumlyanskyy, L., Hawkesworth, C., Billström, K., Bogdanova, S., Mytrokhyn, O., Dhuime, B., Claesson, S., Ernst, R., Whitehouse, M., Bilan, O., 2017. The origin of the Palaeoproterozoic AMCG complexes in the Ukrainian Shield: new U-Pb ages and Hf isotopes in zircon. Precambr. Res. 292, 216–239.

Shumlyanskyy, L.V., Stepanyuk, L.M., Claesson, S., Rudenko, K.V., Bekker, A.Yu., 2018. The U-Pb zircon and monazite geochronology of granitoids of the Zhytomyr and Sheremetiv complexes, the Northwestern region of the Ukrainian Shield. Mineral. J. (Ukraine) 40(2), 63-85 (in Ukrainian).

Shumlyanskyy, L., Ernst, R.E., Albekov, A., Söderlund, U., Wilde, S.A, Bekker, A., 2021. The Statherian (ca. 1800-1750 Ma) Prutivka-Novogol large igneous province of Sarmatia: geochronology and implication for the Nuna/Columbia supercontinent reconstruction. Precambrian Research 358, 106185. https://doi.org/10.1016/j.precamres.2021.106185.

Sides, J.R., Bickford, M.E., Shuster, R.D., Nusbaum, R.L., 1981. Calderas in the Precambrian terrane of the St. Francois Mountains, southeastern Missouri. J. Geophys. Res. 86, 10349–10364.

Sims, P.K., Van Schmus, R., Schulz, K., Peterman, Z., 1989. Tectono-stratigraphic evolution of the Early Proterozoic Wisconsin magmatic terranes of the Penokean orogen. Can. J. Earth Sci. 26, 2145–2158.

Singletary, S.J., Hanson, R.E., Martin, M.W., Crowley, J.L., Bowring, S.A., Key, R.M., Ramokate, L.V., Direng, B.B., Krol, M.A., 2003. Geochronology of basement rocks in the Kalahari Desert, Botswana, and implications for regional Proterozoic tectonics. Precambr. Res. 121, 47–71.

Skridlaite, G., Siliauskas, L., Whitehouse, M., Johansson, Å, Rimsa, A., 2021. On the origin and evolution of the 1.86-1.76 Ga Mid-Baltic Belt in the western East European Craton. Precambrian Research 367 (106403), 1–21. https://doi.org/10.1016/j.precamres.2021.106403.

Skridlaite, G., Wiszniewska, J., Duchesne, J.-C., 2003. Ferro-potassic A-type granites and related rocks in NE Poland and S Lithuania: west of the East European Craton. Precambr. Res. 124, 305–326.

Skridlaite, G., Baginski, B., Whitehouse, M., 2008. Significance of c. 1.5 Ga zircon and monazite ages from charnockites in southern Lithuania and NE Poland. Gondwana Res. 14, 663–674.

Slagstad, T., Culshaw, N.G., Daly, J.S., Jamieson, R.A., 2009. Western Grenville Province holds key to midcontinental Granite-Rhyolite Province enigma. Terra Nova 21, 181–187. https://doi.org/10.1111/j.1365-3121.2009.00871.x.

Slagstad, T., Roberts, N.M.W., Marker, M., Røhr, T.S., Schiellerup, H., 2013. A non-collisional, accretionary Sveconorwegian orogen. Terra Nova 25, 30–37.

Slagstad, T., Roberts, N.M.W., Kulakov, E., 2017. Linking orogenesis across a supercontinent; the Grenvillian and Sveconorwegian margins on Rodinia. Gondwana Res. 44, 109–115.

Slagstad, T., Roberts, N.M.W., Coint, N., Høy, I., Sauer, S., Kirkland, K.L., Marker, M., Røhr, T.S., Henderson, I.H.C., Stormoen, M.A., Skår, Ø., Sørensen, B.E., Bybee, G.M., 2018. Magma-driven, high-grade metamorphism in the Sveconorwegian Province, southwest Norway, during the terminal stages of Fennoscandian Shield evolution. Geosphere 14, 861–882.

Slagstad, T., Marker, M., Roberts, N.M.W., Saalmann, K., Kirkland, C.L., Kulakov, E., Ganerød, M., Røhr, T.S., Møkkelgjerd, S.H.H., Granseth, A., Sørensen, B.E., 2020. The Sveconorwegian orogeny – reamalgamation of the fragmented southwestern margin of Fennoscandia. Precambr. Res. 350, 105877.

Smithies, R., Howard, H., Maier, W., Evins, P., 2009. Blackstone, WA Sheet 4545. 1: 100000 Geological Series.

Smithies, R., Howard, H., Evins, P., Kirkland, C., Kelsey, D., Hand, M., Wingate, M., Collins, A., Belousova, E., Allchurch, S., 2010. Geochemistry, geochronology and petrogenesis of Mesoproterozoic felsic rocks in the west Musgrave Province, Central Australia, and implications for the Mesoproterozoic tectonic evolution of the region. Geological Survey of Western Australia.

Smithies, R.H., Howard, H.M., Evins, P.M., Kirkland, C.L., Kelsey, D.E., Hand, M., Wingate, M.T.D., Collins, A.S., Belousova, E.A., 2011. High-temperature granite magmatism, crust-mantle interaction and the Mesoproterozoic intracontinental evolution of the Musgrave Province, Central Australia. J. Petrol. 52, 931–958.

Smithies, R.H., Spaggiari, C.V., Kirkland, C.L., 2015a. Building the crust of the Albany-Fraser Orogen; constraints from granite geochemistry. Geol. Survey of Western Australia, Report 150, 49p.

Smithies, R.H., Spaggiari, C.V., Kirkland, C.L., Wingate, M.T.D., England, R.N., 2015b. Forrest Zone: geochemistry and petrogenesis. In: Spaggiari, C., Smithies, R. (eds.), Eucla Basement Stratigraphic Drilling Results Release Workshop: Extended Abstracts. Geological Survey of Western Australia, Record 2015/10, pp. 41-51.

Smithies, R.H., Spaggiari, C.V., Kirkland, C.L., Wingate, M.T.D., England, R.N., 2015c. Madura Province: geochemistry and petrogenesis. In: Spaggiari, C., Smithies, R. (eds.), Eucla Basement Stratigraphic Drilling Results Release Workshop: Extended Abstracts. Geological Survey of Western Australia, Record 2015/10, pp. 17-28.

Smithies, R.H., Howard, H.M., Kirkland, C.L., Korhonen, F.J., Medlin, C.C., Maier, W.D., Quentin De Gromard, R., Wingate, M.T.D., 2015d. Piggy-back supervolcanoes - long-lived, voluminous, juvenile rhyolite volcanism in Mesoproterozoic central Australia. J. Petrol. 56, 735–763. https://doi.org/10.1093/petrology/egv015.

Smithies, R.H., Kirkland, C.L., Cliff, J.B., Howard, H.M., Quentin de Gromard, R., 2015e. Syn-volcanic cannibalisation of juvenile felsic crust: Superimposed giant ^{18}O-depleted rhyolite systems in the hot and thinned crust of Mesoproterozoic central Australia. Earth Planet. Sci. Lett. 424, 15–25.

Smits, R., Collins, W., Hand, M., Dutch, R., Payne, J., 2014. A Proterozoic Wilson cycle identified by Hf isotopes in central Australia: implications for the assembly of Proterozoic Australia and Rodinia. Geology 42, 231–234.

Söderlund, U., Möller, C., Andersson, J., Johansson, L., Whitehouse, M., 2002. Zircon geochronology in polymetamorphic gneisses in the Sveconorwegian orogen, SW Sweden: ion microprobe evidence for 1.46-1.42 and 0.98-0.96 Ga reworking. Precambr. Res. 113, 193–225.

Söderlund, U., Hellström, F.A., Kamo, S.L., 2008. Geochronology of high-pressure mafic granulite dykes in SW Sweden; tracking the P-T-t path of metamorphism using Hf isotopes in zircon and baddeleyite. J. Metamorph. Geol. 26, 539–560.

Soesoo, A., Hade, S., 2012. Geochemistry and age of some A-type granitoid rocks of Estonia. LITHOSPHERE 2012 - Symposium (Nov. 6–8, 2012). Espoo, Finland 2012, 97–101.

Soesoo, A., Puura, V., Kirs, J., Petersell, V., Niin, M., All, T., 2004. Outlines of the Precambrian basement of Estonia. Proceedings of the Estonian Academy of Sciences, Geology 53, 149–164.

Soesoo, A., Nirgi, S., Plado, J., 2020. The evolution of the Estonian Precambrian basement: geological, geophysical and geochronological constraints. Proc. Karelian Res. Centre Russ. Acad. Sci. 2, 18–33.

Sørensen, H., 2001. Brief introduction to the geology of the Ilímaussaq alkaline complex, South Greenland, and its exploration history. Geol. Greenland Survey Bull. 190, 7–24.

Spaggiari, C.V., Smithies, R.H., 2015. Eucla basement stratigraphic drilling results release workshop: extended abstracts. Geol. Survey Western Aust., Record 2015 (10), 70p.

Spaggiari, C., Bodorkos, S., Barquero-Molina, M., Tyler, I., Wingate, M., 2009. Interpreted bedrock geology of the south Yilgarn and central Albany-Fraser orogen, Western Australia. Geol. Survey Western Aust., Record 10, 84.

Spaggiari, C., Kirkland, C., Pawley, M., Smithies, R., Wingate, M., Doyle, M., Blenkinsop, T., Clark, C., Oorschot, C., Fox, L., 2011. The geology of the east Albany-Fraser Orogen—a field guide. Geol. Survey Western Aust., Record 23, 97.

Spaggiari, C.V., Kirkland, C.L., Smithies, R.H., Wingate, M.T.D., Belousova, E.A., 2015. Transformation of an Archean craton margin during Proterozoic basin formation and magmatism: The Albany-Fraser Orogen, Western Australia. Precambr. Res. 266, 440–466.

Spencer, C.J., Thomas, R.J., Roberts, N.M., Cawood, P.A., Millar, I., Tapster, S., 2015. Crustal growth during island arc accretion and transcurrent deformation, Natal Metamorphic Province, South Africa: new isotopic constraints. Precambr. Res. 265, 203–217.

Spencer, C.J., Murphy, J.B., Hoiland, C.W., Johnston, S.T., Mitchell, R.N., Collins, W.J., 2019. Evidence for Whole Mantle Convection Driving Cordilleran Tectonics. Geophys. Res. Lett. 46, 4239–4248. https://doi.org/10.1029/2019GL082313.

Srivastava, R.K, Ernst, R.E., Peng, P., (eds.), 2019. Dyke Swarms of the World, A Modern Perspective. Springer, Singapore, 492 pp.

Steenfelt, A., Kolb, J., Thrane, K., 2016. Metallogeny of South Greenland: a review of geological evolution, mineral occurrences and geochemical exploration data. Ore Geol. Rev. 77, 194–245.

Stein, M., Hofmann, A.W., 1994. Mantle plumes and episodic crustal growth. Nature 372, 63–68. https://doi.org/10.1038/372063a0.

Stephens, M.B., 2020. Outboard-migrating accretionary orogeny at 1.9-1.8 Ga (Svecokarelian) along a margin of the continent Fennoscandia. Chapter 8 in Stephens, M.B., Bergman Weihed, J. (eds.), 2020. Sweden: Lithotectonic Framework, Tectonic Evolution and Mineral Resources. Geological Society Memoir 50, Geological Society of London, 237-250.

Stephens, M.B., Bergman Weihed, J. (eds.), 2020. Sweden: Lithotectonic Framework, Tectonic Evolution and Mineral Resources. Geological Society Memoir 50, Geological Society of London, 631 pp.

Stephens, M.B., Bergman, S., 2020. Regional context and lithotectonic framework of the 2.0-1.8 Ga Svecokarelian orogen, eastern Sweden. Chapter 2 in Stephens, M.B., Bergman Weihed, J. (eds.), 2020. Sweden: Lithotectonic Framework, Tectonic Evolution and Mineral Resources. Geological Society Memoir 50, Geological Society of London, 19-26.

Stephens, M.B., Wahlgren, C.-H., 2020a. Polyphase (1.9-1.8, 1.5-1.4 and 1.0-0.9 Ga) deformation and metamorphism of Proterozoic (1.9-1.2 Ga) continental crust, Eastern Segment, Sveconorwegian orogen. Chapter 15 in Stephens, M.B., Bergman Weihed, J. (eds.), 2020. Sweden: Lithotectonic Framework, Tectonic Evolution and Mineral Resources. Geological Society Memoir 50, Geological Society of London, 351-396.

Stephens, M.B., Wahlgren, C.-H., 2020b. Accretionary orogens reworked in an overriding plate setting during protracted continent-continent collision, Sveconorwegian orogen, southwestern Sweden. Chapter 17 in Stephens, M.B., Bergman Weihed, J. (eds.), 2020. Sweden: Lithotectonic Framework, Tectonic Evolution and Mineral Resources. Geological Society Memoir 50, Geological Society of London, 435-448.

Stephens, M.B., Bergström, U., Wahlgren, C.-H., 2020. Regional context and lithotectonic framework of the 1.1-0.9 Ga Sveconorwegian orogen, southwestern Sweden. Chapter 14 in Stephens, M.B., Bergman Weihed, J. (eds.), 2020. Sweden: Lithotectonic Framework, Tectonic Evolution and Mineral Resources. Geological Society Memoir 50, Geological Society of London, 337-349.

Stephens, M.B., Ripa, M., Lundström, I., Persson, L., Bergman, T., Ahl, M., Wahlgren, C.-H., Persson, P.-O., Wickström, L., 2009. Synthesis of bedrock geology in the Bergslagen region, Fennoscandian Shield, south-central Sweden. Sveriges Geologiska Undersökning Ba 58, 259 pp.

St-Onge, M.R., van Gool, J.A.M., Garde, A.A., Scott, D.J., 2009. Correlation of Archaean and Palaeoproterozoic units between northeastern Canada and western Greenland: constraining the pre-collisional upper plate accretionary history of the Trans-Hudson orogen. Geol. Society, London, Spec. Publ. 318, 193–235. https://doi.org/10.1144/SP318.7.

Strickland, A., Wooden, J.L., Mattinson, C.G., Ushikubo, T., Miller, D.M., Valley, J.W., 2013. Proterozoic evolution of the Mojave crustal province as preserved in the Ivanpah Mountains, southeastern California. Precambrian Research 224, 222–241.

Suominen, V., 1991. The chronostratigraphy of southwestern Finland with special reference to Postjotnian and Subjotnian diabases. Geological Survey of Finland Bulletin 356, 100 pp.

Tassinari, C.C.G., Macambira, M.J.B., 1999. Geochronological provinces of the Amazonian Craton. Episodes 22, 174–182.

Tassinari, C.G.C., Cordani, U.G., Nutman, A.P., Schmus, W.R.V., Bettencourt, J.S., Taylor, P.N., 1996. Geochronological Systematics on Basement Rocks from the Rio Negro - Juruena Province (Amazonian Craton) and Tectonic Implications. Int. Geol. Rev. 38, 161–175.

Teixeira, W., Reis, N.J, Bettencourt, J.S., Klein, E.F., Oliveira, D., 2019. Intraplate Proterozoic magmatism in the Amazonian Craton reviewed: geochronology, crustal tectonics and global barcode matches. In Srivastava, R.K, Ernst, R.E., Peng, P., (eds.): Dyke Swarms of the World - A Modern Perspective. Springer Geology, p. 111-154. https://doi.org/10.1007/978-981-13-1666-1_4.

Teixeira, W., Geraldes, M.C., Matos, R., Ruiz, A.S., Saes, G., Vargas-Mattos, G., 2010. A review of the tectonic evolution of the Sunśas belt, SW Amazonian Craton. J. S. Am. Earth Sci. 29, 47–60.

Teixeira, W., Hamilton, M.A., Lima, G.A., Ruiz, A.S., Matos, R., Ernst, R.E., 2015. Precise ID-TIMS U-Pb baddeleyite ages (1110–1112 Ma) for the Rincón del Tigre-Huanchaca large igneous province (LIP) of the Amazonian Craton: implications for the Rodinia supercontinent. Precambrian Res. 265, 273–285.

Teixeira, W., Cordani, U.G., Faleiros, F.M., Sato, K., Maurer, V.C., Ruiz, A.S., Azevedo, E. J.P., 2020. The Rio Apa Terrane reviewed: U-Pb zircon geochronology and provenance studies provide paleotectonic links with a growing Proterozoic Amazonia. Earth Sci. Rev. 202 (103089), 1–35.

Teixeira, J.B.G., Misi, A., da Silva, M.G., 2007. Supercontinent evolution and the Proterozoic metallogeny of South America. Gondwana Res. 11, 346–361.

Terentiev, R.A., Santosh, M., 2020. Baltica (East European Craton) and Atlantica (Amazonian and West African Cratons) in the Proterozoic: The pre-Columbia connection. Earth-Science Reviews 210 (103378), 1–27. https://doi.org/10.1016/j.earscirev.2020.103378.

Terentiev, R.A., Savko, K.A., Santosh, M., 2016. Paleoproterozoic crustal evolution in the East Sarmatian Orogen: petrology, geochemistry, Sr-Nd isotopes and zircon U-Pb geochronology of andesites from the Voronezh massif, Western Russia. Lithos 246–247, 61–80.

Thomas, R.J., 1989. A tale of two tectonic terranes. South African Journal of Geology 92, 306–321.

Thomas, R.J., Eglington, B.M., 1990. A Rb-Sr, Sm-Nd and U-Pb zircon isotopic study of the Mzumbe Suite, the oldest intrusive granitoid in southern Natal, South Africa. S. Afr. J. Geol. 93, 761–765.

Thomas, R.J., Cornell, D.H., Moore, J.M., Jacobs, J., 1994. Crustal evolution of the Namaqua-Natal metamorphic province, Southern Africa. S. Afr. J. Geol. 97, 8–14.

Thomas, R.J., Cornell, D.H., Armstrong, R.A., 1999. Provenance age and metamorphic history of the Quha Formation, Natal Metamorphic Province: a U-Th-Pb zircon SHRIMP study. S. Afr. J. Geol. 102, 83–88.

Thomas, R.J., Bushi, A.M., Roberts, N.M.W., Jacobs, J., 2014. Geochronology of granitic rocks from the Ruangwa region, southern Tanzania – links with NE Mozambique and beyond. J. Afr. Earth Sc. 100, 70–80.

Thomas, R.J., Macey, P.H., Spencer, C., Dhansay, T., Diener, J.F.A., Lambert, C.W., Nguno, A., 2016. The Sperrgebiet Domain, Aurus Mountains, SW Namibia: a ~2020 to 850 Ma window within the Pan-African Gariep Orogen. Precambr. Res. 286, 35–58.

Tohver, E., van der Pluijm, B.A., Van der Voo, R., Rizzotto, G., Scandolara, J.E., 2002. Paleogeography of the Amazon craton at 1.2 Ga: early Grenvillian collision with the Llano segment of Laurentia. Earth Planet. Sci. Lett. 199, 185–200.

Tohver, E., Bettencourt, J.S., Tosdal, R., Mezger, K., Leite, W.B., Payolla, B.L., 2004a. Terrane transfer during the Grenville orogeny: Tracing the Amazonian ancestry of southern Appalachian basement through Pb and Nd isotopes. Earth Planet. Sci. Lett. 228, 161–176. https://doi.org/10.1016/j.epsl.2004.09.029.

Tohver, E., Van der Pluijm, B.A., Mezger, K., Essene, E., Scandorala, J.E., Rizzotto, G.J., 2004b. Significance of the Nova Brasilândia metasedimentary belt in western Brazil: redefining the Mesoproterozoic boundary of the Amazon Craton. Tectonics. https://doi.org/10.1029/2003TC001563.

Tohver, E., Teixeira, W., Van der Pluijm, B.A., Geraldes, M.C., Bettencourt, J.S., Rizzotto, G., 2006. A restored transect across the exhumed Grenville orogen of Laurentia and Amazonia, with implications for crustal architecture. Geology 34, 669–672.

Trevisan, V.G., Hagemann, S.G., Loucks, R.R., Xavier, R.P., Motta, J.G., Parra-Avila, L.A., Petersson, A., Gao, J.-F., Kemp, A.I.S., Assis, R.R., 2021. Tectonic switches recorded in a Paleoproterozoic accretionary orogen in the Alta Floresta Mineral Province, southern Amazonian Craton. Precambrian Research 364, 106324, 43 pp., https://doi.org/10.1016/j.precamres.2021.106324.

Tyson, A.R., Morozova, E.A., Karlstrom, K.E., Chamberlain, K.R., Smithson, S.B., Dueker, K.G., Foster, C.T., 2002. Proterozoic Farwell Mountain - Lester Mountain suture zone, northern Colorado: Subduction flip and progressive assembly of arcs. Geology 30, 943–946. https://doi.org/10.1130/0091-7613(2002)030<0943:PFMLMS>2.0.CO;2.

Ulmius, J., Andersson, J., Möller, C., 2015. Hallandian 1.45 Ga high-temperature metamorphism in Baltica: P-T evolution and SIMS U-Pb zircon ages of aluminous gneisses, SW Sweden. Precambr. Res. 265, 10–39.

Upton, B.G.J., 2013. Tectono-magmatic evolution of the younger Gardar southern rift, South Greenland. Geol. Survey Denmark Greenland Bull. 29, 1–128.

Van Schmus, W.R., Bickford, M.E., Sims, P.K., Anderson, R.R., Shearer, C.K., Treves, S.B., 1993. Proterozoic geology of the western midcontinent basement. In: Reed, J.C., Jr, et al. (eds.), Precambrian Conterminous US. Boulder, Colorado, Geological Society of America, vols. C-2. Geology of North America, p. 239-259.

Van Schmus, W.R., Bickford, M.E., Turek, A., 1996. Proterozoic geology of the east-central Midcontinent basement. In: van der Pluijm, B.A., Catacosinos, P.A. (eds.): Basement and Basins of Eastern North America. Geological Society America Special Paper 308, 7-32.

Vander Auwera, J., Bolle, O., Bingen, B., Liégeois, J.P., Bogaerts, M., Duchesne, J.C., DeWaele, B., Longhi, J., 2011. Sveconorwegian massif-type anorthosites and related granitoids result from post-collisional melting of a continental root. Earth Sci. Rev. 107, 375–397.

Vanderhaege, O., Ledru, P., Thiéblemont, D., Egal, E., Cocherie, A., Tegyey, M., Milési, J., 1998. Contrasting mechanism of crustal growth. Geodynamic evolution of the Paleoproterozoic granite–greenstone belts of French Guiana. Precambr. Res. 92, 165–193.

Vasquez, M.L., Macambira, M.J.B., Galarza Toro, M.A., 2005. Granitoides transamazônicos da Região Iriri-Xingu, Pará – Novos dados geológicos e geocronológicos. In: Horbe, A.M.C., Souza, V.S. (Eds.), Contribuições à Geologia da Amazônia 4, 16–31.

Vasquez, M.L., Macambira, M.J.B., Armstrong, R.A., 2008. Zircon geochronology of granitoids from the western Bacajá domain, southeastern Amazonian craton, Brazil: Neoarchean to Orosirian evolution. Precambr. Res. 161, 279–302.

Vasquez, M.L., Cordani, U.G., Sato, K., Barbosa, J.P.O., Faraco, M.T.L., Maurer, V.C., 2019. U-Pb SHRIMP dating of basement rocks of the Iriri-Xingu Domain, Central Amazonian Province, Amazonian Craton, Brazil. Braz. J. Geol. 49 (3), 20190067.

Volante, S., Pourteau, A., Collins, W.J., Blereau, E., Li, Z.-X., Smit, M., Evans, N.J., Nordsvan, A.R., Spencer, C.J., McDonald, B.J., Li, J., Günter, C., 2020. Multiple P-T–d–t paths reveal the evolution of the final Nuna assembly in northeast Australia. J. Metamorph. Geol. 38, 593–627. https://doi.org/10.1111/jmg.12532.

Wade, B., Barovich, K., Hand, M., Scrimgeour, I., Close, D., 2006. Evidence for early Mesoproterozoic arc magmatism in the Musgrave Block, central Australia: implications for Proterozoic crustal growth and tectonic reconstructions of Australia. J. Geol. 114, 43–63.

Wade, B., Kelsey, D., Hand, M., Barovich, K., 2008. The Musgrave Province: stitching north, west and south Australia. Precambr. Res. 166, 370–386.

Wade, B.P., Payne, J.L., Hand, M., Barovich, K.M., 2007. Petrogenesis of ca 1.50 Ga granitic gneiss of the Coompana Block: filling the 'magmatic gap' of Mesoproterozoic Australia. Aust. J. Earth Sci. 54, 1089–1102.

Wahlgren, C.-H., Stephens, M.B., 2020a. Småland lithotectonic unit dominated by Paleoproterozoic (1.8 Ga) syn-orogenic magmatism, Svecokarelian orogen. Chapter 7 in Stephens, M.B., Bergman Weihed, J. (eds.), 2020. Sweden: Lithotectonic Framework, Tectonic Evolution and Mineral Resources. Geological Society Memoir 50, Geological Society of London, 207-235.

Wahlgren, C.-H., Stephens, M.B., 2020b. Reworking of older (1.8 Ga) continental crust by Mesoproterozoic (1.5-1.4 Ga) orogeny, Blekinge-Bornholm orogen, southeastern Sweden. Chapter 11 in Stephens, M.B., Bergman Weihed, J. (eds.), 2020. Sweden: Lithotectonic Framework, Tectonic Evolution and Mineral Resources. Geological Society Memoir 50, Geological Society of London, 291-312.

Walzer, U., Hendel, R., 2017. Continental crust formation: Numerical modelling of chemical evolution and geological implications. Lithos 278–281, 215–228. https://doi.org/10.1016/j.lithos.2016.12.014.

Wan, B., Yang, X., Tian, X., Yuan, H., Kirscher, U., Mitchell, R.N., 2020. Seismological evidence for the earliest global subduction network at 2 Ga ago. Science Advances 6, no. 32, eabc5491. https://doi.org/10.1126/sciadv.abc5491.

Wang, C.Y., Campbell, I.H., Allen, C.M., Williams, I.S., Eggins, S.M., 2009. Rate of growth of the preserved North American Continental crust: Evidence from Hf and O isotopes in Mississippi detrital zircons. Geochim. Cosmochim. Acta 73, 712–728. https://doi.org/10.1016/j.gca.2008.10.037.

Wang, C., Mitchell, R.N., Murphy, J.B., Peng, P., Spencer, C.J., 2020. The role of megacontinents in the supercontinent cycle. Geology 49, 402–406. https://doi.org/10.1130/G47988.1.

Wang, C.C., Jacobs, J., Elburg, M.A., Läufer, A., Thomas, R.J., Elvevold, S., 2020a. Grenville-age continental arc magmatism and crustal evolution in central Dronning Maud Land (East Antarctica): Zircon geochronological and Hf–O isotopic evidence. Gondwana Res. 82, 108–127.

Wang, C.C., Jacobs, J., Elburg, M.A., Läufer, A., Elvevold, S., 2020b. Late Neoproterozoic-Cambrian magmatism in Dronning Maud Land (East Antarctica): U-Pb zircon geochronology, isotope geochemistry and implications for Gondwana assembly. Precambr. Res. 350, 105880.

Waters, D.J., 1986. Metamorphic zonation and thermal history of pelitic gneisses from western Namaqualand, South Africa. S. Afr. J. Geol. 89, 97–102.

Wegener, A., 1912. Die Entstehung der Kontinente. Geologische Rundschau 3, 276–292.

Wegener A. 1915. Die Entstehung der Kontinente und Ozeane. Friedriech Vieweg & Sohn.

White, R., Powell, R., Clarke, G., 2002. The interpretation of reaction textures in Fe-rich metapelitic granulites of the Musgrave Block, central Australia: constraints from mineral equilibria calculations in the system K2O–FeO–MgO–Al2O3–SiO2–H2O–TiO2–Fe2O3. J. Metamorph. Geol. 20, 41–55.

Whitmeyer, S.J., Karlstrom, K.E., 2007. Tectonic model for the Proterozoic growth of North America. Geosphere 3, 220–259. https://doi.org/10.1130/GES00055.1.

Windley, B.F., 1993. Proterozoic anorogenic magmatism and its orogenic connections. J. Geol. Soc. London 150, 39–50.

Wingate, M., Kirkland, C., Spaggiari, C., Smithies, R., 2015. U-Pb geochronology of the Forrest Zone of the Coompana Province. In: Spaggiari, C., Smithies, R. (eds.): Eucla Basement Stratigraphic Drilling Results Release Workshop: Extended Abstracts. Geological Survey of Western Australia, Record 2015/10, pp. 37-40.

Wiszniewska, J., Krzeminska, E., 2021. Advances in geochronology in the Suwałki anorthosite massif and subsequent granite veins, northeastern Poland. Precambrian Research 361 (106265), 1–20. https://doi.org/10.1016/j.precamres.2021.106265.

Wooden, J.L., Miller, D.M., 1990. Chronologic and isotopic framework for early Proterozoic crustal evolution in the eastern Mojave Desert region, SE California. Journal of Geophysical Research 95, 20133-20146.

Wooden, J.L., Barth, A.P., Mueller, P.A., 2012. Crustal growth and tectonic evolution of the Mojave crustal province: Insights from hafnium isotope systematics in zircons. Lithosphere 5, 17–28. https://doi.org/10.1130/L218.1.

Wooden, J.L., Stacey, J.S., Howard, K.A., Doe, B.R., Miller, D.M., 1988. Pb isotopic evidence for the formation of Proterozoic crust in the southwestern United States. In Ernst, W.G., (ed.): Metamorphism and Crustal Evolution of the Western United States. Englewood Cliffs, New Jersey, Prentice-Hall, p. 68–86.

Zhang, S., Li, Z.-X., Evans, D.A.D., Wu, H., Li, H., Dong, J., 2012. Pre-Rodinia supercontinent Nuna shaping up: a global synthesis with new paleomagnetic results from North China. Earth Planetary Science Letters 353–354, 145–155.

Zhao, G., Sun, M., Wilde, S.A., Li, S., 2004. A Paleo-Mesoproterozoic supercontinent: assembly, growth and breakup. Earth Sci. Rev. 67, 91–123.

Zhao, G., Li, S., Sun, M., Wilde, S.A., 2011. Assembly, accretion, and break-up of the Palaeo-Mesoproterozoic Columbia supercontinent: record in the North China Craton revisited. Int. Geol. Rev. 53, 1331–1356. https://doi.org/10.1080/00206814.2010.527631.